2018

Bio-based carbon fiber from biorefinery lignin and lignin-derived bio-oil

Wangda Qu
Iowa State University

Bio-based carbon fiber from biorefinery lignin and lignin-derived bio-oil

by

Wangda Qu

A dissertation submitted to the graduate faculty

in partial fulfillment of the requirements for the degree of

DOCTOR OF PHILOSOPHY

Major: Mechanical Engineering

Program of Study Committee:
Xianglan Bai, Major Professor
Xinwei Wang
Mark Mba-Wright
Eric Cochran
Simon Laflamme

The student author, whose presentation of the scholarship herein was approved by the program of study committee, is solely responsible for the content of this dissertation. The Graduate College will ensure this dissertation is globally accessible and will not permit alterations after a degree is conferred.

Iowa State University

Ames, Iowa

2018

TABLE OF CONTENTS

Page

LIST OF FIGURES

Page

LIST OF TABLES

Page

ACKNOWLEDGMENTS

First, I would like to express my sincere appreciation to my advisor Dr. Bai. During my entire Ph. D study, she has provided great support both on my research and my life. Her kindly advise and care make me feel being a Ph. D student is indeed a meaningful journey, and I have learned much more than the knowledge itself.

I would like to thank my committee members, Dr. Xinwei Wang, Dr. Eric Cochran, Dr. Mark Wright, and Dr. Simon Laflamme for their guidance and support throughout the course of my research. Without their help and kindly advise, I cannot finish my work in high quality.

I would also like to thank the professors, staffs and colleagues in Biorenewable Research Laboratory. Especially to Dr. Robert Brown, Dr. Marge Rover, Dr. Patrick Johnson, Dr. Patrick Hall, and Mr. Ryan Smith for their great assistance in laboratory work, and maintenance of a clean/safe environment for research.

Last, I would like to express my special thanks to the lab members of Dr. Bai's group (Dr. Shuai Zhou, Dr. Ashokkumar Sharma, Dr. Yuan Xue, Wenqi Li, Yiwei Gao, Joel Bradon, Lusi A, Yixin Luo, and Xiaolin Chen), and my friends in Ames and families in China. Without their company and encouragement, I will not have precious memories during my hard time of Ph.D. study. They make my life at Iowa State University a memorable experience.

ABSTRACT

Due to its light weight and superior mechanical properties, carbon fiber has many attractive applications. However, PAN-based carbon fiber is too costly, which prevent its wide applications. On the other hand, lignin is considered as a low-cost alternative of PAN for carbon fiber production. As ever-increasing amount of lignin is produced from emerging biorefineries as a byproduct, lignin-based carbon fiber could contribute to economic sustainability of the lignin producing industries. In the first section of this work, the potential of producing carbon fiber from a high-ash containing corn stover lignin is investigated. The lignin was pretreated with methanol fractionation and partial acetylation and melt-spun at 165-170 ℃. After stabilization and carbonization, carbon fiber with tensile strength of 0.454 GPa was obtained. In following serious of study, a new concept called “depolymerization followed repolymerization” is proposed to prepare structurally modified lignin precursors in order to improve carbon fiber properties. Specifically, red oak lignin was thermally depolymerized into crude bio-oil via fast pyrolysis, and then repolymerized into carbon fiber precursors through different reaction routes. The aim of the work is to produce a lignin-based carbon fiber precursor with modified structure and molecular orientation.

In first route, the bio-oil, so called pyrolytic lignin (PL) was repolymerized in the presence of acid catalyst to prepare a precursor. The precursor had a T_g of 101 ℃, could be easily melt-spun at 115-120 ℃, and stabilized at 0.3 ℃/min. The resulting carbon fiber had smooth surface and void-free cross section. The average tensile strength of the fiber was 0.855 GPa. In the second route, PL was thermally co-treated with 5 or 20 percent of polyethylene terephthalate (PET), prior to the PL-PET precursor was melt-spun. Results

from FTIR, NMR, thermal, and rheological tests all indicated that PL and PET chemically bonded to improve molecular orientation of the resulting precursor. As a result, PL-PET precursor had decreased spinning temperatures and higher thermal stabilities. Also, PL-PET based carbon fiber had lower I_D/I_G from Raman spectra for improved crystallinity and higher mechanical properties compared to PL-based carbon fiber. In third route, PL was converted to lignin-based polymers through free radical polymerization. To convert PL into radically polymerizable material, PL was functionalized with different amounts of methacryloyls and acetyls and then polymerized by applying Reversible Addition-Fragmentation chain Transfer (RAFT) technique. Three polymers namely PLMAP1, PLMAP2, and PLMAP3 were synthesized. PLMAP1 (fully methacylated PL) was a cross-linked polymer. PLMAP2 (partially methacrylated PL) was a thermoplastic polymer with glass transition temperature (T_g) of 161 ℃ and thermal decomposition temperature (T_d) of 241 ℃. PLMAP3 (partially methacrylated and the fully acetylated PL) had reduced T_g of 130 ℃, while its T_d increased to 250 ℃. PLMAP3 is melt-spinnable and also demonstrated highly attractive properties as ideal carbon fiber precursor. It is carbonizable at 1000 ℃, and has much improved molecular orientation.

CHAPTER 1. INTRODUCTION

1.1 Carbon Fiber

1.1.1 Background of Carbon Fiber

Carbon fiber is a fibrous material with diameter in micrometers and carbon content of more than 92 percent. It possesses a combination of unique properties, making it a good candidate for current advanced materials and engineering composites [1]. First, carbon fiber is lightweight with density of 1.75-2.18 g cm^{-3}, about four times lower comparing to steel [2]. Second, owing to its well-orientated packing of lamellar graphite structure on molecular level, carbon fiber has high tensile strength up to 7 GPa and modulus up to 900 GPa. In terms of strength-to-density (S/D) ratio, it therefore has an even higher value, rendering carbon fiber a lightweight and strong material. Third, carbon fiber has both good heat and creep resistance, making it stable to use over long lifetime. Last, carbon fiber is resistant to most of chemicals, and it can be coated with resin to enhance its applicable fields. Combining these superior features especially its high S/D ratio, carbon fiber has obtained tremendous interests and increasing demand in automobile industry, aerospace, construction, mechanical engineering, sports equipment, and other high-end products [3, 4]. According to a recent report from Oak Ridge National Laboratory, the demand of carbon fiber will increase to more than 150,000 tonnes by the year of 2020 [3]. Currently, the wide application of carbon fiber is still restricted by its high price. In order to make carbon fiber more available to markets, its price has to be reduced. Moreover, the precursors to produce carbon fiber are based on petroleum downstream products. Therefore, the price and resources of carbon fiber precursor can be volatile based on petroleum supply and prices, which will add more uncertainty as well as energy security concerns to related industry.

1.1.2 Precursors and Manufacturing of Carbon Fibers

1.1.2.1 Polyacrylonitrile based carbon fiber

There are primary three types of precursors being used in carbon fiber production- polyacrylonitrile (PAN), pitch, and rayon [5]. Their chemical structures are presented in Fig. 1.1. Among them, at least 90% of the market is occupied by PAN-based carbon fiber, since the pitch and rayon based carbon fiber both have their drawbacks in processing maturity and products quality [4]. PAN can be synthesized from acrylonitrile (AN) via various types of polymerizations. Among those, solution polymerization is the main method used for continuously producing PAN, while it brings issues in product yield and environmental concerns [4]. Suspension polymerization is another common method to obtain high yield of PAN. However it is a discontinuous process [4]. The PAN-based precursor usually has the molecular weight (Mw) of 70000 to 260000 g/mol, with polydispersity index of 1.5 to 3.5 [6]. There are about less than 5 mol% of co-monomers present in PAN, and these co-polymers are known to have apparent impacts on precursor structure and corresponding carbon fiber properties [1].

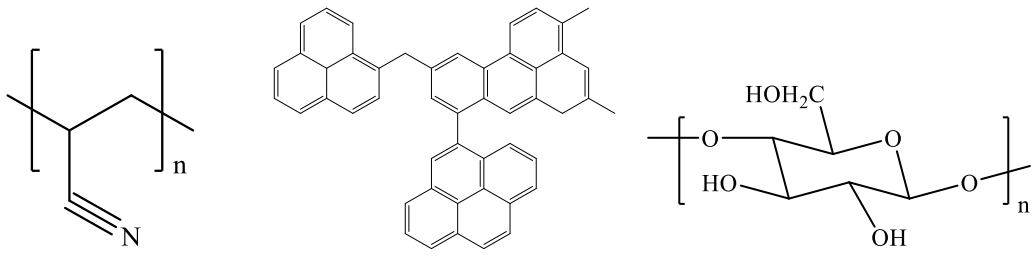

Figure 1.1 Structural illustration of PAN (left), Pitch (middle), and Rayon (cellulose) (right).

Producing carbon fiber from PAN is a long and complicated process, which requires good knowledge and practice of each step, as well as a rational design of equipment and device so that the obtained carbon fiber is uniform and homogeneous. Failure in each step can result in the low quality of carbon fiber intermedium, subsequently adding difficulties in

following steps. PAN can be formed to fiber strings via a process known as spinning. There are different types of spinning techniques such as melt-spinning, wet-spinning, dry spinning and others [7-9]. Melt-spinning is to heat the precursor polymer to above its soften or melting point, and then pull the fibers from the polymer dope. This process is believed to be economic and scalable by simply applying heat. Wet-spinning is to dissolve the precursor polymer into a suitable solvent, and then inject the dopes through another solvent, where the solvent in dopes will be dissolved in the coagulation bath, and the polymer fiber will be formed. Dry-spinning is similar to wet-spinning in dope preparation, while the polymer needs to be dissolved in a much more volatile solvent, and the solvent will be later rapidly evaporated in hot air and the polymer fiber will be remained. Since PAN has a thermal decomposition temperature lower than its melting temperature (~ 300 ℃), PAN is only applicable to use wet-spinning for fiber production. Although pretreatment of PAN or adding plasticizer may facilitate the melting of PAN by alleviating its nitrile interactions [10], the final produced carbon fiber is not comparable to that produced from wet-spinning. The spinning fiber still needs to be further treated before collected, which includes essential steps such as washing, drawing, drying, etc. [4]. This is to render the fiber free of residual solvent and with better molecular orientation. After obtaining the as-spun fiber, it needs to be subject to a series of heat treatments to gradually convert into carbon fiber, which is summarized in Fig. 1.2.

The first step is called stabilization, where the PAN fiber will undergo cyclization, dehydration, oxidation, and crosslinking, and gradually form a ladder structure after the process [11]. Stabilization process can take place either under air or inert atmosphere at temperatures between 200 to 300 ℃. Also, the heating rate has to be well controlled so that

the glass transition temperature is constantly higher than atmosphere temperature, and the fiber could maintain its form over the course of heating. After stabilization, the PAN fiber will transform into more dense fiber with heteroaromatic structure. This cross-linked structure is heat resistant and can therefore be survived in following process called carbonization. To prevent the fiber from shrinking during stabilization, tension is usually applied. Moreover, the applying of tension could help to maintain the orientation along the axis of fiber. Previous researches have shown that applying tension can effectively increase the tensile strength of the final carbon fiber [12].

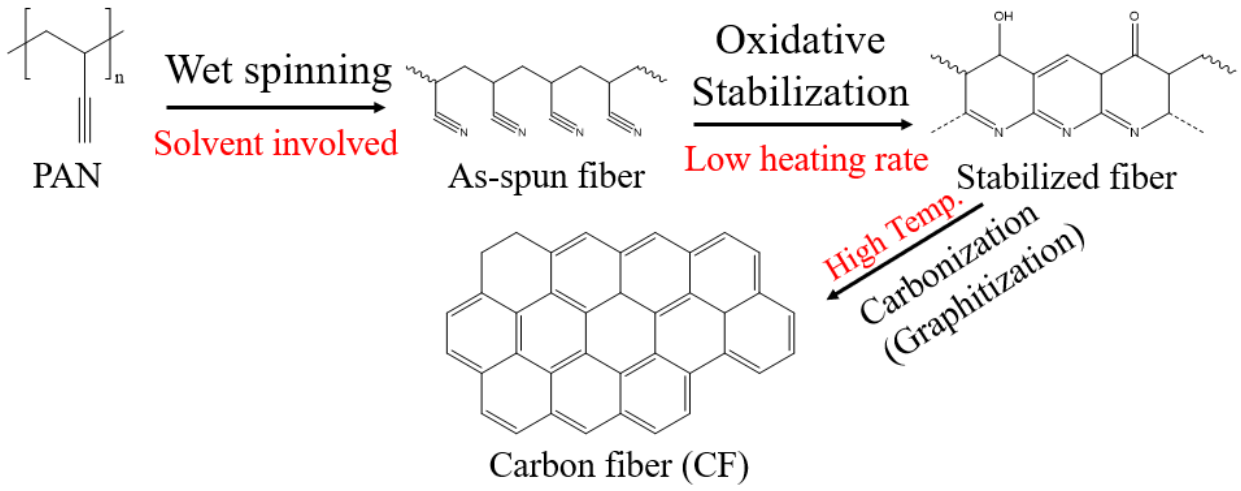

Figure 1.2 Conversion of carbon fiber from PAN.

After stabilization, the stabilized fiber becomes stronger and less flexible compared with the as-spun fiber. The stabilized fiber usually has the carbon content of 62-70%, nitrogen content of 20-24%, oxygen content of 5-10%, and hydrogen content of 2-4% [13]. To convert into carbon fiber, most of the heteroatoms need to be removed by carbonization process. Carbonization is a pyrolysis process occurring under high temperature (1000℃ or higher) and inert atmosphere. During this process, most of the heteroatoms will be eliminated in the forms of HCN, H_2, CO, NH_3, CH_4, H_2O, O_2, etc. and the residual carbon will form a

graphite structure [14]. There will be residual heteroatoms and defects present in the carbon fiber after carbonization, and the perfectness of the structure will determine the properties of carbon fiber. In order to ensure that the fiber has a mild shrinkage when most of the gases are eliminated, Frank et al. suggests that the heating rate need to be well controlled during the early stage in carbonization so that the fiber structure will not be damaged [4].

Following by carbonization, another heating process called graphitization is sometimes conducted to further increase the carbon content and structural ordering of the carbon fiber. Graphitization is usually conducted at temperatures up to 3000 ℃, and more crystallites can form along the axis of carbon fiber [4]. The graphitized carbon fiber has improvement on its modulus, however its tensile strength is usually become lower. For industrial applications, the produced carbon fiber still needs to be sized to activate its surface, meanwhile improving its adhesion with resins [15]. Based on application needs, carbon fiber with different modulus can be produced, and various types of carbon fiber are available on markets [11].

1.1.2.2 Pitch and Rayon-based carbon fibers

As the other two precursors, pitch and rayon are also available in industry, yet with low market share. The PAN-based carbon fiber is mostly used for structural application, while the pitch or rayon-based carbon fiber are generally used for functional purposes due to their relatively low mechanical properties.

Similar with PAN-based carbon fiber, the process for producing carbon fiber from pitch includes spinning, stabilization, carbonization, and graphitization. The main difference is the chemical composition of the precursor. Pitch is a general name of any tarry substances that can be derived from petroleum, coal, asphalt, or other synthetic polymer wastes [4]. It is not pure and does not have specific compositions. Pitch is mainly composed of poly-

aromatics with methyl side chains as shown in Fig 1.1. The typical Mw of pitch is around 1000 g/mol, which has to be low enough so that it can be melt-spun under mild temperatures. Pitch based precursor has high carbon content and high aromatic structures resembling to the structure of carbon fiber. These are both advantages if the structure can be successfully maintained and delivered to following process. However, pitch is sensitive to temperature when spinning, and its rheological properties are inconstant, which will eventually influence its structure and alignment on molecular level [4]. There are isotropic pitch and anisotropic pitch (also named as mesophase pitch) available. The fiber from anisotropic pitch can be orientated along fiber direction during spinning and stretching. In the following process, the aligned poly-aromatics, named as disco nematic liquid crystals, can contribute to form a more directional graphite structure after converting into carbon fiber [16]. As a result, carbon fiber from anisotropic can achieve relatively high tensile strength.

Rayon based carbon fiber is derived from regenerated cellulose. Related researches have been largely investigated during 1950-1970s, but later the market is taken over by the more promising PAN based carbon fiber [4]. The structure of cellulose is shown in Fig. 1.1. The carbon content of cellulose is only about 44.4%, lower than that of PAN or pitch, therefore the yield of rayon-based carbon fiber is generally low. The rayon fiber usually contains impurities such as lignin or hemicellulose. Plus, the alignment of its fibril is discontinuous, and the structure is porous. As a result, the rayon derived carbon fiber only has tensile strength of 0.5-1.2 GPa and modulus of 40-100 GPa [17]. In addition, processing with rayon-based precursor is costly even though the raw material has low cost and large availability.

As abovementioned, currently the most suitable carbon fiber precursor is still PAN. Its high processing cost, petroleum-dependency, and environmental concerns encourage researchers to search for low-cost and renewable precursors.

1.2 Lignin

Fortunately, lignin is such a polymer with several advantages that can be used as carbon fiber precursor [18]. Lignin is the most abundant aromatic resources from nature and the second most available polymer next to cellulose [19]. It is present in most of the terrestrial plants with content varies from 10-40% and to lend rigidity to cell walls [20, 21]. Currently, lignin is a by-product mostly from pulp and paper industry, and the so-called "black liquor" which is the discarded lignin stream has long been underutilized [22]. Also, with the development of biorefinery industry, biorefinery lignin also becomes more available in recent years. According to the U.S. Energy Security and Independence Act of 2007, an estimate of 62 million biorefinery lignin will be produced by the year of 2022 [21]. Therefore, finding value-added applications for biorefinery lignin is of great importance. Lignin has aromatic structures and relatively high carbon content, which make them a good candidate for producing carbon-based materials. Lignin is also bio-degradable and renewable that is desired to maintain an environmentally friendly, sustainable and carbon-neutral community [19].

However, lignin does not have well-defined structures and properties. Its type can be much varied based on botanical species and extraction methods [20]. Lignin is composed of mainly three phenylpropanes units known as p-hydroxyphenyl (H), guaiacyl (G), and syringyl (S) as shown in Fig 1.3. These three units are inter-crosslinked via in-situ free radical polymerization to form a three dimensionally complex network. The interlink bonds mainly include α-O-4, β-O-4, β-β, β-1, β-5, 5-5, and 4-O-5 [23]. With different ratios of

H/G/S units, the plants can be classified into three categories, namely hardwood, softwood, and herbaceous species [24]. Hardwood lignin containing mostly S units is present in dicots plant, it is thereby less branched with both ortho positions on the phenolic ring occupied by methoxyls. Softwood lignin is present in gymnosperm plants (also known as evergreen) and composed of both S and G units, and it can be more branched and reactive than hardwood lignin upon heating. Herbaceous lignin is present in grass or crops, and it is composed of all three types of H, G, and S units. Since lignin is embedded with cellulose and hemi-cellulose, it is impossible to retain original lignin structure when extracting lignin from original resources. The extracted lignin is always deconstructed to some extent through the breaking of instable interlinking bonds such as β-O-4. The molecular weight of lignin can be varied from thousands to tens of thousands Dalton [20].

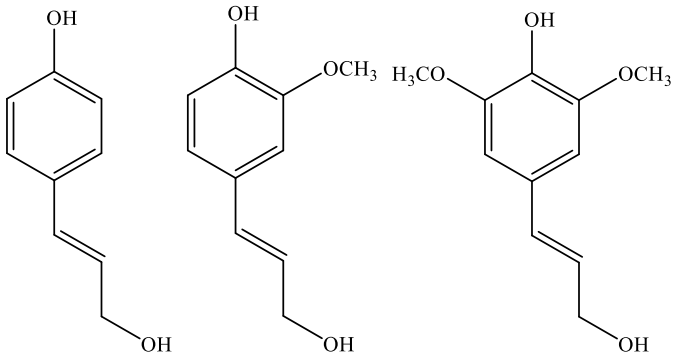

Figure 1.3 H (Left), G (Middle), and S (Right) units of lignin.

1.3 Current Lignin-based Carbon Fiber Research and Challenges

The earliest work using lignin as carbon fiber precursor can date back to 1960s. Over that time, hardwood kraft lignin, softwood kraft lignin, and alkali softwood lignin have been successfully converted into carbon fiber with tensile strength up to 0.785 GPa [25]. The lignin-based carbon fibers were commercially available for a short period of time. Since then, extensive research about lignin-based carbon fiber has been conducted in the following

decades. The reported work in general include 1) raw lignin with minor modification as precursor; 2) chemically modified lignin as precursor; 3) the mixture of lignin and other polymers as precursor.

1.3.1 Raw Lignin as Precursor

Due to its less complexity and low cost, melt-spinning is favorable in spinning fiber from precursors [26]. This will require the precursor to have a suitable melting point, also the melting point to be lower than its decomposition temperature. Plus, the precursor should be chemically stable at the spinning temperature, so that it will not cross-link which will lead to the inconsistency in fiber spinning. In terms of three types of lignin, only hardwood lignin is melt-spinning favorable due to the large presence of its S-type. Baker et al. [27] used an organic solvent purified, Kraft hardwood lignin (HWL-OP) with low content of impurities and high Mw. Upon purified by organic solvent, it was found the HWL-OP had much lower melting point of 128 ℃ compared with HWL with melting point of 202 ℃. The glass transition temperature also dropped to 88 ℃, making the stabilization of HWL-OP at extremely low rate of 0.01 ℃/min to avoid fiber fusing. Finally, the produced carbon fiber only has moderate mechanical properties with tensile strength of 0.52 GPa and modulus of 28.6 GPa. In another work, Kadla et al. [28] used organosolv Alcell and Kraft hardwood lignin (HWKL) to produce carbon fibers. They found the T_g of Alcell and HWKL was 68.2 and 83.3 ℃, respectively, and they could be melt-spun at 138-165 ℃, and 195-228 ℃, respectively. The corresponding mechanical properties of both lignin were low at around 0.4 GPa. Although the T_g of lignin used in their study was lower than that used for the HWL-OP (88 ℃), the heating rates during stabilization was reported at a faster speed (0.2 ℃/min). Kubo et al. [29] also used a hardwood Kraft lignin to produce carbon fiber. The lignin with a T_g of 110 ℃ could be melt-spun at 195-228 ℃. The fiber was stabilized at 0.2 ℃/min and

the resulting carbon fiber had a tensile strength of 0.605 GPa. In summary, although hardwood lignin is believed to be the most readily melt-spinnable precursor, its mechanical properties present as the major bottleneck. In a later work, however, Baker et al. [30] reported that the mechanical properties of carbon fiber processed from a highly purified and pretreated OP86 hardwood lignin could reach up to 1.07 GPa. Although this represents the highest value for lignin-based carbon fiber to date, it is still far lower than the minimum requirement of 1.72 GPa suggested by the Department of Energy for auto-mobile grade carbon fiber [18]. In a more recent work, Li et al. fractionated lignin into water soluble and insoluble fractions [31]. The two fractions were different in Mw, functional groups, and inter-linkages, and were both enhanced for their spinnability. In particular, it was reported that the water insoluble fraction rendered the produced carbon fiber with improved turbostratic carbon structures. Yet, only modulus of carbon fiber was reported and compared with PAN-based carbon fiber in their study.

Raw softwood is less directly used to produce carbon fiber mainly owing to its thermal instability. As mentioned above, softwood lignin contains G-type lignin, making it more reactive under elevated temperature, therefore causing cross-linking and inconsistency during fiber spinning. To improve the melt-spinnability of softwood lignin, Kubo et al. used acetic acid to extract the low Mw fraction (SAL-L) of a softwood lignin (SAL) [32]. The SAL-L had much lower Mw, glass transition temperate and softening temperature. The SA L-L was melt-spun to fiber with tensile strength of 0.0264 GPa. Successful carbonization was also conducted on SAL-L as-spun fiber, however no tensile strength of carbon fiber was reported. On the carbon fiber surface, pores were observed that could be detrimental to

mechanical property. From this point, the spinnability was improved at the expense of lowering the mechanical property of carbon fiber.

Herbaceous lignin is seldom investigated as precursors for carbon fiber production. It is considered as a new type of lignin mainly produced from recent biorefineries. Compared to wood lignin, it contains more G and H type units, thus it is easier to condense and cause thermal instability. Hosseinaei et al. [33] recently reported the spinning of switchgrass lignin was difficult. The so-called S-LS and S-HS switchgrass lignin obtained from different degrees of organosolv fractionation were both tested for melt-spinning. It was found that the lignins were difficult to continuously spinning due to the brittleness of the spun-fiber and foaming of the lignin. Nevertheless, some fiber filaments were still collected and converted into carbon fiber. The tensile strengths for both were less than 0.4 GPa, which was a relatively low value compared to hardwood and softwood lignin-based carbon fibers. Herbaceous lignin contains long aliphatic side chains in its structure, which will be difficult to aromatize and thus release volatiles during conversion to carbon fiber. On the other hand, converting switchgrass lignin into carbon fiber may require less time for stabilization, which is considered as an advantage. This is owing to the presence of H and G units and their preference for cross-linking.

In summary, multiple types of lignin mainly from pulp and paper industry have been tested for producing carbon fiber. Solutions such as increasing lignin's stability, reducing lignin's dispersity, purifying lignin's content, fractionating lignin, could be effective in promoting lignin fiber's processability and quality. However, the overall tensile strength of lignin-based carbon fiber is well below 1 GPa. Since lignin's intrinsic structure was not modified in these approaches, lignin will gradually form into amorphous carbon instead of

well-aligned and crystallized carbon. As a result, it was difficult to produce high quality carbon fiber from the lignins without structural modification.

1.3.2 Chemical Modifications of Lignin and/or Blending with Polymers

To alter the properties of the raw lignin, chemical modifications have been applied to improve the melt spinnability of lignin. Esterification, especially acetylation, has been mostly used to capture the hydroxyls on lignin which are most reactive under elevated temperatures. Also, acetylation could improve the molecular chain movement by decreasing the hydrogen bonding between hydroxyls. Zhang et al. [34] applied acetylation on a non-softening softwood lignin, and reported the occurrence of softening temperature between 156-167 ℃ upon acetylation. Ding et al. [35] applied butylation on a corn stover lignin and found that the modified lignin had reduced molecular interactions, so that uniform electrospinning fiber could be produced without beads on the nanofiber filament. Gordobil et al. [36] used both acetylated alkali lignin and orgasolv lignin as fillers in polylactic acid composites, and found only after acetylation could disperse the lignin evenly in the composites, also the corresponding tensile strength of the composite film was enhanced. However, the contribution of acetylation is mainly on its enhancement of lignin melt processability. The detrimental effect of acetylation arises from its reduced reactivity. After acetylation, the as-spun fiber became less reactive, thus it becomes difficult to cross-link during stabilization step. As a result, even though acetylation makes more diverse types of lignin suitable as melt-spinning precursor, it does not modify the molecular orientation of lignin, thus it has limited contribution on improving the quality of lignin-based carbon fiber.

Lignin was also treated with iodine to improve its thermal stability. Dai et al. [37] reported that the iodine-treated lignin had a denser structure and increased T_g. Correspondingly, the resulting electro-spun carbon fiber had increased tensile strength of

0.089 GPa. In another work, Ma et al. liquified wood with phenol using H_3PO_4 as the catalyst and further melt-spun the mixture[38]. The fiber was then cured in an HCL/HCHO solution, followed by carbonization at 1000 ℃. The resulting carbon fiber had tensile strength up to 1.7 GPa. However, the economic aspect of the process is questionable due to the cost of a large amount of phenol used. Hydrogenation was also applied to enhance the exploded lignin's melt-spinnability as reported by Kubo's et al. [39]. The hydrogenated lignin had improved flowability, and the resulting carbon fiber had a tensile strength of 0.66 GPa.

Blends of lignin and polymers are also commonly used in lignin carbon fiber production. The processability of fiber spinning can be improved with addition of certain polymers in lignin. Also, the molecular orientation of precursor may be improved by mixing lignin with orientated polymers. In previous work, typical polymers such as polyacrylonitrile (PAN) [8], polypropane (PP) [40], polylactic acid (PLA) [41], polyethylene terephthalate (PET) [29], and polyethylene oxide (PEO) [28] have been mixed with lignin to improve the spinnability. PAN is the commercialized precursor of carbon fiber that can yield high quality carbon fiber, but it comes with high costs. Mixing PAN with lignin can partly reduce the precursor cost. However, the tradeoff is lowered carbon fiber quality. Most recently, Jin et al. [8] investigated wet-spinning of lignin-PAN blends with the lignin content up to 50%, and obtained carbon fibers with diameter of ~7 μm. In general, it was found that the tensile strength of PAN-lignin carbon fibers was lower compared to pure PAN carbon fibers. The modulus of the carbon fiber also decreased with the increase of lignin content. The lack of chemical bonding between PAN and lignin is likely the reason for reduced mechanical properties. Kubo et al. [29] used lignin and PP mixture as precursor to produce carbon fiber. Unfortunately, although the melting behavior could be improved by PP addition, the

mechanical properties of lignin-PP based carbon fiber dropped dramatically with increasing amount of PP in the precursor. This is due to the lack of intermolecular interaction between lignin and PP. Also, since PP does not have fixed carbon, it will be decomposed to gases and leave the fiber matrix upon carbonization. The pores on the fibers created by the escaping gas products will ultimately lead to a low quality of carbon fiber. In the same study, PET was also mixed with lignin. Interestingly, they found PET to mix well with lignin. The T_g of lignin-PET was also enhanced, which is beneficial to stabilization. In the study, the quality of the lignin-PET carbon fiber also showed increase. Wang et al. [41] mixed PLA with lignin to evaluate its spinnability and resulting carbon fiber quality. They claimed lignin hydroxyls could form hydrogen-bonding with PLA, thus improving the spinnability of lignin. However, the produced carbon fiber had voids and low quality compared with lignin carbon fibers probably due to the same reason found for the lignin-PP blends. In the study conducted by Kadla et al. [28], PEO was used as a plasticizer to facilitate the melt-spinning of lignin. The authors found that only a maximum 5 wt% of PEO could be used, otherwise lignin-PEO fibers could fuse during stabilization. Since most of the synthetic polymers have poor ability to cross-link, their negative effect on stabilization process is another issue that needs to be noticed. It was also noted that the lignin-PEO carbon fiber did not have evidently increased mechanical properties compared to the counter part of lignin-based carbon fiber.

Lignin isolated from different biomass species were also mixed with each other to produce melt-spinnable precursors. Norberg et al. reported that the melt-spinning is possible for their softwood lignin permeate (SKLP) [9]. They further reported that mixing SKLP with hardwood lignin (HKLP) as softening agent could enhance the melt-spinnability of the SKLP. The resulting carbon fiber appeared to have neat and smooth surface and cross-

section. However, no mechanical properties were reported in their work. This work suggested that hardwood and softwood lignin can be mixed together to overcome the drawbacks of each, i.e. poor spinnability of softwood lignin and slow stabilization rates of hardwood lignin. Specifically, hardwood lignin has relatively low T_g, is less branched, and less reactive. Also, due to the presence of mainly S type lignin, hardwood lignin is favored in melt-spinning process. However, its low reactivity also makes the fiber difficult to be stabilized. On the other hand, softwood lignin is easier to be stabilized yet its melt processability is poor. In another work, Hosseinaei et al. used different ratios of herbaceous lignin (switch grass, SG) and hardwood lignin (yellow polar, YP) to make lignin-based carbon fiber [42]. They confirmed that the two lignins formed a miscible blend, and could be successfully melt-spun into fiber. They also claimed that the spinnability was improved by YP lignin, and the stabilization was enhanced by SG lignin. Finally, highest tensile strength of 0.747 GPa was reported from the 85% YP:15% SG lignin-based carbon fiber.

Overall, lignin processability could be enhanced by the addition of various types of co-polymers. Yet, the major contribution was promoting the melt processability of the precursor. The modification to lignin structures is likely limited. Also, polymers as plasticizers also led to low product yields and porous carbon fiber.

1.4 Objectives and Dissertation Organization

Lignin from pulp and paper industry has been investigated extensively for producing carbon fiber. Although great efforts have been made, the overall quality of lignin-based carbon fiber are still unsatisfactory. One of the critical disadvantages of lignin over PAN or synthetic polymers is that lignin does not have well-defined structure. Instead, it is a randomly cross-linked polymer that intrinsically lack of molecular orientation. As a result, the lignin-based carbon fiber is amorphous with poor mechanical properties. It is also noted

that the biorefinery lignin has been explored less frequently. Carbon fiber as a value-added product from biorefinery lignin could greatly promote economic feasibility of biorefineries.

In the first part of this dissertation, production of carbon fiber from a biorefinery corn stover lignin through melt-spinning is investigated. In the rest of parts of this dissertation, new approaches to produce carbon fiber from structurally modified lignin are explored. Lignin is first depolymerized to crude bio-oil containing various phenolic monomers and oligomers. The bio-oil, namely pyrolytic lignin (PL), is used as a starting material and repolymerized to provide new lignin-based precursors with modified structures for subsequence melt-spinning processes. Compared to raw lignin, PL has several features, such as higher reactivity, condensed structure, reduced inter crosslinking, flowability, smaller molecule sizes, and low dispersity. These features will render pyrolytic lignin a suitable medium to re-polymerize into different lignin-based precursors and eventually carbon fiber with improved properties.

Specifically, in Chapter 2, corn stover lignin is subjected to a two-step pretreatment, followed by melt-spinning to converted into carbon fiber. Through this work, the carbon fiber production from ash-rich biorefinery lignin is examined. In Chapter 3, PL is re-polymerized with the presence of acid catalyst to produce a PL-based precursor, and subsequently processed into carbon fiber. The work aims to evaluate the properties and processability of PL-based materials. In Chapter 4, PL and polyethylene terephthalate (PET) are co-treated and the precursor is subsequently processed into carbon fiber. The goal is to improve molecular orientation of the precursor by reacting PL molecules and the linear PET molecules. The effect of the improved molecular orientation of the precursor on the resulting carbon fiber is further investigated. In Chapter 5, PL is first methacrylated and then

synthesized into a methacrylate polymer via controlled radical polymerization technique. The resulting polymers are characterized and their suitability as an ideal precursor of carbon fiber is evaluated. Finally, in Chapter 6, research summary is given, and a future perspective of the research direction is discussed.

1.5 References

1. Frank, E., F. Hermanutz, and M.R. Buchmeiser, *Carbon fibers: precursors, manufacturing, and properties.* Macromolecular materials and engineering, 2012. **297**(6): p. 493-501.
2. Liu, Y. and S. Kumar, *Recent progress in fabrication, structure, and properties of carbon fibers.* Polymer Reviews, 2012. **52**(3): p. 234-258.
3. Das, S., et al., *Global Carbon Fiber Composites. Supply Chain Competitiveness Analysis*. 2016, Oak Ridge National Laboratory (ORNL), Oak Ridge, TN (United States).
4. Frank, E., et al., *Carbon fibers: precursor systems, processing, structure, and properties.* Angewandte Chemie International Edition, 2014. **53**(21): p. 5262-5298.
5. Goulis, P., et al., *Thermal Treatment of Melt-Spun Fibers Based on High Density PolyEthylene and Lignin.* C, 2017. **3**(4): p. 35.
6. Chung, D., *Carbon Fiber Composites Butterworth*. 1994, Heinemann, Newton, MA.
7. Zhang, M. and A.A. Ogale, *Carbon fibers from dry-spinning of acetylated softwood kraft lignin.* Carbon, 2014. **69**: p. 626-629.
8. Jin, J. and A.A. Ogale, *Carbon fibers derived from wet-spinning of equi-component lignin/polyacrylonitrile blends.* Journal of Applied Polymer Science, 2018. **135**(8): p. 45903.
9. Nordström, Y., et al., *A new softening agent for melt spinning of softwood kraft lignin.* Journal of Applied Polymer Science, 2013. **129**(3): p. 1274-1279.
10. Yu, M., et al., *Process of melt-spinning polyacrylonitrile fiber*. 2014, Google Patents.
11. Huang, X., *Fabrication and properties of carbon fibers.* Materials, 2009. **2**(4): p. 2369-2403.
12. Zhang, M., *Carbon Fibers Derived from Dry-Spinning of Modified Lignin Precursors.* Carbon Fibers Derived from Dry-Spinning of Modified Lignin Precursors. Ph.D. Thesis, Clemson University, Clemson, SC, May, 2016.
13. Bonart, R., *Synthesefasern: Grundlagen, Technologie, Verarbeitung und Anwendung*. 1981: Verlag Chemie.
14. Morgan, P., *Carbon fibers and their composites*. 2005: CRC press.
15. Meek, N., et al., *Synthesis and characterization of lignin carbon fiber and composites.* Composites Science and Technology, 2016. **137**: p. 60-68.
16. Zimmer, J. and J. White, *Disclination structures in the carbonaceous mesophase*, in *Advances in liquid crystals*. 1982, Elsevier. p. 157-213.
17. Dumanlı, A.G. and A.H. Windle, *Carbon fibres from cellulosic precursors: a review.* Journal of Materials Science, 2012. **47**(10): p. 4236-4250.

18. Baker, D.A. and T.G. Rials, *Recent advances in low-cost carbon fiber manufacture from lignin.* Journal of Applied Polymer Science, 2013. **130**(2): p. 713-728.
19. Thakur, V.K., et al., *Progress in green polymer composites from lignin for multifunctional applications: a review.* ACS Sustainable Chemistry & Engineering, 2014. **2**(5): p. 1072-1092.
20. Kai, D., et al., *Towards lignin-based functional materials in a sustainable world.* Green Chemistry, 2016. **18**(5): p. 1175-1200.
21. Ragauskas, A.J., et al., *Lignin valorization: improving lignin processing in the biorefinery.* Science, 2014. **344**(6185): p. 1246843.
22. Azadi, P., et al., *Liquid fuels, hydrogen and chemicals from lignin: A critical review.* Renewable and Sustainable Energy Reviews, 2013. **21**: p. 506-523.
23. Dorrestijn, E., et al., *The occurrence and reactivity of phenoxyl linkages in lignin and low rank coal.* Journal of Analytical and Applied Pyrolysis, 2000. **54**(1-2): p. 153-192.
24. Wang, S., et al., *Lignocellulosic biomass pyrolysis mechanism: a state-of-the-art review.* Progress in Energy and Combustion Science, 2017. **62**: p. 33-86.
25. Otani, S., et al., *Method for producing carbonized lignin fiber*. 1969, Google Patents.
26. Steudle, L.M., et al., *Carbon fibers prepared from melt spun peracylated softwood lignin: an integrated approach.* Macromolecular Materials and Engineering, 2017. **302**(4).
27. Baker, D.A., N.C. Gallego, and F.S. Baker, *On the characterization and spinning of an organic-purified lignin toward the manufacture of low-cost carbon fiber.* Journal of Applied Polymer Science, 2012. **124**(1): p. 227-234.
28. Kadla, J., et al., *Lignin-based carbon fibers for composite fiber applications.* Carbon, 2002. **40**(15): p. 2913-2920.
29. Kubo, S. and J. Kadla, *Lignin-based carbon fibers: Effect of synthetic polymer blending on fiber properties.* Journal of Polymers and the Environment, 2005. **13**(2): p. 97-105.
30. Baker, F., D. Baker, and N. Gallego, *Carbon fibre from lignin.* Proceeding, Carbon, 2010: p. 11-16.
31. Li, Q., et al., *Quality carbon fibers from fractionated lignin.* Green Chemistry, 2017. **19**(7): p. 1628-1634.
32. Kubo, S., Y. Uraki, and Y. Sano, *Preparation of carbon fibers from softwood lignin by atmospheric acetic acid pulping.* Carbon, 1998. **36**(7-8): p. 1119-1124.
33. Hosseinaei, O., et al., *Role of Physicochemical Structure of Organosolv Hardwood and Herbaceous Lignins on Carbon Fiber Performance.* Acs Sustainable Chemistry & Engineering, 2016. **4**(10): p. 5785-5798.
34. Zhang, M. and A.A. Ogale, *Carbon fibers derived from acetylated softwood kraft lignin*, in *Polymer Precursor-Derived Carbon*. 2014, ACS Publications. p. 137-152.
35. Ding, R., et al., *Processing and characterization of low-cost electrospun carbon fibers from organosolv lignin/polyacrylonitrile blends.* Carbon, 2016. **100**: p. 126-136.
36. Gordobil, O., et al., *Physicochemical properties of PLA lignin blends.* Polymer Degradation and Stability, 2014. **108**: p. 330-338.
37. Dai, Z., et al., *High-strength lignin-based carbon fibers via a low-energy method.* RSC Advances, 2018. **8**(3): p. 1218-1224.

38. Xiaojun, M. and Z. Guangjie, *Preparation of carbon fibers from liquefied wood.* Wood science and technology, 2010. **44**(1): p. 3-11.
39. Sudo, K. and K. Shimizu, *A new carbon fiber from lignin.* Journal of applied polymer science, 1992. **44**(1): p. 127-134.
40. Kadla, J.F. and S. Kubo, *Lignin-based polymer blends: analysis of intermolecular interactions in lignin–synthetic polymer blends.* Composites Part A: Applied Science and Manufacturing, 2004. **35**(3): p. 395-400.
41. Wang, S., et al., *Low cost carbon fibers from bio-renewable lignin/poly (lactic acid)(PLA) blends.* Composites Science and Technology, 2015. **119**: p. 20-25.
42. Hosseinaei, O., et al., *Improving processing and performance of pure lignin carbon fibers through hardwood and herbaceous lignin blends.* International journal of molecular sciences, 2017. **18**(7): p. 1410.

CHAPTER 2. POTENTIAL OF PRODUCING CARBON FIBER FROM BIOREFINERY CORN STOVER LIGNIN WITH HIGH ASH CONTENT

(A paper published in *Journal of Applied Polymer Science*)

ABSTRACT

The possibility of producing carbon fiber from an industrial corn stover lignin was investigated in the present study. As-received, high-ash containing lignin was subjected to methanol fractionation, acetylation, and thermal treatment prior to melt spinning. The pretreated lignin precursors were characterized for their physiochemical and thermal properties. Methanol fractionation removed most of the impurities in raw lignin and also selectively removed the molecules with high melting points. However, methanol fractionation or thermal pretreatment could not render melt-spinnable precursors. The precursors were highly viscous and decomposed easily at low temperatures, attributed to the presence of H, G phenolic units and abundant coumarate and ferulate groups in herbaceous lignin. A two-step acetylation of methanol fractionated lignin greatly improved the mobility of lignin, while enhancing the thermal stability of the precursor during melt-spinning. FTIR and 2D-NMR analysis showed that the contents of phenolic and aliphatic hydroxyls, as well as the hydroxycinnamates, decreased in the acetylated precursors. The optimum precursor was a partially acetylated lignin with a glass transition temperature of 85 °C. Upon oxidative stabilization and carbonization, the carbon fibers with an average tensile strength of 0.454 GPa and modulus of 62 GPa were obtained. The Raman spectrometry showed the I_D/I_G ratio of the fiber to be 2.53. Overall, this study explored the potential use of the popular biorefinery-residue lignin for general-grade carbon fibers.

Key words: biopolymers and renewable polymers; fibers; mechanical properties; thermal properties

2.1. Introduction

Carbon fiber is a corrosion resistant material with many potential applications because of its high ratio of tensile strength to density along with its unique thermal and electrical properties [1, 2]. Despite the advantages, carbon fiber is currently used in limited areas due to the high price of polyacrylonitrile (PAN), which accounts for more than 50% of the total production cost of carbon fiber [3-5]. PAN is also derived from petroleum and emits hazardous gas during carbon fiber manufacturing. Thus, finding alternative precursors of carbon fiber has been of great interest for decades [6]. Among potential alternatives, lignin has received significant attention because it is a renewable biopolymer available in large quantities at low cost [5, 7-12]. Similar to PAN, lignin can be spun into fibers followed by oxidative stabilization and carbonization to produce carbon fibers with a turbostratic carbon structure [6]. Compared to PAN, lignin could provide a higher carbon fiber yield because of its relatively high carbon content. The partly-oxidized lignin molecules also potentially reduce the time required for stabilizing the spun fiber of lignin. The ability to melt-spin lignin also provides cost effectiveness, compared to wet-spinning of PAN.

To date, woody biomass-derived lignins produced from the pulping process have been extensively studied for carbon fiber processing. Previous studies showed that the lignin structure has a significant implication in carbon fiber processing [6, 13]. Lignin is an amorphous aromatic polymer and physiochemical and thermal properties of lignin highly depend on the biomass origin and lignin isolation method [14]. Although lignin in general is biosynthesized from three main units, which are p-hydroxyphenyl (H), guaiacyl (G), and syringyl (S) units, the ratios of H, G and S units vary by biomass species [15]. S unit is dominant in hardwood lignin; thus hardwood lignin is chemically stable and less likely to crosslink when it is thermally processed. Accordingly, hardwood lignin has a moderate glass

transition temperature (T_g) and can be melt-spun at ease [16]. However, as-spun fiber of hardwood lignin tends to fuse during stabilization due to its low ability to develop oxidative crosslinking. Unlike hardwood lignin, G unit is the major unit of softwood lignin. Due to its imbalanced aromatic ring structure in G unit, softwood lignin has a strong tendency to develop crosslinking. Thus, softwood lignin is difficult to spin due to its high T_g and low molecular mobility. On the other hand, the crosslinking of softwood lignin fiber promotes solidification of the fiber during stabilization [13, 17]. In the previous studies, lignin was pretreated or chemically modified to improve the processibility of the precursor and the quality of the resulting carbon fibers. For example, Baker et a [12]. fractionated a hardwood kraft lignin in an organic solvent followed by thermal pretreatment to obtain the precursor with more defined properties. Zhang et al. [8] spun fiber from a mixture of an acetylated softwood kraft lignin and acetone. Softwood and hardwood lignin were also mixed with other co-polymers, such as PEO, PET, PP, PVA and PAN to improve the spinnability of the precursors, as well as mechanical properties of the resulting carbon fibers [18-21]. Despite these efforts, the quality of lignin-based carbon fiber was found to be much lower than PAN-based carbon fiber. Baker et al. produced a carbon fiber with a tensile strength of 1.07 GPa from an experimental hardwood lignin and so far it is the lignin-based carbon fiber with highest quality [6]. Other lignin-based carbon fibers mostly have lower tensile strengths in the range of 0.15 to 0.7 GPa [6, 22]. The lack of well-defined molecular orientation in lignin is mainly responsible for the low mechanical properties of lignin-based carbon fiber compared to PAN-based carbon fiber. Although replacing PAN based carbon fiber for structural applications is currently challenging, as a low cost and greener product, lignin-based carbon fiber could still be considered in many general applications where materials with moderately high mechanical properties, low density,

high temperature tolerance, low thermal expansion and thermal conductivity are of interest. For instance, it has been reported that lignin-based carbon fiber is used to produce a high-temperature tolerating insulation material [17].

Compared to woody biomass-derived lignin, herbaceous lignin was seldom used in carbon fiber production. Herbaceous lignin is available from cellulosic biorefineries as a byproduct when agricultural residues and energy crops are used to produce biofuels and chemicals. Herbaceous biomass are popular feedstocks in biorefineries because they can be harvested annually and are the largest biomass sources available in many regions [23]. As biorefineries are rapidly expanding, producing value-added products from herbaceous lignin became an urgent need in order to maintain the economic sustainability in many biorefineries. Accordingly, exploring herbaceous lignin-based carbon fiber could provide a potential opportunity for value-added product from lignin. Herbaceous lignin consists of both H and G units in relatively higher contents, thus showing that thermal and physiochemical properties differ from wood-based lignin [5]. Hosseinaei et al. produced carbon fiber from switchgrass lignin recently [5] and it is currently the only published study about carbon fiber from herbaceous lignin. In their study, an experimental organosolv lignin with high purity was used as the starting material.

In this study, an industrial corn stover lignin was used as the raw material to investigate the possibility of producing carbon fiber from a popular herbaceous lignin. Corn stover is the most abundant cellulosic-agricultural residue in the United States [24] and currently being used as the biomass feedstock by several biorefineries in the country. To produce a melt-spinnable precursor, as-received lignin was subjected to solvent fraction, acetylation and thermal

treatment. The pretreated precursors were characterized and the resulting carbon fiber was evaluated.

2.2. Materials and Methods

2.2.1. Materials

Corn stover organosolv lignin was provided by Archer Daniels Midland (ADM) Company. The lignin was isolated from corn stover using an acetosolv extraction process in the plant. Methanol, hydrochloride acid (HCl), acetic anhydride (AA), and tetrahydrofuran (THF) used in this study were purchased from Fisher Scientific Co.

2.2.2. Lignin Pretreatment

For methanol fractionation, 50 g of raw lignin was dissolved in 250 ml methanol and stirred with a magnetic rod for 15 min at room temperature. After stirring, the solution was filtered twice using a 0.7 μm filter paper followed by a 0.45 μm filter paper to remove insoluble lignin particles and impurities. The methanol soluble lignin was then placed in a vacuum oven at 40 ℃ overnight to evaporate methanol. The resulting methanol fractionated lignin is denoted as “ML” in this study.

For the acid-washing of lignin, raw lignin was washed with a 0.1 N HCl acid solution at a ratio of 10 ml of the acid solution to 1 g of the lignin and stirred for 30 min. The procedure was repeated three times and the filtered solid lignin was rinsed with deionized water until the rinsed water became neutral.

Acetylation of the methanol fractionated lignin was performed in two steps. In the first step, different concentrations of acetic anhydride were added to ML and kept at 85 ℃ for 2 h. In the second step, the acetylated samples were subsequently heated at 140 ℃ for an additional 0.5 h under vacuum ventilation. During the entire process, the mixtures were stirred at 150 rpm. After the two-stage treatments, the acetylated precursors were pelletized and stored at

room temperature. Different levels of acetylation were performed at 0.5, 0.75, 1, 2 and 3 ml g^{-1} of ML, respectively. The resulting precursors are denoted as “0.5AT-ML”, “0.75AT-ML”, “1AT-ML”, “2AT-ML” and “3AT-ML”, respectively. ML was also treated under identical temperatures and reaction times in the absence of acetic anhydride, and the thermally pretreated precursor is denoted as “0AT-ML”.

2.2.3. Fiber Spinning and Processing

Raw lignin and pretreated lignins were extruded using a twin-screw extruder (DACA Instruments, Santa Barbara, CA). The precursors were fed into the extruder preheated to 130 ℃ and circulated within the extruder for 5 min prior to drawing the fibers. The drawn fiber was wound on a roller (DSM, Geleen, Netherlands). During the spinning process, the temperature and rotation speed of the twin-screw, as well as the winding speed at the roller, were adjusted for different types of precursors. Several hundred meters of the fiber were collected during each test.

The as-spun fibers were mounted on a metal rack inside a muffle furnace and subjected to oxidative stabilization at a heating rate of 0.1 ℃ min^{-1} from room temperature up to 250 ℃, and then held at the same temperature for 1 h. The as-spun fiber of 0.75AT-ML was also subjected to a step-wise stabilization by dwelling the fiber at 100 ℃, 120 ℃, 140 ℃, 160 ℃, 180 ℃, and 200 ℃ for 6 h, respectively. The stabilized fibers were placed on a porcelain crucible and carbonized in a tubular furnace. During carbonization, the stabilized fiber was heated from room temperature to 1000 ℃ at 3 ℃ min^{-1} and then held isothermally for 1 h. Argon was used to maintain an inert environment inside the tube furnace.

2.2.4. Characterizations

Proximate analyses of lignin precursors were performed in thermal gravimetric analyzer (TGA/DSC 1 STARe system, Mettler Toledo) using nitrogen with a flow rate of 100

ml min^{-1}. Approximately 30 mg of lignin samples were heated from room temperature to 105 °C at 10 °C min^{-1} and then held at constant temperature for 40 min to remove moisture. The samples were further heated to 900 °C at a heating rate of 10 °C min^{-1} and then held for 20 min. Finally, air was introduced to combust the solid residue. Thermal stability of the samples was also evaluated using TGA. Approximately 30 mg of each sample was heated under a nitrogen environment from room temperature to 900 °C with a heating rate of 10 °C min^{-1}.

Ultimate analysis of the sample was conducted using an elemental analyzer (Vario Micro Cube, Elementar, Germany). Carbon, hydrogen, nitrogen and sulfur contents were measured and oxygen content was determined by the difference. Each test was triplicated and the average results were reported.

Gel permeation chromatography (GPC) analysis was conducted using Dionex Ultimate 3000 series high performance liquid chromatography (HPLC) equipped with a Shodex Refractive Index (RI) and Diode Array Detectors (DAD). Two GPC columns (3 µm, 100 Å, 300×7.5 mm; PLgel, Agilent, p/n PL1110-6320) were calibrated with six monodispersed polystyrene standards ranging from 162 g mol^{-1} to 38640 g mol^{-1}. Tetrahydrofuran was used as the solvent for samples and the eluent in the columns.

Fourier Transform Infrared (FTIR) analysis was conducted using a Thermo Scientific Nicolet iS10 (Thermo Fisher Scientific Inc., Waltham, MA) equipped with a Smart iTR accessory. The wave numbers of the FTIR analysis ranged from 750 cm^{-1} to 4000 cm^{-1} and each sample was scanned 32 times at a resolution of 4 cm^{-1} and interval of 1 cm^{-1}. All FTIR spectra were normalized at 1510 cm^{-1} (aromatic-skeleton vibration) for comparison.

Glass transition temperature (T_g) was determined using a differential scanning calorimeter (DSC, Q2000, TA instruments). Each sample was first rapidly heated to 200 °C

and cooled to 25 °C to eliminate thermal history, and then reheated to 200 °C at a heating rate of 10 °C min^{-1}. Nitrogen with a flow rate of 50 ml min^{-1} was used as the purge gas. The midpoint T_g of the precursor was determined using a TA software.

Mechanical properties of carbon fiber were determined according to ASTM standard (ASTM C1557-03) using a Discovery hybrid rheometer (DHR-2, TA Instruments) with dynamic mechanical analysis (DMA) clamps. The reported results are the average of 20 single fibers.

[$^{1}H^{13}C$] 2D-NMR heteronuclear single-quantum coherence (HSQC) spectroscopies of selected lignins were obtained at 25 °C on a Bruker Biospin Advance 600 MHz spectrometer incorporated with a 5 mm cryogenically cooled z-gradient probe using the Bruker pulse sequence "hsqcetg-psisp.2". A sample concentration of 100 mg lignin per 1 ml of solvent mixture was used. The solvent mixture was composed of dimethyl sulfoxide (DMSO)-d_6 and pyridine-d_5 (v/v: 4/1). The sample was prepared by dissolving 100 mg of sample in the solvent mixture and then holding it in the shaker for 20 min to enhance sample dissolution. Different structural compounds were identified by comparing the acquired 2D-NMR signals with the available literature [25-29].

Raman spectrum of carbon fiber was characterized using a confocal Raman system (Voyage, B&W Tek, Inc. and Olympus BX51). A 532nm Raman laser of 16mW is focused on the fiber with a 50 × lens. A 20 s integration time is used to obtain the spectrum and origin software was used to analyze the acquired Raman spectra with Gaussian-Lorentzian curve fitting.

2.3. Results and Discussion

2.3.1. Proximate and Ultimate Analysis of Raw Lignin and ML

The results of proximate and ultimate analyses for as-received raw lignin and the ML are given in Table 2.1. The ash content of as-received lignin is 6.07%, significantly higher than the ash contents in experimental organosolv lignins, which are usually below 0.2% [30]. The compositions of ash are mainly inorganic salts. Herbaceous biomass is known to contain significantly more impurities than woody biomass [31]. Lignin isolation method and the scale of lignin production also affect the impurity content in lignin. Lignin must be pretreated to remove the impurities prior to fiber spinning. Otherwise, the impurities remaining in carbon fiber could become the source of mechanical defects. The inorganics could also promote the volatile release and the formation of pores in the fibers due to their catalytic effect for thermal decomposition of lignin. Elemental analysis showed that the raw lignin also contained 2% of nitrogen and 0.72% of sulfur. Nitrogen and sulfur in the precursor may react with oxygen to form hazardous gases.

The raw lignin was initially subjected to acid washing with 0.1 N HCl. Since acidic solution dissolves many inorganic salts, acid washing is a common method to purify lignin [2]. However, the ash content after three rounds of washing was still high at 3.97%. It is likely that the raw lignin contained a high amount of acid-insoluble impurities. For example, silica and silicates are not soluble and calcium salts also have lower solubility in acidic solution [32]. Therefore, the raw lignin must be purified by alternative methods. Methanol fractionation was chosen because inorganic impurities have no or low solubility in alcohols [33]. After the fractionation, the ash content reduced to 0.27% in ML, indicating that most impurities remained in methanol-insoluble fraction. Upon the fractionation, ML had a tar-like texture.

The volatile and fixed carbon contents were both higher in ML in comparison to raw lignin, mainly due to the reduced ash content. Carbon content in ML was 58.66%, which is lower than 61.37% in the raw lignin. Hydrogen and oxygen contents, on the other hand, increased in ML. Considering oxygen atoms only appear at the side chains of aromatic rings, ML could have a less aromatically condensed structure than raw lignin. Nitrogen and sulfur contents were also reduced to 0.2% and 0.06% in ML. The ML was further subjected to acetylation and thermal pretreatment and the characterizations of different precursors are described below.

2.3.2. FTIR Analysis

FTIR spectra of raw lignin, ML and pretreated lignins are given in Figure 2.1. The peak appearing at 3250-3400 cm^{-1} is for phenolic and aliphatic hydroxyl groups, and the peak at 2842-3000 cm^{-1} is for C-H in methyl and methylene attached to aromatic rings. The relative peak ratio of 2842-3000 cm^{-1} to 3250-3400 cm^{-1} of the corn stover lignin was higher than the corresponding ratios of hardwood and softwood lignins in their respective FTIR spectra reported in literature [8, 16, 34, 35]. This is because herbaceous lignin contains higher amounts of side chain carbon than woody biomass-based lignin. Coumarate and ferulate groups, commonly found in herbaceous lignin contribute to the C-H peak [5, 36, 37]. In comparison to raw lignin, ML contains a higher amount of hydroxyl group, ascribing to selective extraction of lignin molecules by methanol. Saito et al. also reported that methanol-extracted lignin contains a higher content of hydroxyl group than original lignin [38]. The increased peak at 1709-1738 cm^{-1} corresponds to unconjugated ketones, carbonyls, and conjugated aldehydes and carboxylic acids groups. In herbaceous lignin, γ-positions of lignin side chains are naturally acetylated [23], which also contribute to this peak. In addition, the peak at 2842-3000 cm^{-1} for C-H, 1221-1230 cm^{-1} for C-C, C-O and C=O stretch, 1166 cm^{-1} for conjugated C=O

in ester group and 1030-1035 cm^{-1} for C-O deformation in primary alcohols and unconjugated C=O stretch also increased in ML. ML contains more oxygen containing groups, such as hydroxyl, carboxyl and carbonyl groups, which correspond to the higher oxygen content in ML compared to the raw lignin. Because the signals of the side chains became stronger relative to the peak intensity of the aromatic skeleton (1510 cm^{-1}), the result also confirms that ML has a less aromatically condensed structure than raw lignin. The higher amount of side chain could increase the mobility of lignin during fiber spinning.

Compared to ML, the intensities of the hydroxyl peak (at 3250-3400 cm^{-1}) and carbonyl peak (at 1709-1738 cm^{-1}) decreased in the thermally treated precursor (0AT-ML). The peak around 1030-1035cm^{-1} also decreased. The changes in the peak intensities indicate that lignin structure became condensed upon thermal treatment, and phenolic and aliphatic hydroxyl, and C-O groups participated in the condensation reactions.

The precursors, including 0.5AT-ML, 0.75AT-ML, 1AT-ML, 2AT-ML and 3AT-ML, are produced by the two-step acetylation. Acetylation is frequently used to treat lignin as it could improve solubility of lignin in organic solvents. Acetylation was also used to inhibit yellowing of paper caused by the formation of free radicals from lignin [39]. In terms of carbon fiber production, a softwood kraft lignin was acetylated to reduce the reactivity of hydroxyl groups and enhance the mobility of the lignin molecules [40]. Corn stover lignin has an increased amount of side chains in comparison to softwood lignin, and thus may have better precursor mobility. However, G and H units in corn stover lignin also promote crosslinking. The reactivity of H unit is higher than G unit because both of the ortho positions in P-hydroxylphenol become the potential sites for crosslinking. Crosslinking of lignin molecules during melt-spinning increases the precursor viscosity, causing a difficulty of fiber spinning.

Thus, capping the hydroxyl group by acetylation could improve melt-spinnablity of lignin [8]. The intensities of the peak at 3250-3400 cm^{-1} remarkably decreased in the acetylated precursors even with the lowest amount of acetic anhydride. On the other hand, the intensities of the peaks shown at 1702 cm^{-1} for C=O, 1360-1365 cm^{-1} for aliphatic C-H stretch in CH_3 and 1221-1230 cm^{-1} for C-C, C-O, and C=O increased with the increasing degree of acetylation. This confirms that phenolic and aliphatic hydroxyl groups are acetylated, and that carbonyl and methyl groups are newly added. The hydroxyl peak nearly disappeared at 3AT-ML, indicating that hydroxyl groups were almost completely acetylated under the reaction condition.

The degree of acetylation in the acetylated precursor was estimated based on the FTIR spectra using following equation [41] :

$$\text{Acetylation degree } (\theta) = 1 - \frac{[\text{H (OH)/H (aromatic)}]\text{after acetylation}}{[\text{H (OH)/H (aromatic)}]\text{before acetylation}}$$

where H (OH) is the peak intensity of hydroxyl stretching at approximately 3400 cm^{-1}, and H (aromatic) is the peak intensity of aromatic skeleton vibration at 1510 cm^{-1}. The results are plotted in Figure 2.2.

The value of θ is 0 in ML and 0.96 in 3AT-ML. Although θ monotonically increased with increasing concentrations of acetic anhydride, the increases were faster with lower concentrations of acetic anhydride. As the concentration of acetic anhydride further increased above 1 ml g^{-1} lignin, θ values increased slowly. This result is likely related to the variations in the reactivity of difference types of hydroxyl groups in lignin toward to acetylation. According to Pu and Ragauskas [39], phenolic OH is preferentially acetylated within a shorter reaction time. The preference of acetylation is in the order of phenolic OH > β-side chain OH > α-side chain OH.

Nevertheless, it should also be noted that fully acetylating lignin may not be desirable since the absence of hydroxyl groups could hinder the ability of the precursor fiber to crosslink during oxidative stabilization, thus forming fusible fiber. Previously, Zhang et al. also reported that a fully acetylated softwood lignin fiber could not be stabilized even with a heating rate as low as 0.01 °C min^{-1} [42]. Therefore, the softwood lignin was partially acetylated in their study so the acetylated fibers could be stabilized. In this study, processability of all the acetylated precursors was tested. Among the acetylated lignins, however, 0.75AT-ML with the θ value of 0.59 was characterized in greater detail in below to evaluate the effect of acetylation on the precursor properties and performance.

2.3.3. 2D-NMR Analysis

The 2D-NMR of ML, 0AT-ML and 0.75AT-ML are compared in Figure 2.3. Raw lignin was also tested, but the results are not shown. The signals of some lignin structures were not clearly observed with raw lignin, possibly affected by strong solvent peaks and the presence of high impurity content.

Aryl ether linkages, methoxyl group, S, G and H groups were detected in ML as they are characteristics in lignin. Ferulate, courmaric groups and tricin structures were also detected in ML lignin. Due to the abundancy of ferulate and courmaric groups, herbaceous lignin has overall longer aliphatic side chains than woody biomass-based lignin. Particularly, corn stover contains higher amounts of the hydroxycinnamate acids than many other herbaceous biomass plants [43]. These longer and linear side chain groups may provide some molecular linearity in the lignin, which is potentially beneficial for improving the quality of carbon fiber. However, the aliphatic side chain linkages are also susceptible for thermal decomposition, causing lignin instability. The signal of polysaccharide residue was also found in ML. The presence of

polysaccharide residue in lignin is undesired because polysaccharides can decompose during thermal processing to form pores in the fibers.

There were no significant changes in the signals of methoxyl and aryl ether linkage in 0AT-ML after ML was thermally treated. The temperature for thermal treatment was 140 °C, not high enough to cause β-O-4 cleavage or demethoxylation. Ferurate and courmate groups were also not affected by thermal treatment. Polysaccharides still remained in this precursor. In 0.75AT-ML, the signals for acetyl group (AcMe) newly appeared. Due to acetylation of phenolic and aliphatic hydroxyl groups, the signals of H and G groups, as well as aryl ether and tricin groups decreased. Compared to the corresponding signals in 0AT-ML, the signals of C_α and C_β in ferulate and p-coumarate groups decreased significantly after acetylation. This change was unexpected, since the acetylation of phenolic OH in the hydroxycinnamates should not shift the signals of C_α and C_β. The disappearance of the signals suggest that the unsaturated C_α=C_β is either cleaved or saturated during the acetylation. Considering acetic acid is the byproduct of acetylation and is known to catalyze repolymerization of lignin-derived bio-oil [44], it is likely that acetic acid catalyzed repolymerization reactions to saturate the C_α=C_β bonds. Attachment of other groups at C_α=C_β may result in a lignin with a slightly more branched structure. However, it also results in more stable lignin structure. It is also found that the signals of polysaccharide disappeared at 0.75AT-ML, probably because OH groups in polysaccharides were also acetylated.

2.3.4. GPC Analysis

The molecular weight distributions of selected lignins are given in Table 2.2. Weight average molecular weights (Mw) and polydispersity index (PDI) of raw lignin are 3263 Da and 2.91, which are typical for organic lignins [32]. The average Mw of ML was 1299 Da, significantly lower than raw lignin. The PDI also decreased to 1.89, indicating large Mw compounds were selectively removed along with the impurities by methanol fraction. Although the precursors with lower Mw usually have better mobility, low Mw lignin could also easily devolatilize at relatively low temperatures during spinning or cause fiber fusion during oxidative stabilization. For the reason, solvent fractionated lignins and other low Mw precursors were often thermally treated prior to fiber spinning in previous studies to increase its Mw [9].

The Mw of 0AT-ML was 3180 Da, indicating thermal treatment of ML caused repolymerization. The PDI of the precursor also increased to 3.19. The reactivity toward repolymerization varies by the functional groups in individual lignin molecules, which resulted in the thermally treated precursor with a broader molecule distribution. Ideally, carbon fiber precursor should have high Mw and low PDI for structural uniformity [6].

The average Mw and PDI of 0.75AT-ML were 3594 Da and 3.39, both slightly higher than the corresponding values of 0AT-ML. Although acetylation could suppress the crosslinking polymerization of the molecules, replacing phenolic and aliphatic hydroxyls in individual molecules by acetyl groups increases the Mw. Also, since 0.75AT-ML is a partially acetylated precursor (θ=0.59), the unacetylated free OH groups allow crosslinking during the thermal treatment catlyzed by acetic acid byproduct. The possibility of acetic acid catalyzed repolymerization of C=C bonds was discribed above.

2.3.5. Glass Transition Temperature

Glass transition temperatures (T_g) of different precursors are compared in Table 2.3. For fiber spinning, T_g of the precursor has to be low enough so the precursor can be melt before it decomposes. However, the T_g of precursor fiber also has to be high enough so the fiber can be stabilized during oxidation process without fusion or liquid droplet formation. Raw lignin has a T_g of 148 ºC, similar to that of a softwood kraft lignin previously reported [7], although the Mw of the corn stover lignin in this study is only about a half of the Mw of the softwood lignin in the referenced study. Baker et al. [6] previously indicated that T_g of lignin precursor relates to the ratio of G and S unit. The precursor with higher G to S ratio has higher T_g, because G unit is reactive for crosslinking whereas S unit is relatively stable. The corn stover lignin contains H unit in addition to G unit, thus leading to high T_g even though the Mw of the corn stover lignin was much lower. The impurities in the raw lignin also contribute to the increased T_g of lignin [45]. The T_g decreased to 93 ºC in ML, because low Mw molecules have better mobility in the same type of lignin. For example, Saito et al. reported that T_g of a softwood kraft lignin decreased from 153 ºC to 117 ºC after methanol extraction due to a decreased Mw [38]. After thermal treatment, T_g of corn stover lignin increased to 111 ºC at 0AT-ML. Repolymerization increased Mw and crosslinking among the molecules, which reduced the mobility of the precursor molecules. In comparison, the T_g of 0.75AT-ML was only 85 ºC despite the fact that the average Mw of the acetylated precursor was even higher than the Mw of 0AT-ML. This result confirms that the presence of hydroxyl groups in lignin greatly contributes to the intermolecular force and limits the mobility of molecules [5]. Replacing hydroxyl with acetyl groups has weakened the intermolecular forces and lowered the T_g of the lignin.

2.3.6. Thermal Stability

TGA curves of raw lignin, ML, 0AT-ML, and 0.75AT-ML are given in Figure 2.4 to compare thermal stability of different precursors. Decomposition temperatures (T_d) are the temperature corresponding to 5% mass losses in the samples and are also listed in Table 2.3. Thermal stability plays an important role in determining the spinning performance of precursor [46]. In general, a precursor should have high thermal stability at the spinning temperatures, so that the melt-spinning is not interrupted by the formation of bubbles. Bubbling and devolatilization during precursor spinning could create pores in the fiber and eventually lower the mechanical properties of the carbon fiber. The thermal pretreatment could increase the Mw of the precursor, thus improving thermal stability of the precursor during fiber processing [47]. However, the lignin with a high Mw and T_g may become difficult to melt spin and could also decompose before it melts. In the case of raw lignin, the mass loss started at a temperature below 100 ºC and T_d was 194 ºC. In addition to the evaporated moisture, the high content of inorganic impurities in raw lignin could have catalyzed thermal decomposition of lignin occurring at lower temperatures.

ML precursor also started to devolatilize at low temperatures and T_d decreased to 160 ºC due to its lower Mw. Since melt-spinning of lignin is usually conducted at a temperature range below 200 ºC (because aryl ether linkages in lignin start to cleave at temperatures above 200 ºC), the mass loss of the precursors at this temperature range could be indicative of undesired bubbling and volatile release during the melt-spinning process. For 0AT-ML, no mass loss was observed at temperatures below 150 ºC, showing an improved thermal stability after thermal pretreatment. However, further increasing the temperature reduced the stability of the precursor and T_d was recorded at 197 ºC. Previously, Sun et al. [48] investigated rheology of softwood lignin at different melting temperatures and indicated that

repolymerization is the main reaction at temperatures below 190 ºC and thermal decomposition becomes dominant at higher temperatures. Herbaceous lignin contains a higher amount of side chain than softwood lignin, and decomposition reaction preferentially occurs at lower temperatures. Ferulate and coumarate groups are still abundant in the thermally pretreated precursor and could contribute to the release volatiles. Decomposition of ferulate and courmarate produces CO_2 and vinyl phenols as the major products.

Compared to non-acetylated precursors, 0.75AT-ML had a remarkably better thermal stability. With this precursor, negligible mass loss was observed at temperature below 200 ºC and T_d also increased to 233 ºC. Thermal decomposition of acetylated lignin occurs at higher temperatures compared to non-acetylated sample because acetylation hinders the cleavage of aryl ether linkages and other weaker bonds [39]. In a previous study, it was suggested that hydroxycinnamate groups and aliphatic OH are the main causes of volatile release in switchgrass lignin [5]. Acetylation of phenolic OH on coumarate and ferulates and saturation of C_α=C_β, also likely increased thermal stability of the acetylated precursor.

The lignin with low T_g usually results in lower carbon fiber yield. However, it may not be the case with the acetylated precursor of corn stover. It was found that the amount of residue carbon at 900 ºC for 0.75AT-ML was higher than the carbon residues of ML and 0AT-ML. Although raw lignin produced similar amount of solid residue, it also includes inorganic ash. Higher residue carbon in acetylated lignin could be an indicator of a higher carbon fiber yield. The two-step acetylation increased thermal stability and carbonization of the precursor, which are both beneficial to carbon fiber processing.

2.3.7. Performance of Fiber Processing and Properties of Carbon Fiber

All lignin precursors produced in this study, including raw lignin and the pretreated precursors (ML, 0AT-ML, 0.5AT-ML, 0.75AT-ML, 1AT-ML, 2AT-ML and 3AT-ML), were

subjected to melt-spinning. The raw lignin did not melt below 200 ℃. Further raising the extruder temperature slightly improved the melting of the lignin, but the lignin also started to decompose. It is likely that the melting temperature of raw lignin is higher than its decomposition temperature. The similar melting behavior was also reported with a softwood kraft lignin [8]. ML precursor melted better than raw lignin at lower temperatures, indicating the lignin molecules with higher melting temperatures were selectively removed as methanol-insoluble during the solvent fractionation. However, severe devolatilization took place with the extruder temperature of 150 ºC, whereas the viscosity of the melted ML at this temperature was still too high to extrude.

The 0AT-ML precursor could be extruded at a temperature range of 140 to 200 ºC due to its improved thermal stability and precursor mobility at higher extrusion temperatures. However, spinning fiber for an extended time was still difficult due to the high viscosity of the precursor. The as-spun fiber was also too brittle to handle. The high viscosity of 0AT-ML precursor is due to crosslinking polymerization of the lignin at elevated temperatures. Previously, Hosseinaei et al. reported that switchgrass organosolv lignin with T_g of 118 ºC could be melt-spun at 190-195 ºC [5]. Although 0AT-ML has a lower T_g than the switchgrass lignin reported in the literature, it could not be spun at a similar temperature range. When the extruder temperature exceeded 200 ℃, bubbling and forming of the precursor at the extruder outlet was significant and fiber spinning became impractical. The excessive bubbling and forming at higher temperatures could be attributed to decomposition of aryl ether, the hydroxylcinamates and other aliphatic side chain groups. Poor spinning performances of the above precursors were predictable based on their TGA profiles in Figure 2.4. Because the melt-spinning process is conducted in air, oxygen further enhances the thermal decomposition of

lignin. For instance, in addition to CO_2 and vinylphenols, vanillin, acetovanillone and vanillic acid can also formed during oxidative thermal decomposition of ferulate acid [49].

All acetylated precursors, except 0.5AT-ML, demonstrated better melt-spinnability than the non-acetylated lignins. The precursor of 0.5AT-ML was still thermally instable and too viscous for spinning, attributed to its low acetylation degree ($\theta = 0.35$). It was also found that the extruder temperature had to be adjusted with different acetylated precursors for best spinning performance. As shown in Table 2.4, the optimum spinning temperatures were lower for the precursors with higher degrees of acetylation. Apparently, the decreased intermolecular forces in acetylated precursors reduced the viscosity of the precursors, so the fiber can be spun at lower temperatures.

The as-spun fibers of the acetylated precursors were subjected to oxidative stabilization. The extent of fiber fusion upon stabilization is also summarized in Table 2.4. The as-spun fibers from 3AT-ML and 2AT-ML fused severely after stabilization at a heating rate of 0.1 $^{o}C\ min^{-1}$. The fibers of 1AT-ML and 0.75AT-ML also stick together, but fused less significantly. Ideally, the precursor fiber should turn into non-fusible, solid fiber by oxidative stabilization within a reasonable time. At this stage, crosslinking among the fiber molecules is highly desired in order to form a rigid fiber structure. Oxygen is mainly introduced into the precursor fiber molecules as carbonyl and carboxyl groups, although some minor degrees of dehydration, decarboxylation and decarbonyzation could be expected. Since acetylated precursor has a reduced ability to crosslink, the precursor fiber molecules still have mobility and fuse together during stabilization at elevated temperatures. Apparently, the lignin has to be acetylated at the optimum degree to ensure the acetylated precursor is spinnable yet the precursor fiber can be stabilized within an acceptable time. Among the actylated presursor

fibers, 0.75AT-ML was least fusible due to its lower degree of acetylation. Thus, this precursor fiber was selected and subjected to the step-wise stablization as described. Upon stablization for prolonged time, fiber fusion was greatly diminished and the integrity of the stabilized fiber was much enhanced. The stablized fiber was further carbonized to produce carbon fiber.

Raman spectrum of the carbon fiber is shown in Figure 2.5. The G band (1595 cm^{-1}) is related to the stretching of the C-C bond in graphitic materials and the D band (1365 cm^{-1}) is associated with structural disorder. The ratio of peak intensities of I_D/I_G is often used to estimate the level of disorder in the fiber. A higher ratio of I_D/I_G corresponds to the fiber with more defects. The I_D/I_G ratio of the carbon fiber produced from 0.75AT-ML was 2.53. This ratio is lower than the corresponding ratio value of acetylated softwood lignin-based carbon fibers carbonized at same temperature, which was reported to be 2.88 [42]. Li et al. [50] suggested that a lignin precursor with a higher content of linear molecular linkages could result in a carbon fiber with better crystallinity and lower I_D/I_G. The lengths of aliphatic side chains are overall longer in corn stover lignin in comparison to softwood lignin, which may explain the lower I_D/I_G ratio obtained in this study. However, further research is needed to confirm this theory. Frank et al. [22] previously pointed out that the molecular linearity is the most critical factor in determining the quality of carbon fiber and it must be established before the fiber is oxidized and carbonized.

The average diameter and mechanical properties of the carbon fibers produced from 0.75AT-ML are summerized in Table 2.5. Distributions of the tensile strength with diameter of the 20 single fibers are also ploted in Figure 2.6.

The carbon fiber has an average tensile strength of 0.454 GPa and modulus of 62 GPa. The average strain of the carbon fiber is 0.73%, which is similar to that of switchgrass lignin-

based carbon fiber [5], but lower than the corresponding value of carbon fibers produced from woody biomass based lignins [6]. As it can be seen from Figure 2.6, some fibers had relatively lower tensile strength than other fibers despite their similar diameters, suggesting these fibers have more structural defects than others. Recall that the ash content in ML was 0.27%, still higher than the recommended ash content in lignin as a carbon fiber precursor (< 0.1%) [2]. As described earlier, the carbon fiber with inorganic impurities result in lower mechanical properties. In this study, the average diameter of carbon fiber was 39.1 μm, considerably larger than the diameters of commercial grade carbon fibers. In general, the mechanical properties of carbon fiber is inversely correlated to the diameter of the fiber. During stabilization, oxidization occurs from the outermost layer of the fiber to form a hard shell. The hard shell could then act as a physical barrier to prevent oxygen from penetrating into the inner side of the fiber, preventing the fiber from being sufficienctly stablized. Thus, the fiber with thinner diameter is highly preferred in order to achieve higher mechanical properties. It has been reported that reducing the fiber diameter from 22.5 to 5.8 μm increased the tensile strength of an acetylated softwood lignin-based carbon fiber from 0.52 GPa to 1.04 GPa [8]. Applying tension during stabilization and carbonization of fiber in future study could reduce the diameter of the fibers and potentially improve the mechanical properties of corn stover lignin-based carbon fiber. However, it should also be noted that the detrimental effects of pores and impurities on mechanical properties of the fiber could also be magnified in the fiber with smaller diameters. Thus, the lignin must have a high purity prior to fiber spinning. The purity of the corn stover lignin could be improved in future studies by repreating the solvent fractionation process or using other filtration methods.

2.4 Conclusions

In the present study, an industrial corn-stover lignin high in ash content was successfully converted into carbon fiber. The methanol fractionation is used to purify raw lignin and selectively removed the lignin with high Mw. However, neither ML nor thermally pretreated ML (0AT-ML) was spinnable, due to the coupled effect of higher viscosity of the precursors upon melting and precursor devolatilzations at low temperatures. These problems were caused by the crosslinking of G, H units and thermal decomposition of aliphatic side chains in the corn stover lignin. On the other hand, the two-step acetylation of ML rendered thermally stable and spinnable precursors. Substitution of phenolic and aliphatic hydroxyl groups by acetylation reduced intermolecular forces to enhance the mobility of the precursor. The hydroxycinnamate groups also decreased upon acetylation, which contributed to the improved thermal stability of the precursor. However, partial acetylation of the lignin was recommended since the lignin with a low acetylation degree was not spinnable, whereas highly acetylated precursor fibers easily fuse. The optimum precursor in this study had an acetylation degree of 0.59, T_g of 85 ºC and Mw of 3594 Da. The average tensile strength and modulus of the carbon fiber produced upon oxidative stabilization of the 0.75AT-ML precursor fiber followed by carbonization at 1000 ºC were 0.454 GPa and 62 GPa. The I_D/I_G ratio of the carbon fiber at Raman spectroscopy was 2.53.

Overall, this study demonstrated potential uses of a biorefinery agricultural-residue lignin for carbon fiber and showed challenging issues to tackle. Lignin pretreatment was necessary to increase thermal instability of the lignin caused by decomposition of hydroxycinnamate groups and other aliphatic side chain groups. The ash content was 0.27% in the present study after methanol extraction, which is still higher than the recommended ash content in a lignin precursor for carbon fiber. Improving the precursor purity and optimizing

manufacturing processes in future studies could lead to corn stover lignin-based carbon fiber with higher mechanical properties.

2.5 Figures and Tables

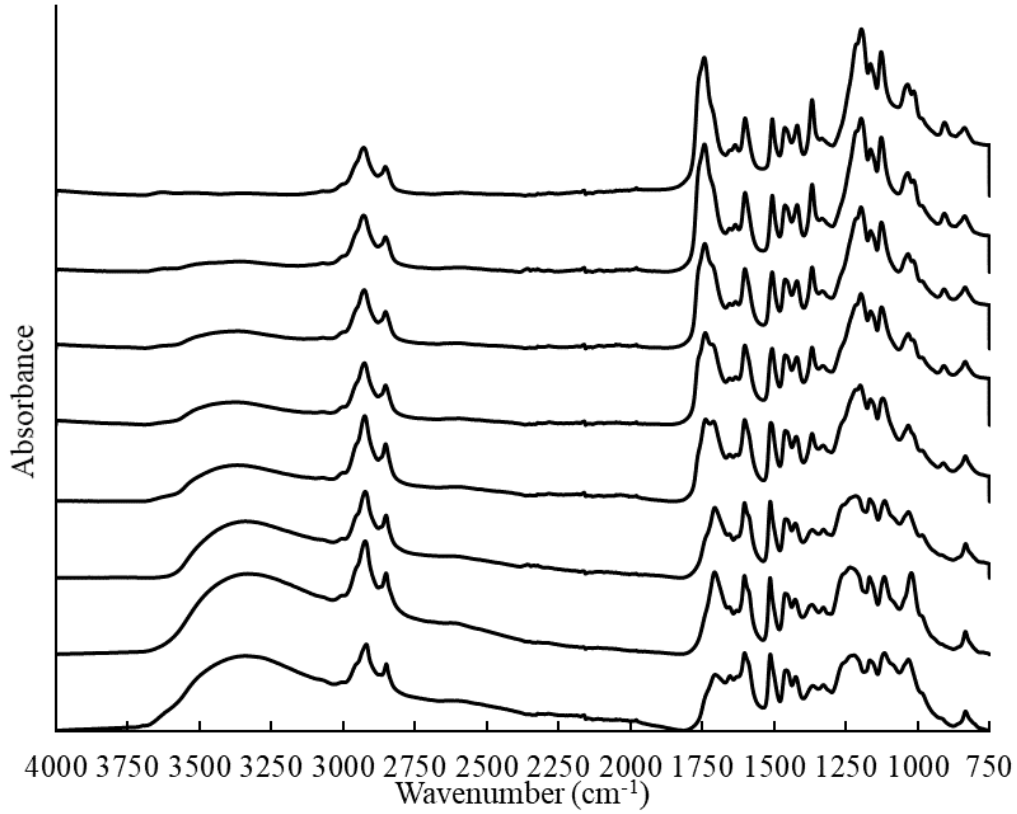

Figure 2.1 FTIR spectra of different lignin precursors

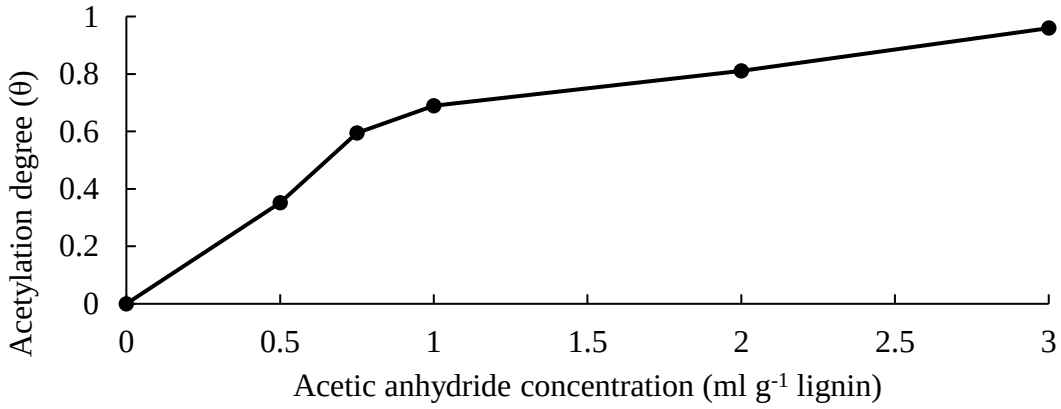

Figure 2.2 Correlation between acetic anhydride concentrations and acetylation degrees

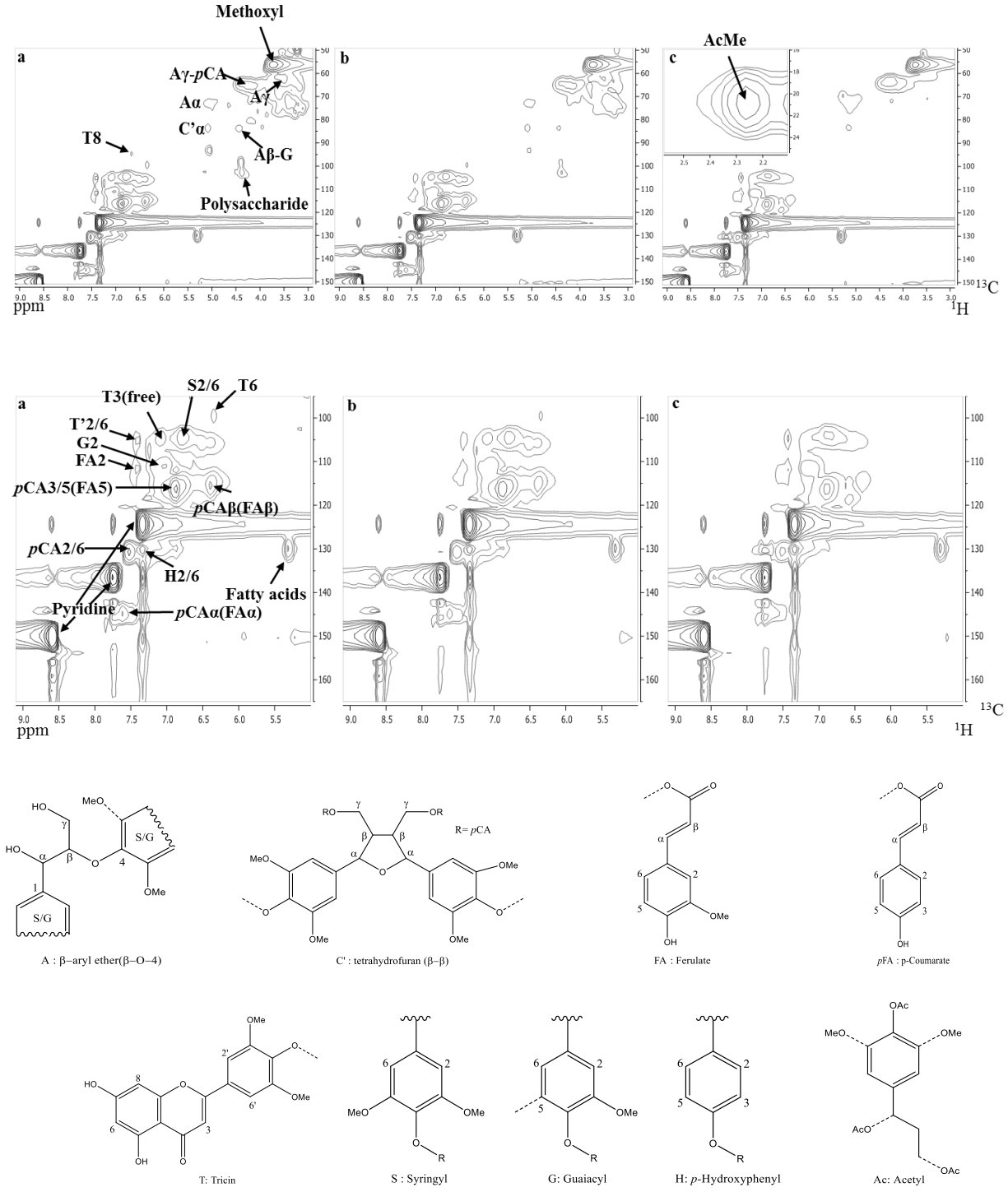

Figure 2.3 2D-NMR spectra of selected lignin precursors (a: ML. b: 0AT-ML. c: 0.75AT-ML Top: Full region. Bottom: Selected region.)

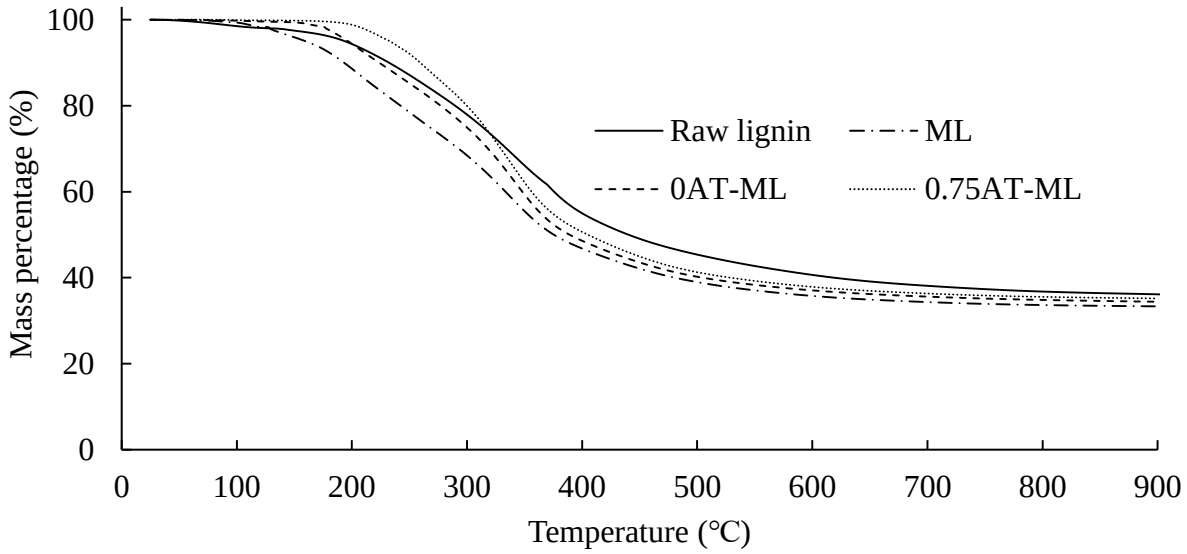

Figure 2.4 TGA curves of selected lignin precursors

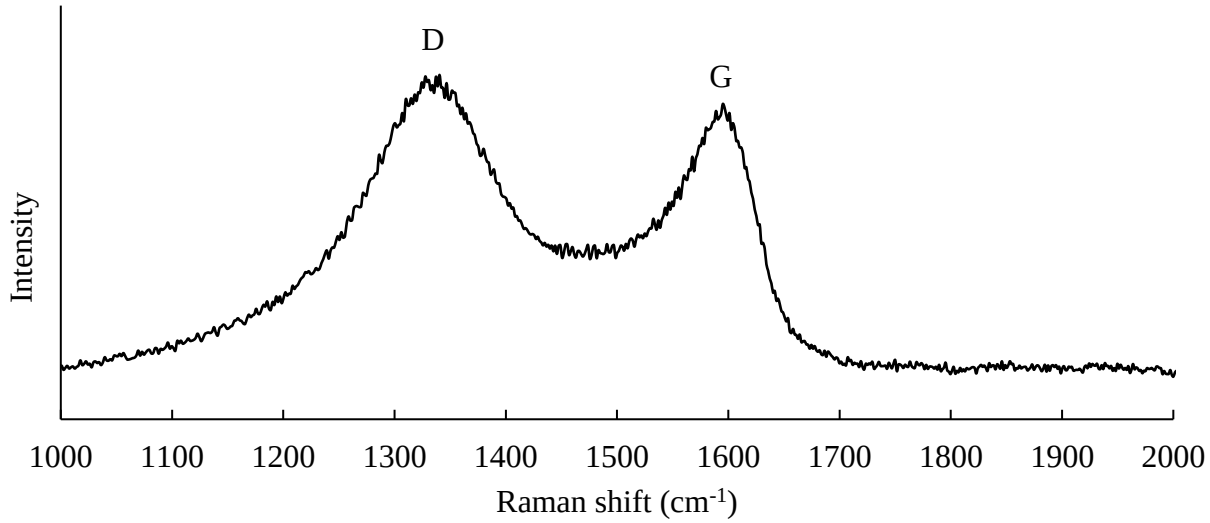

Figure 2.5 Raman spectrum of carbon fiber produced from 0.75AT-ML

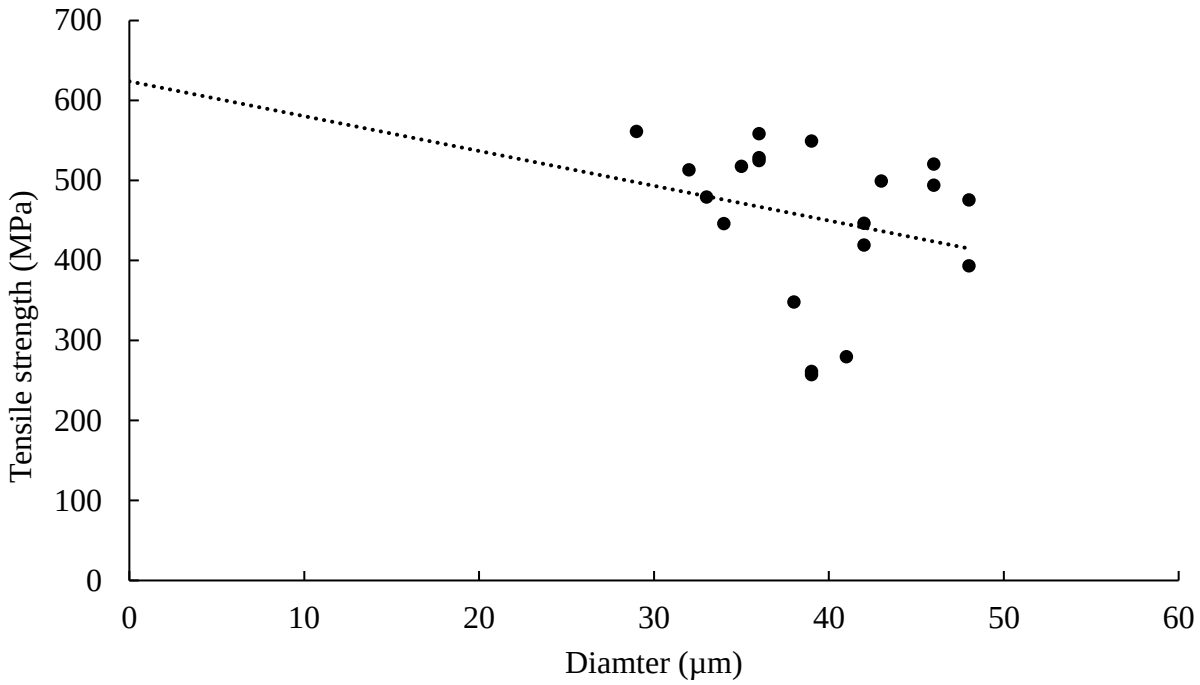

Figure 2.6 Tensile strengths and corresponding diameters of carbon fibers produced from 0.75AT-ML

Table 2.1 Proximate and ultimate analyses of raw lignin and ML

	Raw lignin	ML
Proximate analysis (%)		
Moisture content	3.87	3.66
Volatiles	62.52	65.03
Fixed carbon	27.55	31.04
Ash	6.07	0.27
Ultimate analysis (%)		
Carbon	61.34	58.66
Hydrogen	4.67	5.32
Nitrogen	2.00	0.72
Sulfur	0.20	0.06
Oxygen[a]	31.79	35.24

[a] By difference

Table 2.2 Molecular weights and polydispersity index (PDI) of different lignin precursors

	Raw lignin	ML	0AT-ML	0.75AT-ML
Mw (Da)	3263	1278	3180	3594
Mn (Da)	1121	674	997	1060
PDI	2.91	1.89	3.19	3.39

Table 2.3 Glass transition temperatures (T_g) and decomposition temperatures (T_d) of different lignin precursors

	Raw lignin	ML	0AT-ML	0.75AT-ML
T_g (℃)	147	93	111	85
T_d(℃)[a]	194	160	197	233

[a] Determined by the TGA profiles, the temperatures correspond to 5% of weight losses

Table 2.4 Spinning and stabilization conditions of different lignin precursors

Samples	3AT-ML	2AT-ML	1AT-ML	0.75AT-ML	0.5AT-ML	0AT-ML	Raw lignin
Melt spinning temperature (℃)	135-140	140-145	165-170	165-170	NS[a]	NS	NS
Fiber fusion[b]	S	S	M	L	-	-	-

[a] Not spinnable
[b] Based on observation (“S”=Severe, “M”=Medium, “L”=Light)

Table 2.5 Mechanical properties of carbon fibers produced from 0.75AT-ML

Properties $\mu \pm \sigma$[a]	Diameter (μm)	Tensile stength (GPa)	Modulus (GPa)	Strain (%)
	39.1 ± 5.4	0.454 ± 0.098	62 ± 14	0.73 ± 0.08

[a] μ refers to mean value, and σ refers to standard deviation.

2.6 References

1. Frank, E., F. Hermanutz, and M.R. Buchmeiser, *Carbon fibers: precursors, manufacturing, and properties.* Macromolecular materials and engineering, 2012. **297**(6): p. 493-501.
2. Gellerstedt, G., E. Sjöholm, and I. Brodin, *The wood-based biorefinery: A source of carbon fiber?* The Open Agriculture Journal, 2010. **3**: p. 119-124.
3. Yang, J., et al., *Preparation of isotropic pitch-based carbon fiber using hyper coal through co-carbonation with ethylene bottom oil.* Journal of Industrial and Engineering Chemistry, 2016. **34**: p. 397-404.
4. Kim, J.W. and J.S. Lee, *Preparation of carbon fibers from linear low density polyethylene.* Carbon, 2015. **94**: p. 524-530.
5. Hosseinaei, O., et al., *Role of Physicochemical Structure of Organosolv Hardwood and Herbaceous Lignins on Carbon Fiber Performance.* Acs Sustainable Chemistry & Engineering, 2016. **4**(10): p. 5785-5798.
6. Baker, D.A. and T.G. Rials, *Recent advances in low-cost carbon fiber manufacture from lignin.* Journal of Applied Polymer Science, 2013. **130**(2): p. 713-728.
7. Nordström, Y., et al., *A new softening agent for melt spinning of softwood kraft lignin.* Journal of Applied Polymer Science, 2013. **129**(3): p. 1274-1279.
8. Zhang, M. and A.A. Ogale, *Carbon fibers from dry-spinning of acetylated softwood kraft lignin.* Carbon, 2014. **69**: p. 626-629.
9. Qu, W., et al., *Repolymerization of pyrolytic lignin for producing carbon fiber with improved properties.* Biomass and Bioenergy, 2016. **95**: p. 19-26.
10. Kadla, J., et al., *Lignin-based carbon fibers for composite fiber applications.* Carbon, 2002. **40**(15): p. 2913-2920.
11. Sudo, K. and K. Shimizu, *A new carbon fiber from lignin.* Journal of applied polymer science, 1992. **44**(1): p. 127-134.
12. Baker, D.A., N.C. Gallego, and F.S. Baker, *On the characterization and spinning of an organic-purified lignin toward the manufacture of low-cost carbon fiber.* Journal of Applied Polymer Science, 2012. **124**(1): p. 227-234.
13. Ragauskas, A.J., et al., *Lignin valorization: improving lignin processing in the biorefinery.* Science, 2014. **344**(6185): p. 1246843.
14. Zhou, S., et al., *Lignin Valorization through Thermochemical Conversion: Comparison of Hardwood, Softwood and Herbaceous Lignin.* Acs Sustainable Chemistry & Engineering, 2016. **4**(12): p. 6608-6617.
15. Laurichesse, S. and L. Avérous, *Chemical modification of lignins: Towards biobased polymers.* Progress in Polymer Science, 2014. **39**(7): p. 1266-1290.
16. Norberg, I., et al., *A new method for stabilizing softwood kraft lignin fibers for carbon fiber production.* Journal of Applied Polymer Science, 2013. **128**(6): p. 3824-3830.
17. Paul, R., et al., *Recent Progress in Producing# 11; Lignin-Based Carbon Fibers for Functional Applications*. CAMX 2015, Dallas, TX, Oct. 26-29, 2015.
18. Kubo, S. and J. Kadla, *Lignin-based carbon fibers: Effect of synthetic polymer blending on fiber properties.* Journal of Polymers and the Environment, 2005. **13**(2): p. 97-105.

19. Kadla, J.F. and S. Kubo, *Lignin-based polymer blends: analysis of intermolecular interactions in lignin–synthetic polymer blends.* Composites Part A: Applied Science and Manufacturing, 2004. **35**(3): p. 395-400.
20. Seydibeyoğlu, M.Ö., *A novel partially biobased PAN-lignin blend as a potential carbon fiber precursor.* BioMed Research International, 2012. **2012**.
21. Brodin, I., et al., *Oxidative stabilisation of kraft lignin for carbon fibre production.* Holzforschung, 2012. **66**(2): p. 141-147.
22. Frank, E., et al., *Carbon fibers: precursor systems, processing, structure, and properties.* Angewandte Chemie International Edition, 2014. **53**(21): p. 5262-5298.
23. Buranov, A.U. and G. Mazza, *Lignin in straw of herbaceous crops.* Industrial crops and products, 2008. **28**(3): p. 237-259.
24. Carpenter, D., et al., *Biomass feedstocks for renewable fuel production: a review of the impacts of feedstock and pretreatment on the yield and product distribution of fast pyrolysis bio-oils and vapors.* Green Chemistry, 2014. **16**(2): p. 384-406.
25. Luterbacher, J.S., et al., *Lignin monomer production integrated into the γ-valerolactone sugar platform.* Energy & Environmental Science, 2015. **8**(9): p. 2657-2663.
26. Constant, S., et al., *New insights into the structure and composition of technical lignins: a comparative characterisation study.* Green Chemistry, 2016. **18**(9): p. 2651-2665.
27. Foston, M., et al., *NMR a critical tool to study the production of carbon fiber from lignin.* Carbon, 2013. **52**: p. 65-73.
28. Rencoret, J., et al., *Isolation and structural characterization of the milled wood lignin, dioxane lignin, and cellulolytic lignin preparations from brewer's spent grain.* Journal of agricultural and food chemistry, 2015. **63**(2): p. 603-613.
29. Ralph, S.A., et al., *NMR database of lignin and cell wall model compounds.* US Forest Prod. Lab., Madison, WI https://www.glbrc.org/databases_and_software/nmrdatabase/NMR_DataBase_2009_Complete.pdf (accessed May, 2017).
30. Kubo, S. and J.F. Kadla, *Poly (ethylene oxide)/organosolv lignin blends: Relationship between thermal properties, chemical structure, and blend behavior.* Macromolecules, 2004. **37**(18): p. 6904-6911.
31. Platace, R. and A. Adamovics. *CONTENT OF LIGNING AND ASH IN GRASS BIOMASS DEPENDING ON FERTILISER TYPE AND RATE*. in *13th International Scientific Conference Engineering for Rural Development, Jelgava, Latvia. Volume 13, 29-30 May, 2014*. 2014. Latvia University of Agriculture.
32. Vishtal, A.G. and A. Kraslawski, *Challenges in industrial applications of technical lignins.* BioResources, 2011. **6**(3): p. 3547-3568.
33. Pinho, S.P. and E.A. Macedo, *Solubility of NaCl, NaBr, and KCl in water, methanol, ethanol, and their mixed solvents.* Journal of Chemical & Engineering Data, 2005. **50**(1): p. 29-32.
34. Pandey, K., *A study of chemical structure of soft and hardwood and wood polymers by FTIR spectroscopy.* Journal of Applied Polymer Science, 1999. **71**(12): p. 1969-1975.

35. Mainka, H., et al., *Characterization of the major reactions during conversion of lignin to carbon fiber.* Journal of Materials Research and Technology, 2015. **4**(4): p. 377-391.
36. Molinari, H.B.C., et al., *Grass cell wall feruloylation: distribution of bound ferulate and candidate gene expression in Brachypodium distachyon.* Frontiers in plant science, 2013. **4**: p. 50.
37. Monteil-Rivera, F., et al., *Isolation and characterization of herbaceous lignins for applications in biomaterials.* Industrial Crops and Products, 2013. **41**: p. 356-364.
38. Saito, T., et al., *Methanol fractionation of softwood kraft lignin: Impact on the lignin properties.* ChemSusChem, 2014. **7**(1): p. 221-228.
39. Pu, Y. and A.J. Ragauskas, *Structural analysis of acetylated hardwood lignins and their photoyellowing properties.* Canadian journal of chemistry, 2005. **83**(12): p. 2132-2139.
40. Uraki, Y., et al., *Thermal mobility of β-O-4-type artificial lignin.* Biomacromolecules, 2012. **13**(3): p. 867-872.
41. Saralegi, A., et al., *Thermoplastic polyurethanes from renewable resources: effect of soft segment chemical structure and molecular weight on morphology and final properties.* Polymer International, 2013. **62**(1): p. 106-115.
42. Zhang, M., *Carbon Fibers Derived from Dry-Spinning of Modified Lignin Precursors.* Carbon Fibers Derived from Dry-Spinning of Modified Lignin Precursors. Ph.D. Thesis, Clemson University, Clemson, SC, May, 2016.
43. Hatfield, R.D., et al., *Grass lignin acylation: p-coumaroyl transferase activity and cell wall characteristics of C3 and C4 grasses.* Planta, 2009. **229**(6): p. 1253-1267.
44. Meng, J., et al., *Toward understanding of bio-oil aging: Accelerated aging of bio-oil fractions.* ACS Sustainable Chemistry & Engineering, 2014. **2**(8): p. 2011-2018.
45. Lin, S.Y. and C.W. Dence, *In Handbook of Methods in Lignin Chemistry, T.E. Timell Eds.; Springer Science & Business Media, 2012, Chapter 4.*
46. Lin, J., J.-B. Shang, and G.-J. Zhao, *The preparation and characterization of liquefied wood based primary fibers.* Carbohydrate polymers, 2013. **91**(1): p. 224-228.
47. Qin, W. and J. Kadla, *Carbon fibers based on pyrolytic lignin.* Journal of Applied Polymer Science, 2012. **126**(S1).
48. Sun, Q., et al., *A study of poplar organosolv lignin after melt rheology treatment as carbon fiber precursors.* Green Chemistry, 2016. **18**(18): p. 5015-5024.
49. Fiddler, W., et al., *Thermal decomposition of ferulic acid.* Journal of agricultural and food chemistry, 1967. **15**(5): p. 757-761.
50. Li, Q., et al., *Quality carbon fibers from fractionated lignin.* Green Chemistry, 2017. **19**(7): p. 1628-1634.

CHAPTER 3. REPOLYMERIZATION OF PYROLYTIC LIGNIN FOR PRODUCING CARBON FIBER WITH IMPROVED PROPERTIES

(A paper published in *Biomass and Bioenergy*)

ABSTRACT

Lignin is a promising precursor of low-cost carbon fibers. However, the mechanical properties of carbon fibers produced from melt-spinning of raw lignin are poor, restricted by the randomly cross-linked polymer structures of lignin. In the present study, carbon fibers were produced from lignin-derived phenolic oil. Pyrolytic lignin was isolated from pyrolysis oil of red oak and washed with toluene to remove volatile impurities. Upon repolymerizing with a mass fraction of 0.5% of sulfuric acid, the toluene-washed pyrolytic lignin became solid with the glass transition temperature (T_g) of 101 °C and the average molecular weight of 1267 Da. The repolymerized pyrolytic lignin was further processed into carbon fibers through melt-spinning, oxidative stabilization and carbonization at 1000 °C. The average tensile strength and modulus of the fibers were 0.855 GPa and 85 GPa, while the highest values of individual fibers were 1.014 GPa and 122 GPa, respectively. The present study suggests that the quality of the carbon fiber produced from pyrolytic lignin could be further improved by process optimization.

Key words: fast pyrolysis, pyrolytic lignin, repolymerization, carbon fiber, acid catalyst

3.1 Introduction

Carbon fiber is a light weight material with superior mechanical properties and corrosion resistance. Thus, carbon fiber can be used as reinforced composites in automobile and aerospace industries, construction, sports equipment and more [1-3]. Despite great potential, the application of carbon fibers is currently limited, mainly due to the high cost of the precursor. Currently, a large portion of carbon fibers in the market are produced from polyacrylonitrile (PAN), and the precursor alone costs as much as 51% of the production cost of the carbon fiber [2]. PAN is derived from petroleum and releases toxic gas during carbon fiber processing, raising various environmental concerns [4, 5]. Low-cost carbon fibers made from non-petroleum precursors could enable the application of carbon fibers in large scale. The Department of Energy suggested that the alternative carbon fibers with a tensile strength of 1.72 GPa and modulus of 172 GPa, and with cost below 11-15.40 \$ kg^{-1}, could be widely used in the automobile industry to reduce vehicle weight and improve fuel economy [6, 7]. Lignin derived from lignocellulosic biomass has been of particular interest as an alternative precursor since it naturally contains a six-membered-ring aromatic structure and is abundantly available at low cost [8, 9].

Lignin-based carbon fibers have been studied for nearly 50 years. The historical background of the development and recent advances have been thoroughly reviewed by Baker [7]. In the previous studies, carbon fibers were produced from lignin either by thermal processing, chemical modification or mixing lignin with other polymers. Although various types of lignin have been tested and the fiber manufacturing process was also carefully optimized, the quality of lignin-based carbon fibers is still too low to be considered for structural applications [6, 10-12]. To date, the lignin-derived carbon fiber with the highest quality was reported by Oak Ridge National Lab with tensile strength and modulus of 1.07

GPa and 83 GPa, respectively. The fibers were made by melt-spinning an organic-solvent purified, Kraft hardwood lignin with a low glass transition temperature (Tg = 86 °C) after thermal treatment. In general, lignin-based carbon fibers have tensile strength lower than 0.500 GPa.

The quality of lignin-based carbon fibers is low, attributed to the intrinsic nature of lignin structure. Lignin structure is also affected by its biomass origin and isolation method [13, 14]. Lignin is a phenyl propane-based macropolymer and is linked with carbohydrates through covalent bonds in biomass. To separate lignin from the rest of biomass, chemical treatments involving salts, acids, and/or organic solvents are commonly employed. Technical lignin produced either from paper, pulping or cellulosic biorefineries usually contain considerable amounts of organic and inorganic impurities derived from the biomass plant, the extraction process, as well as, lignin handling and storage. These impurities have to be removed from the lignin prior to carbon fiber production through acid washing, which otherwise cause various defects within the fibers. A melt-spinning method is generally used to process lignin due to its low cost. When lignin is melt-spun at elevated temperatures, the cleavage of weak ether and ester bonds in the lignin polymer release volatile products and create void spaces within the fibers [15] ultimately reducing the mechanical strength of the fibers. More importantly, lignin is a three-dimensional polymer formed by random cross linking of its three precursor monomers. Due to the lack of molecular orientation and linearity within the polymer, the resulting fibers have amorphous structures, corresponding to low mechanical strength of the fibers.

While technical lignin is polymeric material isolated from biomass by the removal of carbohydrates through chemical or biochemical process, pyrolytic lignin is depolymerized

lignin produced by heat. When lignocellulosic biomass is rapidly heated to 450 °C to 600 °C in an inert environment and the pyrolysis vapor is quenched, up to a mass fraction of 75% of biomass can be recovered as bio-oil. Due to its robust process and low capital cost, pyrolysis is one of the major liquefaction technologies of biomass. During pyrolysis, phenolic monomers and oligomers produced from lignin (i.e., pyrolytic lignin) are condensed and form a complex mixture along with carbohydrate-derived sugars, furans, acids, ketones and aldehydes in bio-oil. Although accounting for a mass fraction of 20% to 30% of bio-oil [16], pyrolytic lignin is usually referred to as the less-preferred product because it increases the viscosity of bio-oil during storage and could even cause phase separation [17]. This is because pyrolytic lignin is unstable and has a tendency for polymerization. On the other hand, pyrolytic lignin can be extracted from bio-oil by simple water-washing and upgraded independently for other value-added applications. Potential applications of pyrolytic lignin include bio-adhesive [18], resin [19], bioasphalt [20], solid fuel [21], as well as, carbon fiber [22]. For example, Sahaf et al. [23] studied rheological and tunable thermoplastic properties of pyrolytic lignin and reported that pyrolytic lignin could be considered for hot melt adhesive applications. On the other hand, pyrolytic lignin as the precursor of carbon fiber can potentially provide several advantages over lignin. While it has some structural similarities with lignin [24], pyrolytic lignin is made of smaller phenolic units with reactive functional groups, such as phenolic hydroxyl groups, carbonyl groups and vinyl groups [16]. Thus, pyrolytic lignin has the potential to be re-polymerized [25] into more desirable structures versus lignin. Compared to as-received technical lignin, pyrolytic lignin may contain fewer impurities because the majority of impurities in biomass remain in biochar instead of bio-oil when biomass is pyrolyzed.

In the present study, carbon fibers were produced from pyrolytic lignin derived from the fast pyrolysis of red oak. Pyrolytic lignin isolated from the heavy fraction of bio-oil was repolymerized with acid catalyst prior to spinning into fibers. Both the precursor and carbon fibers were characterized in this work.

3.2 Experimental

3.2.1 Preparation of Pyrolytic Lignin

Red oak (Quercus Rubra) was purchased from Wood Residues Solutions (Montello, WI). It was first ground by a mill cut, and then pyrolyzed in a pilot-scale, fluidized bed reactor at Iowa State University's BioCentury Research Farm. Pyrolysis temperature was 500 °C and bio-oil was collected in a five-stage bio-oil condensation system. Detailed reactor configuration and the composition of bio-oil collected in each condenser was previously reported elsewhere [26]. Bio-oil collected in the first condenser consisted of pyrolytic sugars and phenols. It was water-washed three times to remove sugars. The remaining water-insoluble fraction was designated as pyrolytic lignin and used in this study.

3.2.2 Pretreatment of Pyrolytic Lignin

Pyrolytic lignin was subsequently washed with toluene in a mass ratio of 1:1 three times for 15 min and then centrifuged at 66.67 Hz for 20 min to remove any residual water and toluene. The toluene-washed pyrolytic lignin was further heated at 90 °C for 15 min to remove any volatiles. Each time, 10 g to 15 g of toluene-washed pyrolytic lignin was placed in a 200 ml beaker and set on a heating plate. A funnel with its cone-side downward was placed right above the beaker. The neck-side of the funnel was connected to a vacuum tube to facilitate the removal of volatiles. For thermal treatment, the pyrolytic lignin was heated in an oil bath at 105 °C for 2 h with a magnetic stirring bar at 2.5 Hz. A mass fraction of 0.5% of sulfuric acid

(SA) was added dropwise into the pyrolytic lignin to catalyze polymerization reaction [27, 28]. The produced precursor was designated as SA treated precursor in this study.

3.2.3 Characterization of Pyrolytic Lignin

Dionex Ultimate 3000 series high performance liquid chromatography (HPLC) together with a Shodex Refractive Index (RI) and Diode Array Detectors (DAD) was used to conduct gel permeation chromatography (GPC) analyses for relative molecular weight distribution. Two GPC columns (3 μm, 100 Å, 300 × 7.5 mm; PLgel, Agilent, p/n PL1110-6320) were calibrated with six monodispersed polystyrene standards ranging from 162 g mol^{-1} to 38640 g mol^{-1}. Tetrahydrofuran was used as the solvent for samples and the eluent in the columns.

An Agilent 7890B gas chromatography (GC) with Agilent 5977A mass-selective-detector (MSD) and flame ionization detector (FID) system was used to identify the chemical composition in the pyrolytic lignin and precursors. The capillary column used in the GC was a ZB-1701 (60 m × 250 μm × 0.25 μm). The injection temperature was 250 ºC and the oven temperature was kept at 40 ºC for 3 min, and then ramped to 280 ºC with 3 ºC min^{-1}.

A Thermo Scientific Nicolet iS10 (Thermo Fisher Scientific Inc., Waltham, MA) equipped with a Smart iTR accessory was used to conduct Fourier Transform Infrared (FTIR) analysis to determine the functional groups in the pyrolytic lignin and precursors. With wave numbers ranging from 750 cm^{-1} to 4000 cm^{-1}, each sample was scanned 32 times at a resolution of 4 cm^{-1} and interval of 1 cm^{-1}.

Thermogravimetric analysis (TGA) was conducted using a Mettler Toledo TGA/DSC instrument. The samples were heated at a rate of 10 °C min^{-1} from 25 °C to 1000 °C under nitrogen with a flow rate of 100 ml min^{-1}. The experiment was duplicated for reproducibility.

Glass transition temperature (T_g) was determined by using a differential scanning calorimeter (DSC, Q20, TA instruments). Each sample was heated to 125 °C with a heating rate of 10 °C min^{-1}. Nitrogen was used as the purge gas with a flow rate of 50 ml min^{-1}. The midpoint Tg of precursor was determined by using a TA software.

The CHNS elemental analysis of the pyrolytic lignin and precursor were conducted using Elementar (vario MICRO cube) elemental analyzer.

3.2.4 Production of Carbon Fiber

About 6 g of pyrolytic lignin was fed into a twin-screw microcompounder (DACA Instruments, Santa Barbara, CA) and extruded at 115 °C to 120 °C. The fibers were wound onto a roller (DSM, Geleen, Netherlands) at up to 100 m min^{-1}. The oxidative stabilization of the spun fibers were conducted in a muffle furnace by heating the fibers up to 280 °C at a heating rate of 0.3 °C min^{-1} and then held for 1 h. Carbonization was performed in a tubular furnace under an argon environment. The stabilized fibers were heated at 3 °C min^{-1} up to 1000 °C, and held for 1h.

3.2.5 Characterization of Carbon Fibers

Tensile strength of single fiber was measured using a dynamic mechanical analyzer (DMA) (Q800, TA Instruments), the stress-strain curve was obtained by stretching fiber at 30 ºC under a strain rate of 50 μm min^{-1} [29]. The diameter of each fiber was measured by an electronic digital micrometer with a resolution of 1 μm and further confirmed with scanning electron microscope.

The microstructure of the carbon fiber samples was examined using a scanning electron microscope (SEM, Quanta-FEG 250, FEI) at 10 kV accelerating voltage. Segments of the

samples were mounted onto double-stick carbon tape on a 45° incline. Samples were coated with 5 nm of iridium for conductivity.

3.3 Results and Discussion

3.3.1 Properties of Pyrolytic Lignin

Pyrolytic lignin and pyrolytic lignin after toluene wash were a dark black, viscous liquid at room temperature. The viscosity of the pyrolytic lignin initially decreased at elevated temperatures but later increased as thermal treatment progressed. Upon cooling to room temperature, the SA treated pyrolytic lignin became solid.

3.3.1.1 GPC analysis

Relative weight average molecular weight (Mw) and polydispersity index (PDI) of the pyrolytic lignin before and after it was toluene-washed, and SA treated are listed in Table 3.1. The relative Mw distribution of the pyrolytic lignin treated differently is also given in Figure 3.1. As shown, the pyrolytic lignin before the toluene wash had a relative Mw of 566 Da and PDI of 2.44. In the GPC chromatogram, the relative Mw of the major peak was 158 Da while two minor peaks appeared at 84 Da and 452 Da, respectively. Since the theoretical Mw of a phenolic unit is around 180 Da [30], the pyrolytic lignin is a mixture of phenolic monomers and oligomers. The phenolic monomers usually have a lower viscosity than oligomers. The precursor with too low of a viscosity is difficult to spin into continuous fibers, and easily creating void spaces within the fibers due to its volatility during the melt spinning process. Therefore, the pyrolytic lignin was toluene-washed to remove low Mw compounds. The non-polar solvent fraction also preferentially removes less reactive compounds with lower degree of polymerization [31]. After toluene washing, the content of phenolic monomers with relative Mw less than 200 Da were substantially decreased and the Mw of the pyrolytic lignin increased

to 810 Da. The PDI value also decreased slightly, indicating that the toluene-washed pyrolytic lignin had a narrower Mw distribution after washing. Baker et al. [3] suggested that lignin with a narrower Mw distribution was more desirable as a precursor.

The addition of a small amount of sulfuric acid (SA) during thermal treatment increased the Mw of the pyrolytic lignin to 1267 Da. Acid catalyzes polymerization of lignin-derived phenolic compounds. For instance, carboxylic acids (acetic acid, formic acid etc.) in bio-oil are known to promote polymerization of phenols during bio-oil storage [28]. Due to its strong acidity, a small amount of SA was enough to increase Mw of the precursor at relatively short reaction time. A higher concentration of SA results in the precursor charring, making it unable to be melt-spun. The corresponding Mw distribution of the pyrolytic lignin showed a significant decrease in low Mw phenols, accompanied by the formation of higher Mw oligomers. The PDI value was found to increase from 2.42 before treatment to 2.73 after treatment. The polydispersity of SA treated precursor increased slightly, suggesting that the reactivity of the functionalities in phenolic oligomers are varied, which resulted in a wider range of molecular distribution after polymerization. Sulfuric acid is an effective catalyst for polymerization reaction and it could protonate carbonyl, vinyl and hydroxyl groups to promote the overall reactivity of pyrolytic lignin.

Table 3.1. Relative weight average molecular weight (Mw) and polydispersity of pyrolytic lignin before and after treatments.

Pyrolytic lignin	Mw (Da)	Mn (Da)	Polydispersity	Total intensity percentage (%) (Molecular weight < 200 Da)
Without toluene wash	566	232	2.44	37.1
After toluene wash	810	335	2.42	16.3
SA treated	1267	464	2.73	11.9

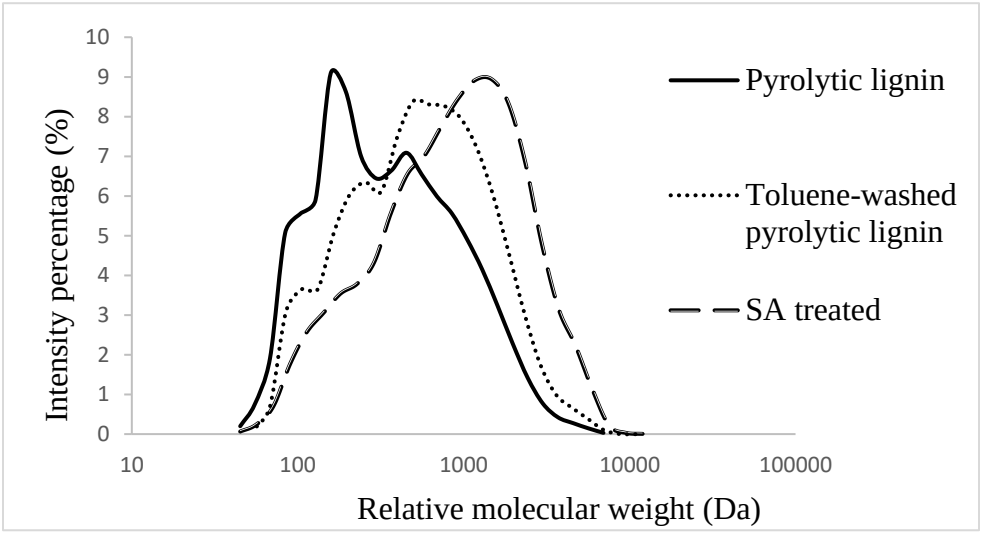

Figure 3.1 Relative molecular weight distribution of pyrolytic lignin before and after pretreatment.

3.3.1.2 GC/MS analysis

The compositions of the pyrolytic lignins with different treatments are compared in Figure 3.2. Phenolic oligomers are not shown in the chromatograms due to their low volatility in the GC column. The major phenolic monomers in the water-washed pyrolytic lignin include syringol, 1,2,4-trimethoxybenzene, 3',5'-dimethoxyacetophenone, 2,6-dimethoxy-4-(2-propenyl)-phenol, etc. Carbohydrate-derived organics, such as 1,2-cyclopentanedione, 2-cyclopenten-1-one, and levoglucosan were also found in the residues. After the toluene wash, peak intensities of the carbohydrate-derived organics and the majority of phenolic monomers decreased. However, the peak intensities of phenolic monomers that appear at retention times greater than 61 min did not change much. The phenolic monomers with higher retention times

have longer side chains and larger Mw. Apparently, the phenolic monomers with lower Mw have better solubility in toluene versus the higher Mw phenols. After acid-catalyzed polymerization, an overall decrease in the peak intensities of the compounds, regardless of their retention times, was observed. Particularly, the phenols with side chain C=C and C=O virtually disappeared, because these functional groups have a higher tendency for polymerization.

3.3.1.3 FTIR analysis

FTIR spectra of the pyrolytic lignin were also compared in Figure 3.3. The different peaks were normalized using the peak that appears at 1510 cm^{-1}, which represents aromatic-skeleton vibration. The peak at 3368 cm^{-1}, corresponding to an OH stretch, was the highest in water-washed pyrolytic lignin. It could be related to phenolic OH and residual water remaining in the sample. The peak was reduced in the toluene-washed pyrolytic lignin, due to the removal of water and some phenols. The remainders of the peaks in the FTIR spectra were similar for water-washed and toluene-washed pyrolytic lignin. The SA treatment decreased the OH band significantly, indicating that polymerization occurred through phenolic OH sites. The intensities of other IR bands also changed significantly SA treatment. The band appearing at 1700 cm^{-1}, represents conjugated aldehydes and carboxylic acid, decreased after the treatment since carbonyl groups are highly reactive. The blunt band appearing around 1634 cm^{-1} for both the water-washed and toluene-washed pyrolytic lignin is related to levoglucosan and other carbohydrate-derived residue compounds. It nearly disappeared after SA treatment. The band at 1602 cm^{-1} corresponds to aromatic skeletal vibrations plus C=O stretch also decreased due to the reactivity of C=O bond for polymerization.

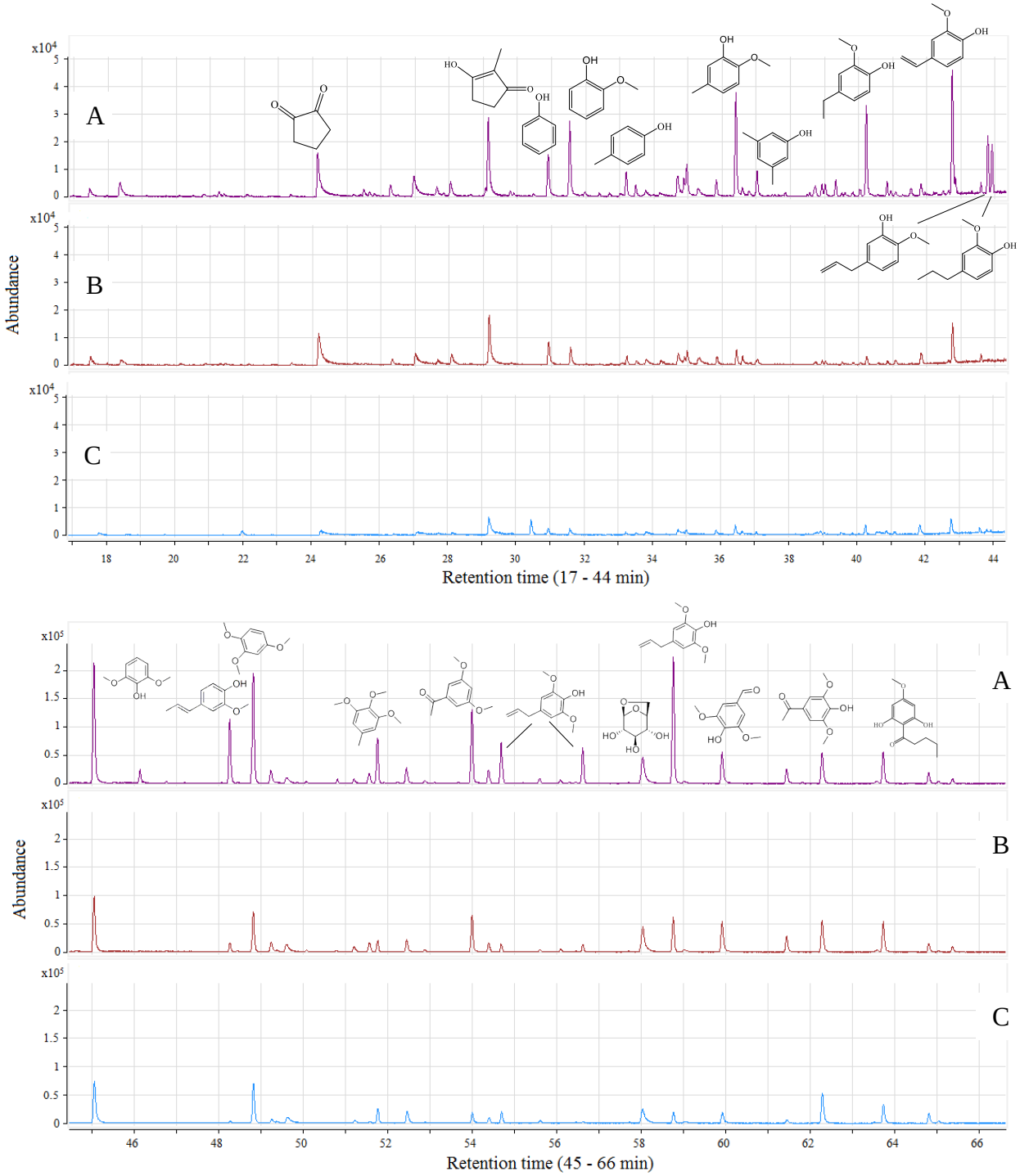

Figure 3.2 GC/MS chromatogram of pyrolytic lignin: A) Pyrolytic lignin; B) Toluene-washed pyrolytic lignin; C) SA treated precursor; Top: retention time (17-44 min); Bottom: retention time (45-66 min).

The bands that appear at 1500 cm^{-1} or below are related to different bond stretches associated with phenolic aromatic structures. For example, the band at 1200 cm^{-1} corresponds to C-C, C-O, and C=O stretch in the guaiacol structure; the bands at 1104 cm^{-1} and 1035 cm^{-1} represent aromatic C-H in plane deformation. Distinguishing these bands from each other became more difficult after the SA treatment, suggesting that the character of the phenolic structure disappears and a more condensed polyaromatic structure is formed. Previously, we noted that the aforementioned bands disappear in pyrolysis char of lignin due to its high polyaromatic structure [32]. The band that appears at 958 cm^{-1} related to –HC=CH out-of-plane deformation decreased, possibly due to the polymerization of vinyl or propyl bonds. Interestingly, the band that appears at 2842 cm^{-1} did not change significantly during the SA treatment. This suggests that demethoxylation or demethylation was negligible during polymerization of the pyrolytic lignin.

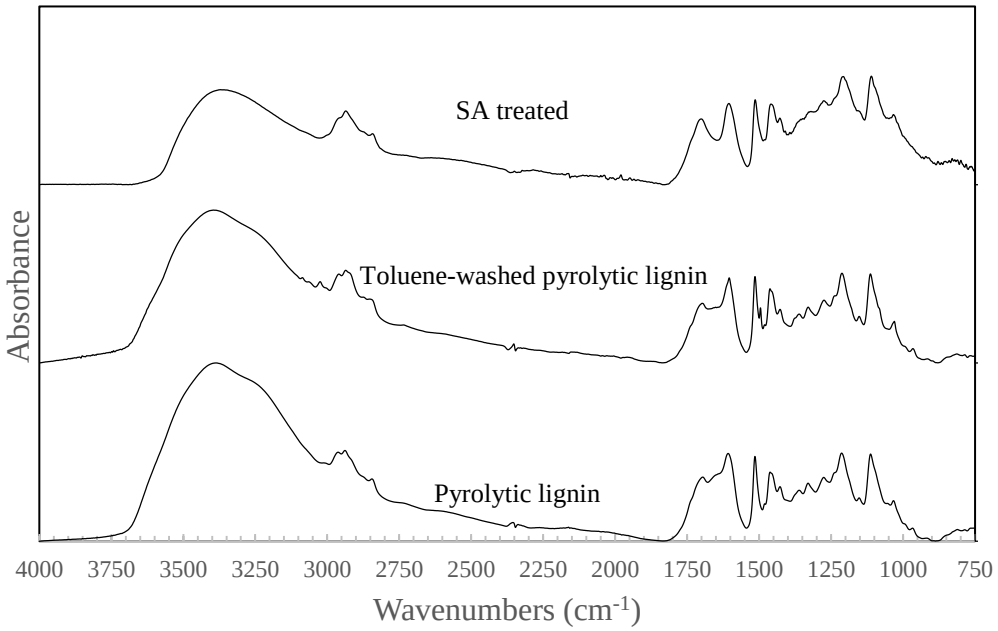

Figure 3.3 FTIR spectra of pyrolytic lignin before and after pretreatment.

3.3.1.4 Thermal stability

Thermal stability of the pyrolytic lignin was investigated using thermogravimetric analysis (TGA) and the TGA profiles are compared in Figure 3.4. The mass loss of toluene-washed pyrolytic lignin began below 100 °C, probably due to incomplete removal of water, toluene and other low molecular weights products remaining in the pyrolytic lignin. In comparison, the SA treatments greatly improved the thermal stability of the pyrolytic lignin. The major mass loss did not begin until the temperature was above 150 °C (mass loss < 1%). The SA-treated pyrolytic lignin had a good thermal stability and the higher mass residue (i.e., 35%) at the end of the heating, which corresponds to the results obtained from GPC and FTIR, indicating it contained compounds with higher Mw and more condensed structure.

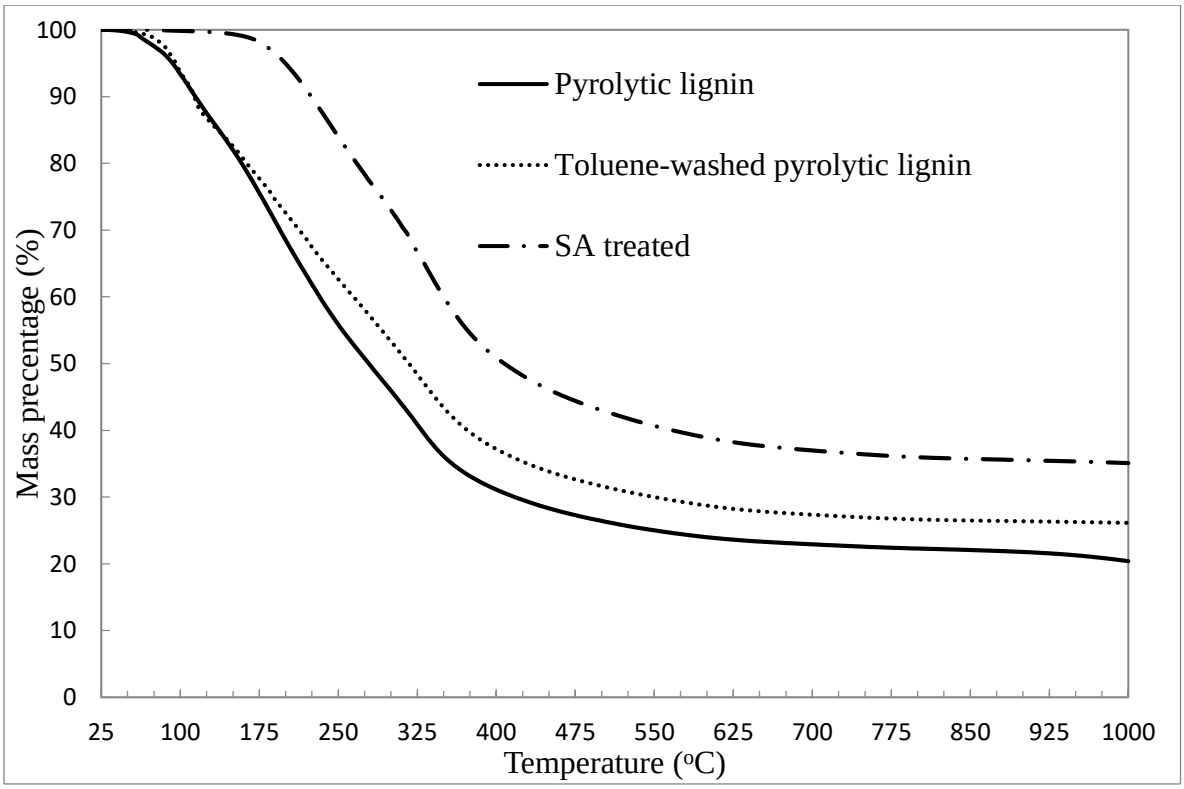

Figure 3.4 TGA profiles of toluene-washed pyrolytic lignin and SA treated precursor.

3.3.1.5 Elemental composition of pyrolytic lignin

The elemental analysis of the pyrolytic lignin before and after treatment is given in Table 3.2. The carbon content in pyrolytic lignin before the toluene wash was 54.84% and the oxygen content was 38.52%. After the toluene wash, carbon content increased to 61.73% and the oxygen content decreased to 31.34% since the residual water was removed. After the SA treatment, the carbon content further increased to 64.35%, whereas, oxygen content decreased. Hydrogen content also decreased, suggesting that condensation polymerization during the SA treatment possibly produced water as the byproduct, which was then evaporated. The concentration of sulfur increased since the sulfur would remain in the pyrolytic lignin after polymerization.

Table 3.2 Elemental composition of pyrolytic lignin before and after pretreatments.

Pyrolytic lignin	C (%)	H (%)	N (%)	S (%)	O (%)*
Before toluene-wash	54.84	5.89	0.74	0.01	38.52
After toluene-wash	61.73	6.21	0.71	0.01	31.34
SA treated	64.46	5.64	0.62	0.13	29.15

* By difference.

3.3.1.6. Differential Screening Calorimetry

The DSC curves of the SA-treated pyrolytic lignin were measured and the results are shown in Figure 3.5. The sharp peak on the DSC curve, as the indicator of glass transition temperature (T_g), was not found. Instead, the DSC curve of the pyrolytic lignin was relatively smooth over the course of measurement. This is due to the nature of pyrolytic lignin, which is a mixture of various phenolic compounds. However, small dip was identified on the curve and the T_g could be assigned, which was 101 °C. It is known that hardwood lignin usually has a lower T_g than the lignin originating from other biomass species [33], and this could also apply

to pyrolytic lignin derived from hardwood lignin. The degree of cross-linking and Mw could impact T_g of the materials. Increased Mw and more condensed aromatic structure in the SA-treated pyrolytic lignin are likely responsible for the T_g.

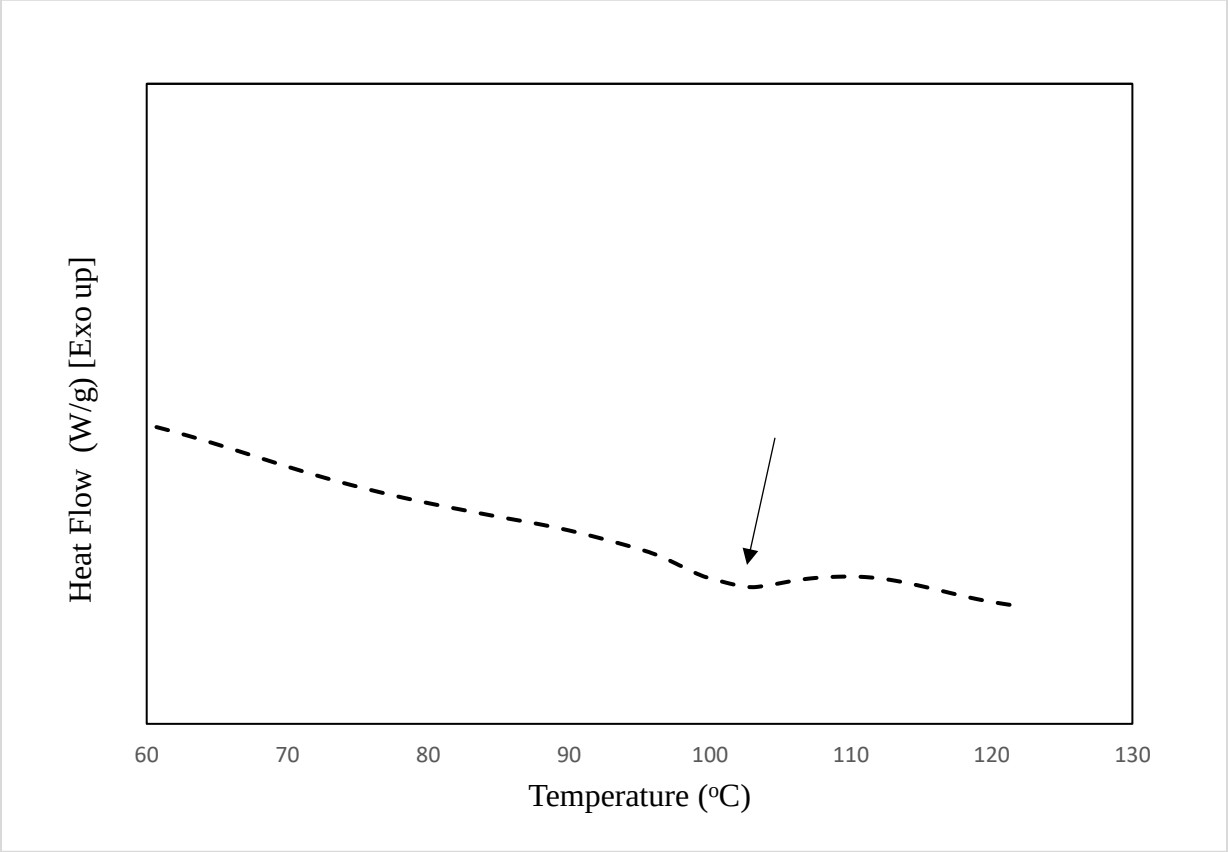

Figure 3.5 DSC profiles of the SA treated precursor (Tg = 101 °C).

3.3.2 Carbon Fiber Processing

The water-washed and toluene-washed pyrolytic lignins were highly viscous at room temperature. Increasing temperature to 80 ºC reduced the viscosity of the liquid sufficiently allowing fibers to be spun continuously. However, the spun fibers fused together upon cooling to room temperature. This was due to the low Mw and T_g of the precursors. By further increasing the spinning temperature, the viscosity of the pyrolytic lignins reduced, making them unable to form a continuous fiber. In comparison, the SA treated pyrolytic lignin was able to spin into fibers continuously upon heating. The fiber-spinning temperature was

determined based on the TGA and DSC results previously shown. A spinning temperature higher than its softening point is preferred, while high temperature could cause decomposition and volatilization of the precursor. Therefore, the spinning temperature was initially set at 115 ºC for the SA treated pyrolytic lignin. Based on the TGA analyses, the mass loss of the precursor at the temperature was negligible and no volatile formation was expected during the fiber spinning process.

The spun fibers were subjected to oxidative thermal stabilization. Stabilization is a critical step in determining the overall properties of carbon fibers. The fiber is converted from a thermoplastic material into a thermoset material after stabilization. Usually, a low heating rate is required to assure adequate oxidation, and cross-linking among inter and intra molecules occurs with increasing temperature. The T_g of the fiber needs to be higher than the stabilization temperature in the course to retain the rigidity of the fiber and prevent thermal fusion. Tension was not applied to the fiber during stabilization. However, it was noticed that the fibers that vertically hung on the metal rack stretched during the stabilization due to gravity. After stabilization, the stabilized fibers become stronger and more flexible than the as-spun fibers.

Carbonization removes most of the other organic elements in the fibers and increases carbon content. A condensed polyaromatic structure is also formed during carbonization. CHN analysis indicated that the carbon content exceeded 93% after carbonizing the fibers at 1000 ºC.

3.3.3 Characterization of Carbon Fiber and Discussion

As shown in Table 3.3, the average tensile strength and modulus of the carbon fibers produced from the SA-treated pyrolytic lignin were 0.855 GPa and 85 GPa, respectively. The maximum values of individual fiber reached a tensile strength of 1.014 GPa and modulus of 122 GPa. The average diameter of the fibers was 36 μm. SEM images of the carbon fibers

produced from the SA treated pyrolytic lignin are shown in Figure 3.6. It could be observed that carbon fiber produced from pyrolytic lignin based precursor in this study is smooth and solid.

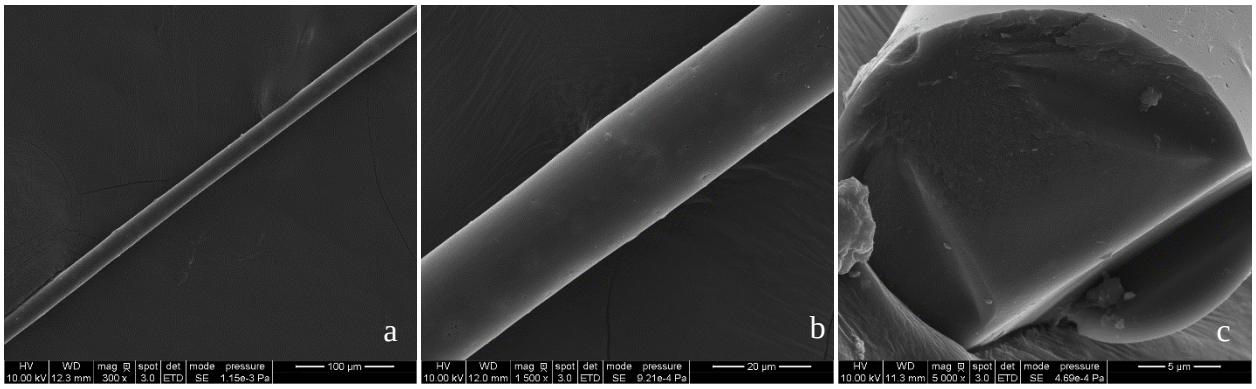

Figure 3.6 SEM images of carbon fibers produced from SA treated precursor

In the present study, carbon fibers were made from pyrolytic lignin by the repolymerization of lignin-derived phenolic monomers and oligomers. However, repolymerization of the depolymerized lignin does not reversibly form lignin. During fast pyrolysis, a high level of thermal energy is provided to lignin within an extremely short time to promote rapid dissociation of chemical bonds. As a result, the ether and ester bonds that connecting aromatic ring units cleave and various chemical reactions occur. Not only a number of phenolic monomers and oligomers are formed, but CO_2, CO, CH_4 and H_2O are also released through decarboxylation, decarbonylation, demethylation and dehydrogenation [34]. The pyrolytic lignin is ready to repolymerize due to the reactivity, but rearrangement of the phenolics would form a modified polymer rather different from the original lignin [35].

Table 3.3 compares the properties of the carbon fibers produced in the present study with two types of lignin-based carbon fibers reported in literature. The reference carbon fibers are made from a hardwood lignin [3] or acetylated softwood lignin [36] through well-optimized processes, representing the highest quality a lignin-based carbon fiber can achieve, to date.

While the mechanical properties of the carbon fibers obtained from the SA treated pyrolytic lignin were nearly comparable to the two reference carbon fibers, the quality of the pyrolytic lignin-based carbon fibers could be further improved by optimizing the precursor and processing conditions.

Table 3.3 Comparison of mechanical properties of carbon fibers produced in the present work with the best-quality lignin-based fibers from previous studies.

Sample	Tensile strength (GPa)	Modulus (GPa)	Strain (%)	Diameter (μm)	Tension
SA treated	0.855 ± 0.159(1.014)*	85 ± 37 (122)	1.01 ± 0.3	29 - 50	No
Kraft hardwood [3]	1.07	83	1.29	<10	Yes
Acetylated softwood [36]	0.510 ± 0.05	30 ± 2	1.7 ± 0.1	22.5	No
	1.05 ± 0.07	35 ± 3	3.0 ± 0.2	5.9 ± 0.2	Yes

*Values in parentheses stands for the highest value obtained among all tests.

The diameters of the carbon fibers produced in the present study were significantly larger than that of the reference fibers which are below 10 μm. It is known that the tensile strength of the fiber is highly dependent of fiber diameter [37]. The thinner the fiber obtained, the higher tensile strength it will retain. Improving the sheer force of the fibers during the spinning process by using a smaller sized die and higher fiber spinning rate could reduce the fiber diameter. Applying tension during stabilization and carbonization can also reduce the diameter of the fibers. Applying tension would also improve the orientation of the fiber molecules, therefore, increasing the mechanical property of the fibers [38]. Meng and Ogale [39] reported the length of the acetylated softwood lignin fibers stretched as much as 8 times when tension was applied during stabilization process. By applying tension during both stabilization and carbonization, they were able to produce the carbon fibers with diameter of 7

μm, a tensile strength of 1.01 GPa and modulus of 53 GPa. Without tension, the tensile strength of the carbon fiber was 0.53 GPa.

While stabilization time depends on the T_g of the fibers, the Mw of the pyrolytic lignin and T_g can be manipulated by adjusting the concentration of SA and/or pretreating temperature and time. The precursor fibers with higher T_g can be stabilized in shorter times. However, too high T_g is not preferred as it may produce a precursor that becomes difficult to spin into fiber.

Although, further optimization is still needed, the properties of the pyrolytic lignin based carbon fibers in the present study are comparably high. Pyrolytic lignin is structurally different from lignin. Wang et al. [14] previously reported that pyrolytic lignin contains newly formed unconjugated C-O functional groups and a fewer amount of methoxyl groups in comparison to lignin. Therefore, repolymerizing the lignin-derived phenolic monomers and oligomers may have resulted in a modified polymer with an improved potential as the precursor in comparison to lignin.

3.4 Conclusions

Carbon fibers were made from pyrolytic lignin isolated from the heavy fraction of bio-oil. Pyrolytic lignin is a mixture of phenolic monomers and oligomers derived from the thermal decomposition of lignin. The pyrolytic lignin was first washed with toluene to remove low-Mw compounds and to narrow the Mw distribution. The pyrolytic lignin was repolymerized in the presence of an acid catalyst to increase both thermal stability and the T_g of the precursor. After melt-spinning, oxidative stabilization and carbonization, the average tensile strength and modulus of the carbon fibers were 0.855 GPa and 85 GPa, respectively. Individual carbon fiber obtained a tensile strength as high as 1.014 GPa and a modulus of 122 GPa. The results of the present study suggest that pyrolytic lignin is a promising precursor for the production of low-cost carbon fibers.

3.5 References

1. Frank, E., F. Hermanutz, and M.R. Buchmeiser, *Carbon fibers: precursors, manufacturing, and properties.* Macromolecular materials and engineering, 2012. **297**(6): p. 493-501.
2. Liu, Y. and S. Kumar, *Recent progress in fabrication, structure, and properties of carbon fibers.* Polymer Reviews, 2012. **52**(3): p. 234-258.
3. Baker, D.A. and T.G. Rials, *Recent advances in low-cost carbon fiber manufacture from lignin.* Journal of Applied Polymer Science, 2013. **130**(2): p. 713-728.
4. Norgren, M. and H. Edlund, *Lignin: recent advances and emerging applications.* Current Opinion in Colloid & Interface Science, 2014. **19**(5): p. 409-416.
5. Pan, X., et al., *Biorefining of softwoods using ethanol organosolv pulping: Preliminary evaluation of process streams for manufacture of fuel-grade ethanol and co-products.* Biotechnology and bioengineering, 2005. **90**(4): p. 473-481.
6. Kadla, J., et al., *Lignin-based carbon fibers for composite fiber applications.* Carbon, 2002. **40**(15): p. 2913-2920.
7. Saito, T., et al., *Methanol fractionation of softwood kraft lignin: Impact on the lignin properties.* ChemSusChem, 2014. **7**(1): p. 221-228.
8. Li, Q., et al., *Molecular weight and uniformity define the mechanical performance of lignin-based carbon fiber.* Journal of Materials Chemistry A, 2017. **5**(25): p. 12740-12746.
9. Norberg, I., et al., *A new method for stabilizing softwood kraft lignin fibers for carbon fiber production.* Journal of Applied Polymer Science, 2013. **128**(6): p. 3824-3830.
10. Luo, J., et al., *Lignin recovered from the near-neutral hemicellulose extraction process as a precursor for carbon fiber.* BioResources, 2011. **6**(4): p. 4566-4593.
11. Qiao, W., et al., *Carbon fibers and films based on biomass resins.* Energy & fuels, 2005. **19**(6): p. 2576-2582.
12. Prauchner, M., et al., *Biopitch-based general purpose carbon fibers: Processing and properties.* Carbon, 2005. **43**(3): p. 591-597.
13. Wang, S., et al., *Pyrolysis behaviors of four lignin polymers isolated from the same pine wood.* Bioresource technology, 2015. **182**: p. 120-127.
14. Wang, S., et al., *Comparison of the pyrolysis behavior of pyrolytic lignin and milled wood lignin by using TG–FTIR analysis.* Journal of Analytical and Applied Pyrolysis, 2014. **108**: p. 78-85.
15. Baker, D.A., N.C. Gallego, and F.S. Baker, *On the characterization and spinning of an organic-purified lignin toward the manufacture of low-cost carbon fiber.* Journal of Applied Polymer Science, 2012. **124**(1): p. 227-234.
16. Mohan, D., C.U. Pittman, and P.H. Steele, *Pyrolysis of wood/biomass for bio-oil: a critical review.* Energy & fuels, 2006. **20**(3): p. 848-889.
17. Rover, M.R., et al., *Stabilization of bio-oils using low temperature, low pressure hydrogenation.* Fuel, 2015. **153**: p. 224-230.
18. Hüttermann, A., C. Mai, and A. Kharazipour, *Modification of lignin for the production of new compounded materials.* Applied microbiology and biotechnology, 2001. **55**(4): p. 387-394.

19. Effendi, A., H. Gerhauser, and A.V. Bridgwater, *Production of renewable phenolic resins by thermochemical conversion of biomass: a review.* Renewable and Sustainable Energy Reviews, 2008. **12**(8): p. 2092-2116.
20. Williams, R.C., et al. *Utilization of fractionated bio oil in asphalt*. in *88th annual meeting of the Transportation Research Board, Washington, DC*. 2009.
21. Stevens, J. and D.J. Gardner, *Enhancing the fuel value of wood pellets with the addition of lignin.* Wood and Fiber Science, 2010. **42**(4): p. 439-443.
22. Qin, W. and J. Kadla, *Carbon fibers based on pyrolytic lignin.* Journal of Applied Polymer Science, 2012. **126**(S1).
23. Sahaf, A., et al., *Rheological Properties and Tunable Thermoplasticity of Phenolic Rich Fraction of Pyrolysis Bio-Oil.* Biomacromolecules, 2013. **14**(4): p. 1132-1139.
24. Fratini, E., et al., *SANS analysis of the microstructural evolution during the aging of pyrolysis oils from biomass.* Langmuir, 2006. **22**(1): p. 306-312.
25. Hilten, R.N. and K. Das, *Comparison of three accelerated aging procedures to assess bio-oil stability.* Fuel, 2010. **89**(10): p. 2741-2749.
26. Pollard, A., M. Rover, and R. Brown, *Characterization of bio-oil recovered as stage fractions with unique chemical and physical properties.* Journal of Analytical and Applied Pyrolysis, 2012. **93**: p. 129-138.
27. Zhou, S., et al., *Effect of sulfuric acid concentration on the yield and properties of the bio-oils obtained from the auger and fast pyrolysis of Douglas Fir.* Fuel, 2013. **104**: p. 536-546.
28. Meng, J., et al., *Toward understanding of bio-oil aging: Accelerated aging of bio-oil fractions.* ACS Sustainable Chemistry & Engineering, 2014. **2**(8): p. 2011-2018.
29. Thunga, M., et al., *Bio-renewable precursor fibers from lignin/polylactide blends for conversion to carbon fibers.* Carbon, 2014. **68**: p. 159-166.
30. Bayerbach, R., et al., *Characterization of the water-insoluble fraction from fast pyrolysis liquids (pyrolytic lignin): Part III. Molar mass characteristics by SEC, MALDI-TOF-MS, LDI-TOF-MS, and Py-FIMS.* Journal of analytical and applied pyrolysis, 2006. **77**(2): p. 95-101.
31. Wang, S., et al., *Multi-step separation of monophenols and pyrolytic lignins from the water-insoluble phase of bio-oil.* Separation and Purification Technology, 2014. **122**: p. 248-255.
32. Zhou, S., R.C. Brown, and X. Bai, *The use of calcium hydroxide pretreatment to overcome agglomeration of technical lignin during fast pyrolysis.* Green Chemistry, 2015. **17**(10): p. 4748-4759.
33. Nordström, Y., et al., *A new softening agent for melt spinning of softwood kraft lignin.* Journal of Applied Polymer Science, 2013. **129**(3): p. 1274-1279.
34. Yang, H., et al., *Characteristics of hemicellulose, cellulose and lignin pyrolysis.* Fuel, 2007. **86**(12): p. 1781-1788.
35. Bayerbach, R. and D. Meier, *Characterization of the water-insoluble fraction from fast pyrolysis liquids (pyrolytic lignin). Part IV: Structure elucidation of oligomeric molecules.* Journal of Analytical and Applied Pyrolysis, 2009. **85**(1-2): p. 98-107.
36. Zhang, M. and A.A. Ogale, *Carbon Fibers Derived from Acetylated Softwood Kraft Lignin*, in *Polymer Precursor-Derived Carbon*. 2014, American Chemical Society. p. 137-152.

37. Tagawa, T. and T. Miyata, *Size effect on tensile strength of carbon fibers.* Materials Science and Engineering: A, 1997. **238**(2): p. 336-342.
38. Ozbek, S. and D. Isaac, *Strain-induced density changes in PAN-based carbon fibres.* Carbon, 2000. **38**(14): p. 2007-2016.
39. Zhang, M., J. Jin, and A.A. Ogale, *Carbon Fibers from UV-Assisted Stabilization of Lignin-Based Precursors.* Fibers, 2015. **3**(2): p. 184-196.

CHAPTER 4. MELT-SPINNABLE LIGNIN-BASED POLYMER WITH IMPROVED MOLECULAR ORIENTATION THROUGH CO-POLYMERIZATION OF PYROLYTIC LIGNIN AND POLYETHYLENE TEREPHTHALATE TOWARD CARBON FIBER PRODUCTION

(A paper under review in *Composite Part A: Applied Science and Manufacturing*)

ABSTRACT

The lack of molecular orientation and flow orientability in the precursor is considered to be the most critical issue of lignin-based materials that leads to the poor quality of resulting carbon fibers. To obtain a lignin-based melt-spinnable polymer with better molecular orientation, lignin-derived phenolic oil is co-polymerized with polyethylene terephthalate (PET) in this study. The phenolic oil, called pyrolytic lignin (PL), facilitated the chain scission and fragmentation of PET, and the fragmentized PET subsequently co-polymerized with PL to form PL-PET polymers containing linear PET backbones. Co-polymerization with PET was also found to increase thermal stability and decrease T_gs of the polymers, despite increasing molecular weights. Dynamic rheology tests confirmed that the PL-PET polymers have better chain alignment and flow orientability. PL-PET polymers were also found to have increased strains of their stabilized fibers, higher tensile strengths, and lowered I_D/I_G ratios of the resulting carbon fibers by Raman spectra analysis.

Key words: A:Carbon fibres, B: Chemical properties; B: Mechanical properties; E: Melt-spinning

4.1 Introduction

Carbon fiber is a lightweight material with excellent mechanical properties. As an advanced material, carbon fiber has applications in many areas including aerospace, sporting goods, construction, wind turbine and automobile industries. However, the high cost of polyacrylonitrile (PAN), which is the main precursor of carbon fiber, limits its widespread applications [1, 2]. For decades, extensive research has been devoted to search for low-cost alternatives of PAN. Lignin has been considered a promising alternative precursor of carbon fiber due to its aromaticity, renewable nature, and large availability at low cost [3, 4]. Various types of lignin derived from different biomass species and extraction methods could be used as the starting materials to manufacture carbon fiber. To date, many different approaches have been developed to improve the processability of lignin precursors and the quality of the resulting carbon fiber. For example, inorganic impurities in lignin, which otherwise cause structural defects in carbon fiber, were removed by prewashing lignin with an acidic solution or employing higher-purity organosolv lignin as the starting materials [5]. The volatile content was removed by pretreating the lignin in a vacuum oven at elevated temperatures prior to fiber spinning to avoid porous carbon fibers [6]. The polydispersity of lignin was reduced by fractionating lignin using organic solvents, thus enabling lignin with narrower molecular distribution [7, 8]. The difficulties in melt-spinning of softwood lignin and stabilization of hardwood lignin as-spun fiber were overcome by blending them prior to processing [9]. In addition, lignin was either mixed with other polymers [6], or chemically modified (hydrotreatment, acetylation, etc.) to improve its processability [10-12]. Despite the efforts, the tensile properties of lignin-based carbon fibers are only comparable to low-quality, pitch-based carbon fiber, far inferior to commercial grade PAN-based carbon fiber [13]. It has been pointed out that the lack of molecular orientation and intrinsic heterogeneity in lignin severely

limits the quality of resulting carbon fiber [3, 13]. Shear-induced uniaxial orientation is well-known to play a critical role in the tensile properties of nearly all synthetic fibers ranging from Kevlar to Rayon to PAN-based carbon fiber resins. While PAN is a well-defined and linear polymer with good flow orientability, lignin is a three-dimensional aromatic polymer that is formed via random crosslinking of its three basic phenylpropane units [14]. Upon stabilization followed by carbonization, the PAN precursor could develop a well-organized turbostratic graphitic structure, whereas the irregular lignin precursor that is absent of molecular orientation forms an amorphous carbon material with significant structural defects [15]. Frank et al. [13] pointed out that the molecular orientation must be achieved before the precursor fiber is stabilized or carbonized, because high temperature processing cannot improve its molecular orientation. Overall, the inherent deficiency in lignin structure is the fundamental cause for the low quality of lignin-based carbon fibers. However, few of the current approaches modified lignin at molecular levels to improve its molecular orientation.

One of the potentially viable approaches to improve molecular orientation could be introducing linear backbone of well-defined polymer into lignin through co-polymerization. However, it is difficult to achieve this goal without modifying lignin prior to co-polymerization. This is because lignin has low reactivity and poor miscibility with most polymers. The large molecular size of lignin also prevents the lignin from forming a new polymer using other polymer chain as its backbone. In previous studies, lignin was co-extruded with linear polymers such as polylactic acid (PLA) [16] or polypropylene (PP) [17]. However, co-polymerization did not occur. Instead, the polymers merely acted as plasticizers to improve the spinning performance. Porous carbon fibers were formed as the result of the co-extrusion since PLA or PP depolymerized or volatilized during the high-temperature processing. Poor

miscibility of lignin and the polymers could also introduce voids in resulting carbon fibers. Moreover, the absence of fixed carbon in PLA or PP, and the lack of chemical bonding between lignin and the polymers are likely to make the precursors incapable of forming condensed structures during carbon fiber processing. The improved blending of lignin and other polymers was occasionally reported. For example, Kubo et al. [17] co-extruded lignin and polyethylene terephthalate (PET) and reported that PET and lignin have better miscibility. Ding et al. [11] butylated lignin prior to blending with PAN to improve the miscibility between lignin and PAN. These previous studies confirm that it is difficult to co-polymerize lignin with other polymers without any pretreatment.

To prepare a lignin-based co-polymer, lignin-derived phenolic oil called pyrolytic lignin, was co-polymerized with PET in the present study. PET is a thermoplastic polyester containing repeated benzene ring units on its polymer chain [18]. While PET is a petroleum-derived polymer, bio-based PET has also become increasingly available in recent years [19]. Compared to other common plastics, PET has a relatively high fixed carbon content, and thus is better suited as carbon material [20, 21]. PET also does not emit toxic gas during carbonization [20]. It is desired that the co-polymer could utilize the linear molecular chain of PET as the backbone to improve its molecular orientation. Pyrolytic lignin is not a technical lignin extracted from biomass using conventional methods. Instead, it is a thermally depolymerized lignin. A term of “pyrolytic lignin” (PL) is commonly used, since it is obtained by depolymerizing lignin or lignin containing biomass using fast pyrolysis technique [22]. When lignin is pyrolyzed, various C-C and C-O bonds between monomeric units cleave and as a result, the macromolecular network of lignin is completely destroyed. Various reactions, such as hydrogen abstraction and transfer, free radical coupling, dehydration, demethylation,

decarbonization and decarboxylation, could occur during pyrolysis. Finally, a viscous liquid containing various sizes of phenolic monomers and oligomers are obtained through quenching the arising vapors. Therefore, the average molecular weight (Mw) of PL is much smaller than its parent lignin (hundreds vs. thousands). PL has a good solubility in many common organic solvents due to its low Mw [23]. Pyrolytic lignin is also known for its high reactivity, which can repolymerize even during cold storage. Reactive functionalities such as hydroxyl, carbonyl and vinyl groups present in PL could easily initiate secondary reactions and repolymerization. The presence of free radicals among PL was also confirmed in previous study [24]. PL also has an improved spinnability and high carbon content compared to lignin, and thus can be used as the starting material for carbon fiber production [25, 26].

As described above, PL has many unique characteristics compared to technical lignin. Especially, its higher reactivity and low Mw compared to lignin may render itself a much more attractive starting material for co-polymerization. In this work, PL and PET were co-polymerized and the properties and characteristic performance of the resulting polymer were assessed.

4.2 Experimental Section

4.2.1 Materials

PL was produced in the BioCentury Research Farm at Iowa State University [27]. The bio-oil collected in first condenser was water washed to isolate lignin-derived PL as the water insoluble. The detailed characterization of the PL is reported in our previous work [26, 27]. PET powders with the Mw of 25000 Da and 99.9% purity was purchased from Shanghai GuanBu Electromechanical Technology Co., Ltd, China.

4.2.2 Precursor Production and Fiber Processing

Twenty grams of PL and PET (5% or 20% of PL weight equivalent) were placed inside a beaker and heated in a silicone oil bath at 200 ℃. After stirring the mixture of PL and PET using a magnetic bar for 90 mins, the resulting product was cooled to room temperature and pelletized. The newly obtained co-polymers were designated as PL-5PET and PL-20PET. For comparison, PL alone was also treated at the same conditions and the resulting polymer was designated as PL-0PET. In this work, PL-0PET was also mixed with 5% or 20% of PET at room temperature and the mixtures are designated as PL-5PET (p) and PL-20PET (p). In the mixtures, the mass percentage of PET is 5% or 20% of the initial mass of PL before the treatment. The PL-PET (P) mixtures were only used as controls to compare with PL-PET co-polymerized polymers, and not further processed for carbon fiber. The polymers were extruded in a twin-screw micro compounder (DACA Instruments, Santa Barbara, CA) preheated at 200 ℃. Extrudates were drawn into fibers and wound on a roller (DSM, Geleen, Netherlands) at a speed of 100 m/min. During the spinning, the temperature of the extruder was slightly adjusted for optimal spinning performance. Oxidative stabilization of the drawn fibers was conducted in a convection oven. For comparison, the polymers were heated to 260 ℃ at different heating rates of 0.1, 0.3, or 0.5 ℃/min, and then kept at the final temperature for additional 1 hr. The stabilized fibers were carbonized in a tubular furnace purged by argon gas. During carbonization, the furnace was heated to 1000 ℃ at a heating rate of 3 ℃/min and then held for 1 hr.

4.2.3 Characterizations

Elemental composition was determined using an elemental analyzer (Vario Micro Cube, Elementar, Germany). Gel permeation chromatography (GPC) analysis was conducted using Dionex Ultimate 3000 series high performance liquid chromatography (HPLC) equipped

with a Shodex Refractive Index (RI) and Diode Array Detectors (DAD). Two GPC columns (3 µm, 100 Å, 300×7.5 mm; PLgel, Agilent, p/n PL1110-6320) were calibrated with six monodispersed polystyrene standards ranging from 162 g/mol to 38640 g/mol. Tetrahydrofuran (THF) was used as the solvent and eluent in the column. Fourier Transform Infrared (FTIR) analysis was conducted using a Thermo Scientific Nicolet iS10 (Thermo Fisher Scientific Inc., Waltham, MA) equipped with a Smart iTR accessory. [$^{1}H^{13}C$] 2D-NMR heteronuclear single-quantum coherence (HSQC) spectroscopies were obtained at 25 ℃ using a Bruker Biospin Advance 600 MHz spectrometer. The solvent was composed of dimethyl sulfoxide (DMSO)-d6 and pyridine-d5 at a 4 to 1 volume ratio. Thermal stability of the precursors was evaluated using a thermal gravimetric analyzer (TGA/DSC 1 STARe system, Mettler Toledo). Approximately 30 mg of each sample was heated under a nitrogen environment from room temperature to 1000 ℃ at a heating rate of 10 ℃/min. TGA was also used to simulate stabilization (using air) and carbonization (using nitrogen) of as-spun fibers with programmable heating processes that correspond to actual experiments. Glass transition temperature (T_g) was determined using a differential scanning calorimeter (DSC, Q2000, TA instruments). Each sample was first rapidly heated to 200 ℃ and then cooled to 25 °C to eliminate thermal history. Finally it was reheated to 200 ℃ at a heating rate of 10 ℃/min. Rheology measurements of the polymers were performed using a Discovery hybrid rheometer (DHR-2, TA Instruments) with 25 mm parallel-plate geometry. A dynamic frequency sweep (0.1 rad/s to 100 rad/s) was conducted at 200 ℃ with strain of 1.25%. For isothermal test with changing retention time, the angular frequency was fixed at 10 rad/s and strain at 1.25%. Mechanical properties of the stabilized fibers were also determined using the same rheometer with dynamic mechanical analysis (DMA) clamps using ASTM Standard C1557, and the

average of 20 fiber filaments were reported. Raman spectrum of carbon fiber was characterized using a confocal Raman system (Voyage, B&W Tek, Inc. and Olympus BX51). A 532 nm Raman laser of 1.84 mW was focused on the fiber with a 20 × lens. A 10s integration time was used to obtain the spectrum and origin software was used to analyze the acquired Raman spectra with Gaussian-Lorentzian curve fitting. The microstructure of the carbon fiber samples was examined using a scanning electron microscope (SEM, Quanta-FEG 250, FEI) at 10 kV accelerating voltage.

4.3 Results and Discussions

4.3.1 Co-polymerization of PL and PET

Pyrolytic lignin (PL) is a mixture of phenolic monomers and oligomers with an average Mw of 566 Da. Upon treatment, PL-5PET, PL-20 PET and PL-0PET were all viscous liquid at 200 ℃. Once cooled down to room temperature, the liquids turned into homogenous dark-brown solids. In comparison, PL-5PET (p) and PL-20PET (p) were light brown solids due to the presence of un-melted white PET particles among the mixtures (Fig. 4.1). The melting temperature of PET is 245~250 ℃, which is considerably higher than 200 ℃ for producing the polymers. The melting property of PET was alternated due to the co-treatment with PL.

PL, PL-0PET, and the THF soluble fractions of PL-5PET and PL-20PET were subjected to GPC analysis and their Mw distributions are plotted in Fig. 4.2. The phenolic oligomers in PL are highly reactive, and elevated temperatures could accelerate polycondensation and repolymerization reactions, leading to the increase of Mw for PL-0PET. The repolymerization also increased the PDI from 2.44 for PL to 2.97 for PL-0PET. Since PET is insoluble in THF, the GPC curves of PL-0PET, PL-5PET and PL-20PET should be identical if PL and PET molecules did not react. The GPC curves of the PL-PET precursors, however, both shifted to the higher Mw region in comparison to PL-0PET. In fact, the shift was more

obvious for PL-20PET than it for PL-5PET. The PDI were 2.80 in both PL-5PET and PL-20PET, slightly lower compared to PL-0PET. These changes are indicative of the formation of new molecular structures in the PL-PET polymers. Specifically, the peaks representing smaller Mw (23 and 26 min) decreased in PL-PET polymers, suggesting that PL converted into higher Mw compounds when co-polymerized with PET.

Unlike the PL-0PET that was fully soluble in THF, the PL-PET polymers were partly insoluble (3.7% for PL-5PET and 15.2% for PL-20PET). The masses of the dark-brown colored THF-insoluble fractions were smaller than the initial masses of PET (55% lower for PL-5PET, 43% lower for PL-20PET). These insoluble fractions are likely to have higher Mws than the soluble fractions since higher Mw usually reduces the solubility of a compound in organic solvents. In terms of preparing carbon fiber, a precursor with higher Mw is preferred because a longer molecular chain contributes to the structural continuity during fiber processing. In the present study, both the THF soluble and insoluble parts were used for carbon fiber processing.

The mass yields of PL-0PET, PL-5PET and PL-20PET are compared. The yield of PL-0PET was 55%, indicating volatiles released when PL repolymerizes. Although repolymerization is the major reaction pathway of PL at 200 ℃, light gases can be produced from polycondensation, dehydration, decarboxylation and decarbonylation reactions. The yields of the PL-5PET (55.3%) and PL-20PET (58.6%) were both higher compared to the yield of PL-0PET, mainly owing to higher thermal stability of PET. Since PET does not decompose at temperatures below 375 ℃, predicted yields of the PL-5PET (57.1%) and PL-20PET (62.5%) can be calculated under an assumption that there is no mass loss from PET fraction. The experimental yields were lower than the predicted yields in both PL-5PET and PL-20PET.

The results suggest that the co-polymerization between PL and PET involves volatile generation.

The FTIR spectra of different polymers are given in Fig. 4.3. The spectra of PL-5PET (p) and PL-20PET (p) are also plotted for comparison. Identifications of the peaks are based on literature [28-32]. Typical FTIR peaks of PET include C=O at 1720 cm^{-1}, CH_2 wagging at 1340 cm^{-1}, C-C-O group at 1240 cm^{-1} and 1093 cm^{-1}, and 1,4-aromatic substitution at 1014 cm^{-1} and 1120 cm^{-1}. On the other hand, the peaks representing OH (3412-3460 cm^{-1}), aromatic skeletal vibrations plus C=O stretch (1593-1605 cm^{-1}), aromatic skeletal vibrations (1505-1515 cm^{-1}), and aromatic and aliphatic C-H (1422-1430 cm^{-1}, 2842-3000 cm^{-1}) were pronounced in PL-0PET. When comparing the spectrum of PL-5PET to PL-5PET (p), and PL-20PET to PL-20PET (p), the intensities of several typical peaks standing for PET decreased in the PL-PET polymers. Specifically, the peak at 1720 cm^{-1} for C=O, 1405 cm^{-1} for aliphatic C-H, 1340 cm^{-1} for CH_2 wagging, 1240 cm^{-1} and 1093 cm^{-1} for C-C-O group, 1014 cm^{-1} and 858 cm^{-1} for aromatic C-H decreased. Also, the hydroxyl peak at 3412-3460 cm^{-1} decreased in PL-5PET but increased in PL-20PET compared to the peaks at their corresponding physical mixtures. The presented result suggests that chain scissions and fragmentations occurred to PET when it was co-treated with PL. On the other hand, the increased Mws of the PL-PET polymers compared to PL or PL-0PET also suggests that the fragmentized PET could further co-polymerize with PL. The FTIR peaks of aromatic ring vibrations appearing at 1505 cm^{-1} and 1593 cm^{-1} did not change in the PL-PET polymers compared to their physical mixtures, showing the aromatic ring opening did not occur during the co-polymerization. Thus, the co-polymerization must took place at the side chains of PL and PET.

The molecular structures of the polymers were further investigated by analyzing their HSQC spectra given in Fig. 4.4. In the spectrum of PL, the peak signals for methoxyl, S and G units, benzaldehyde and cinnamaldehyde end group can be seen. However, the peaks of aryl ether linkages commonly found in lignin are not observed in PL since the linkages are mostly destroyed during pyrolysis. Compared to the spectrum of PL, the peak signals at aliphatic region ($\delta H/\delta$C 3.0-6.0/50-100 ppm) and aromatic region ($\delta H/\delta$C 6.0-8.0/100-150 ppm) both decreased significantly at PL-0PET. The disappearance of the peaks is likely associated with repolymerization reactions and the decrease in functionalities. The peak signals of PL-derived aromatic region are similar in PL-5PET and PL-20PET. However, they are different compared to the peak signals of PL-0PET. The peaks of S and G units shifted slightly to the right side, and the peak for benzaldehyde end group also decreased in the PL-PET polymers. These changes indicate the modification of PL structures by co-polymerization with PET. In PL-PET polymers, the peak centering at $\delta H/\delta$C 8.05/130.50 ppm stands for benzene rings in PET structure, and the peak signal at $\delta H/\delta$C 4.67/64.29 ppm represents ethylenedioxy in PET. The appearance of these peaks confirms that the PL-PET polymers have PET backbones. Having the PET chain in the backbone, it is expected that the PL-PET polymers have an improved molecular orientation. Additionally, several new peaks were also identified at the region near to the PET backbone peaks (marked in circles). These peaks are associated with newly formed bonds between PET fragments with PL.

Elemental compositions of the precursors are shown in Table 4.1. Carbon content of PL-0PET was 69.51%, higher than most of the lignin-based materials reported in literature [33]. The carbon content was high because of the condensed aromatic structure formed during PL repolymerization. The carbon content only slightly decreased to 68.89% in PL-5PET and

67.21% in PL-20PET. Compared to the contents in their corresponding physical mixtures, the C and H contents were lower whereas the O content was higher in PL-5PET and PL-20PET. The differences again indicated the release of volatile products during the co-polymerization.

4.3.2 Thermal Properties

Thermal property is an important parameter that affects the precursor spinnability, as well as performance of the as-spun fibers in the subsequent stabilization process. Precursors with low thermal stability could cause precursor degradation at elevated temperatures, which will not only form fibers with voids, but also cause fouling in the extruder [34]. The TGA results are provided in Fig. 4.5 and Table 4.2. The T_d (i. e., the temperature for 5% mass loss) of PL-0PET, PL-5PET, and PL-20PET were 271 ℃, 287 ℃, and 303 ℃, respectively. The T_d increased in the PL-PET polymers, contributed by the stable PET backbone. From the DTG curves, the maximum mass loss occurred at around 330 ℃ for PL-0PET and PL-5PET, while it occurred at 370 ℃ for PL-20PET. PL-20PET had a higher mass loss at the temperature range between 370 ℃ and 600 ℃, ultimately leading to a lower amount of fixed carbon at 1000 ℃. However, the amount of fixed carbon in PL-20PET was evidently higher than the amount in PL-20PET (p) (37.97% vs. 34.42%). Unexpectedly, the amount of fixed carbon in PL-5PET (42.21%) was even higher than that in PL-0PET (40.09%), despite the amount of fixed carbon in pure PET being only 17.75%. These results demonstrated that the PL-PET polymers have better thermal stability at elevated temperatures.

The measured T_g values are given in Table 4.2. The T_gs of PET and PL-0PET were 75 ℃ and 110 ℃, respectively. The T_g is higher in PL-0PET, attributed by its amorphous structure inherited from the parent lignin and the crosslinking among the phenolic molecules during the thermal treatment. On the contrary, PET had a T_g as low as 75℃ despite its higher Mw, due to

its linear molecular structure and good flow orientability. The noncovalent intermolecular forces in PET are easily overcome due to the absence of crosslinking among individual PET molecules. Such orientated molecular structure is desired during melt-spinning fibers. The T_g values of PL-5PET and PL-20PET were 97 ℃ and 83 ℃, respectively. Single T_gs were found, indicating that the PL-PETs homogeneous materials [35]. According to Utracki [36], the T_g of a non-reacting mixture can be calculated based on equation (1) given below:

$$\frac{1}{T_{g(blend)}} = \sum_i \frac{w_i}{T_{gi}} \qquad (1)$$

where $T_{g\ (blend)}$ is the glass transition temperature of the blended material; w is the weight fraction of a component material in the blend; and T_{gi} is the glass transition temperature of the corresponding component. Compared to the $T_{g(blend)}$s, significantly lower T_gs were obtained with PL-5PET and PL-20PET. The lower T_gs of the PL-PET polymers indicate that molecular flowability were enhanced by co-polymerization.

Based on the physical, chemical and thermal properties of the PL-PET polymers described above, the reaction pathway of PL and PET is proposed in Fig. 4.6. Highly reactive PL can initiate the chain scissions of PET polymers at lower temperatures. The pathways for PET decomposition include thermal, oxidative and hydrolysis [37, 38]. Thermal decomposition generates PET fragments with vinyl end groups (PET-COO-CH=CH_2, PET-I) and carboxylic acid end groups (PET-COOH, PET-II). Oxidative decomposition could result in aromatic alcohol fragments (PET-COO-CH_2-CH_2-OH, PET-III) in addition to PET-I and PET-II. Also, water produced from PL polycondensation could initiate an autocatalyzed hydrolysis of PET to generate PET-II and PET-III fragments containing carboxylic acid and alcohol end groups. These PET fragments could further react with the phenolic compounds in PL to form new polymers. As shown in the figure, transesterification between PET-I and PL-I

forms PLPET-I and simultaneously releases acetaldehyde as a byproduct (Reaction I). Acetaldehyde can also be produced from thermal decomposition of PET alone. Polymerization could occur at vinyl groups in PET-I and PL-II (Reaction II). PET-II could react with PL-III to form PLPET-III and release water in the meanwhile (Reaction III). The FTIR peak representing OH groups increased at PL-20PET as described above, possibly due to the water formation. As illustrated, PET-II could also be decarboxylated to form PET-IV, which may explain the decreased peak at 1720 cm^{-1} in the FTIR spectra of the PL-PET polymers. PET-III and PL-I could form PLPET-IV through transesterification and simultaneously release ethylene glycol (Reaction IV). Alternatively, PET-III could be converted to PET-II and release acetaldehyde. Although fragmentation reduces the Mw, the Mws of the PET fragments are expected to be significantly higher than the PL compounds. Thus, the PL-PET polymers are likely to have the linear, long aromatic backbone of PET with small lignin-derived phenolic monomers and oligomers branching of it.

Several phenomena observed in the present study can be explained based on the proposed reaction pathways. The T_gs of the PL-PET polymers decreased since the new polymers have a PET backbone. Such a linear aromatic-chain backbone can greatly increase molecular orientation and flow orientability of the polymers. Thermal stability of the PL-PET polymers increased, though not solely due to the stable PET backbone. The elimination of aliphatic side chains in PET and PL during co-polymerization could result in condensed aromatic structures with shorter side chains, which would also increase the thermal resistance of the polymers. The volatile products released from co-polymerization of PL and PET fragments, such as acetaldehyde, ethylene glycol, water and carbon dioxide, can explain the lower experimental yields of the PL-PET polymers.

4.3.3 Melt Rheology

Fig. 4.7 showed the complex viscosity of the polymers as a function of sweep frequency measured at 200 ℃. Despite their higher Mws, the viscosity of the PL-PET polymers was lower compared to PL-0PET. The lower viscosity indicates that the molecule chains can be detangled more easily. Also, the slope of the viscosity decrease was steepest with PL-20PET, showing its molecular chains can be aligned faster when external force is applied. This result indicates that the PL-PET polymers have lower degrees of crosslinking and better polymer chain mobility. Isothermal viscosity as a function of retention time was measured at 200 ℃. Isothermal viscosity can reflect flow behavior of a material during fiber spinning. Baker [39] proposed that a suitable viscosity range of a material in favor of melt-spinning is from 100 to 1000 Pa·s. In Fig.4.7, the viscosity was initially within 10~50 Pa·s for all three polymers. Although their viscosities increased at extended times, their values were well below 1000 Pa·s after 10 min for good melt-spinnability of the polymers. Due to the extensive crosslinking at the elevated temperature, the viscosity increase was fastest with PL-0PET. Increasing viscosity along with time is undesirable since it may cause inconsistency in the quality of the spun-fiber and lead to the extruder clogging. In comparison, the viscosity increased much more slowly in the PL-PET polymers, because of their reduced reactivity and improved flow orientability. Hydroxyl groups abundantly present in PL are the main sites for polycondensation and crosslinking reactions. The content of OH groups was reduced in the PL-PET polymers since this reactive group was partly consumed during co-polymerization of PL and PET, as postulated Fig. 4.6.

4.3.4. Performance during Fiber Spinning

Actual spinning temperatures of the polymers were in well accordance with the rheological results given above. The optimum extruding temperature for best spinning

performance was 205~210 ℃ for PL-0PET. In comparison, the optimum temperatures reduced to 200~203 ℃ for PL-5PET, and 197 ℃ for PL-20PET. The viscosity of the precursor is usually reversely correlated with the spinning temperature. Since the viscosities of the PL-PET polymers were lower than that of PL-0PET, they can be spun at lower temperatures. This finding is contrary to the results previously reported by Kubo et al. [17]. They reported that due to the higher melting temperature of PET (245 ℃), the spinning temperature increased with increasing amount of PET in the lignin-PET blends. In the present study, not only the spinning temperatures were reduced by the addition of PET, but also PL-20PET that containing a higher amount of PET had a lower spinning temperature compared to PL-5PET. The appearances of as-spun fibers of the polymers are given in Fig. 4.8.

4.3.5. Performance during Stabilization and Carbonization

Table 4.3 summarized the fusing conditions of as-spun fibers during oxidative stabilization. Many synthetic polymers have good molecular orientation and flow orientability for drawing fibers. However, they are too stable to crosslink during oxidative stabilization. For example, only extreme conditions, such as soaking in highly concentrated sulfuric acid, could be applied to crosslink polyethylene fibers [40]. On the other hand, multiple functional groups in lignin or PL can develop crosslinking reactions through multiple reactions [41]. Compared with PL-0PET, the PL-PET polymers had a lower tolerance to the faster heating rate during stabilization due to their reduced reactivity for crosslinking. This result corresponds with the findings from the FTIR spectra, DSC and rheological tests. Even though the PL-PET polymers have larger Mws than PL-0PET, they are slightly more difficult to be crosslinked during the stabilization process due to the decreased OH contents and their low T_gs. For equivalent comparison, the as-spun fibers of the PL-PET polymers were stabilized at 0.3 ℃/min. The

yields after stabilization were simulated using TGA and the results are given in Table 4.4. It is noteworthy that the TGA simulated yields are expected to be lower than the yields of fully stabilized fibers due to the limited contact surface between the fibers and air when the fibers were placed inside the sample cup. The results showed that the PL-PET as-spun fibers have higher stabilization yields than PL-0PET fibers.

Strains of the stabilized fibers derived from the three polymers were also measured. High strain implies that the fiber could be stretched extensively before it breaks. Thus, the molecular orientations of different fibers can be evaluated to a certain extent by comparing their strains. PET has a high strain due to the flexibility of the linear molecular chain [42]. On the other hand, the strain of lignin-based fiber is usually low due to its crosslinked and highly restricted structure [16]. The average strain of PL-0PET stabilized fiber was 2.38%. In comparison, the strain increased by 50% in the stabilized fibers of PL-5PET (3.57%) and by 19% in the stabilized fibers of PL-20PET (2.84%). The molecular orientation was higher with the PL-PET polymers in comparison to PL-0PET, which is also reflected on their stabilized fibers. It should be noted that the increase of the strain was less dramatic with PL-20PET, despite that whose molecular orientation is expected to be better than PL-5PET. This inconsistency is probably caused by the knots observed on the fiber surfaces (Fig. 4.8), which could be less-reacted PET. Even in very small amounts, these imperfections can lead to fiber heterogeneity and structural inconsistency.

The performance of the polymers during carbonization is also evaluated. The fibers without condensed six-member carbon ring-like structure or the lack of the ability to form aromatic rings during carbonization, will ultimately have a low carbonization yield. In Table 4.4, the TGA simulated carbonization yield of PET was only 9.6%, despite the presence of an

aromatic ring in its basic monomer unit. This is because the aliphatic side chains on the aromatic backbone fail to crosslink and aromatize during carbonization. On the other hand, the yield of carbonized PL-0PET was 49.6% because of its condensed aromatic structure. The carbonization yields of PL-5PET and PL-20PET were 37.8% and 37.2%, respectively. Recall that from Table 4.2, the fixed carbon of PL-5PET was higher than that of PL-0PET. The fixed carbon of a material was commonly used as an indicator to predict the yield of the resulting carbon fiber [43]. The PL-PET polymers may have a reduced ability to crosslink during oxidative stabilization because they are less reactive than PL-0PET.

Raman spectroscopy was used to investigate the graphitic structures of PL and the PL-PET based carbon fibers. As shown in Fig. 4.9, D peak at around 1370 cm^{-1} is an indicator of SP_2 carbon stretching in graphitic region, and G peak at 1600 cm^{-1} is an indicator of structural disorder or imperfection [44]. As expected, the G peak became sharper and narrower for the PL-PET carbon fibers compared to that of PL-0PET carbon fiber. The intensity ratio of the D peak and G peak (I_D/I_G) is commonly used as a quantitative measure to compare the structural disorder in different carbon materials. Usually a lower I_D/I_G ratio implies a better ordered structure. In the present study, the I_D/I_G ratio was 2.25 in PL-0PET carbon fiber. The I_D/I_G ratio further decreased to 2.19 and 2.01 in PL-5PET and PL-20PET carbon fiber. This result indicates that the PL-PET based carbon fibers have improved the graphitic structure with reduced disorder. The improved structures of the carbon fibers must be a result of the improved molecular orientation in the PL-PET polymers since stabilization and carbonization processes cannot improve the molecular orientation [13]. More graphitic clusters are expected to be formed in the PL-PET based carbon fibers compared to non-orientated PL-0PET based carbon fiber.

The morphology of the carbon fibers was also examined by SEM. As seen in Fig. 4.10, swellings on the surface of the PL-0PET based carbon fiber are likely caused by the gas products trapped inside the carbon fiber during fiber processing. The swellings were not observed on the surface of the PL-PET carbon fibers. Instead, a few shallow nanopores were observed on the fiber surfaces. The cross-sections of the PL-PET carbon fibers were smooth and solid, much more uniform in comparison to PL-0PET carbon fiber. It is also noted that the texture of the PL-0PET carbon fiber was slightly different from that of the PL-PET carbon fibers. A rather rough and ribbon-like structure was observed in the PL-0PET carbon fiber while these structures were not observed in the PL-PET carbon fibers. Previously, Thunga [16] reported that the smooth cross-section of carbon fiber could support fiber integrity. Since the PL-PET polymers have improved thermal stability and lower reactivity, the volatile emission during spinning or carbonization process is expected to be much milder compared to that of PL-0PET. Thus, the resulting fibers have smoother surfaces. The mechanical properties of PL-0PET, PL-5PET and PL-20PET were also compared in table 4.4. It could be seen PL-PET based carbon fibers had both improved tensile strengths and modulus than PL-0PET carbon fibers owing to its improved structure. PL-PET carbon fibers also slightly decreased in strain at failure indicating they became more brittle. Overall, the mechanical properties of PL-PET carbon fibers had great potential to achieve higher values upon optimizing the co-polymerization between PL and PET.

4.4. Conclusions

In this work, PL was co-polymerized with PET to produce a lignin-based melt-spinnable polymer with improved molecular orientation. The highly reactive PL was able to initiate chain scission and fragmentation of PET at a temperature significantly lower than standard degradation temperature of PET. The resulting PET fragments containing carboxylic,

vinyl, and hydroxyl groups further reacted with the PL molecules to form the PL-PET polymers, which have linear backbone of PET. The co-polymerization was found to lower T_gs and improve thermal stability of the PL-PET polymers despite of their increased Mws. During melt rheology testing, complex viscosity decreased with the PL-PET polymers because of reduced crosslinking and improved flow orientability in their polymer chains. The melt spinning temperature was lowest with PL-20PET due to the higher content of linear backbones and better molecular orientation. The improved molecular orientation in the PL-PET polymers also resulted in the stabilized fibers with higher strains and carbonized fibers with lower I_D/I_G ratios and higher tensile strengths. This preliminary study demonstrated an approach to improve molecular and flow orientability of lignin-based polymer. Overall, PL has much more attractive properties toward co-polymerization in comparison to conventional technical lignin. The study also showed several aspects that require future investigation in order to manufacture high-quality carbon fibers from PL-PET polymers. For instance, PET content and co-polymerization conditions (temperature, time, with or without catalyst) could to be optimized in future studies to prevent PET leftover or the formation of excessive volatiles within the polymers or fibers. PL can also be co-polymerized with other linear polymers (e.g. PAN) using the similar approach.

4.5 Tables and Figures

Table 4.1 Elemental analysis of different polymers

	C (%)	H (%)	O (%)	N (%)	S (%)
PL-0PET	69.51	4.93	25.26	0.28	0.02
PET	62.5	4.17	33.33	0	0
PL-5PET	68.89 (68.93)*	4.85 (4.86)*	25.98 (25.94)*	0.26	0.01
PL-20PET	67.21 (67.64)*	4.39 (4.73)*	28.17 (27.41)*	0.22	0.01

* The values inside parentheses are predicted values based on PL-PET(p)

Table 4.2 Thermal properties of different polymers

	PET	PL-0PET	PL-5PET	PL-20PET
T_d (℃)	399	271	287	303
Fixed carbon (%)	17.75	40.49	42.21 (38.60)*	37.97 (34.42)*
T_g (℃)	75	110	97	83
T_g (blend)** (℃)	-	-	106	98

* The values in parentheses are predicted values based on PL-PET (p).

** The values under the assumption if PL and PET do not react.

Table 4.3 Fusing conditions of different polymers after stabilization at varied heating rates

Heating rate (℃/min)	PL-0PET	PL-5PET	PL-20PET
0.1	■	■	■
0.3	■	■	▒
0.5	■	▒	⁘

■ : Good fiber integrity

▒ : Mild fusion, fibers are separable

⁘ : Severe fusion

Table 4.4 Yields and mechanical properties of different carbon fibers

	PL-0PET	PL-5PET	PL-20PET	PET
Stabilization yield (%)	87.5	88.3	89.9	96.0
Carbonization yield (%)	49.6	37.8	37.2	9.6
Tensile strength (MPa)	534(±100.1)	677(±64.2)	641.5(±50.2)	NA
Modulus (GPa)	50.7(±9.21)	62.4(±8.01)	64.4(±3.64)	NA
Strain at failure (%)	1.07(±0.15)	1.06(±0.12)	0.99(±0.05)	NA

Figure 4.1 PL-20PET (left) and PL-20PET (p) (right) after milled into powders.

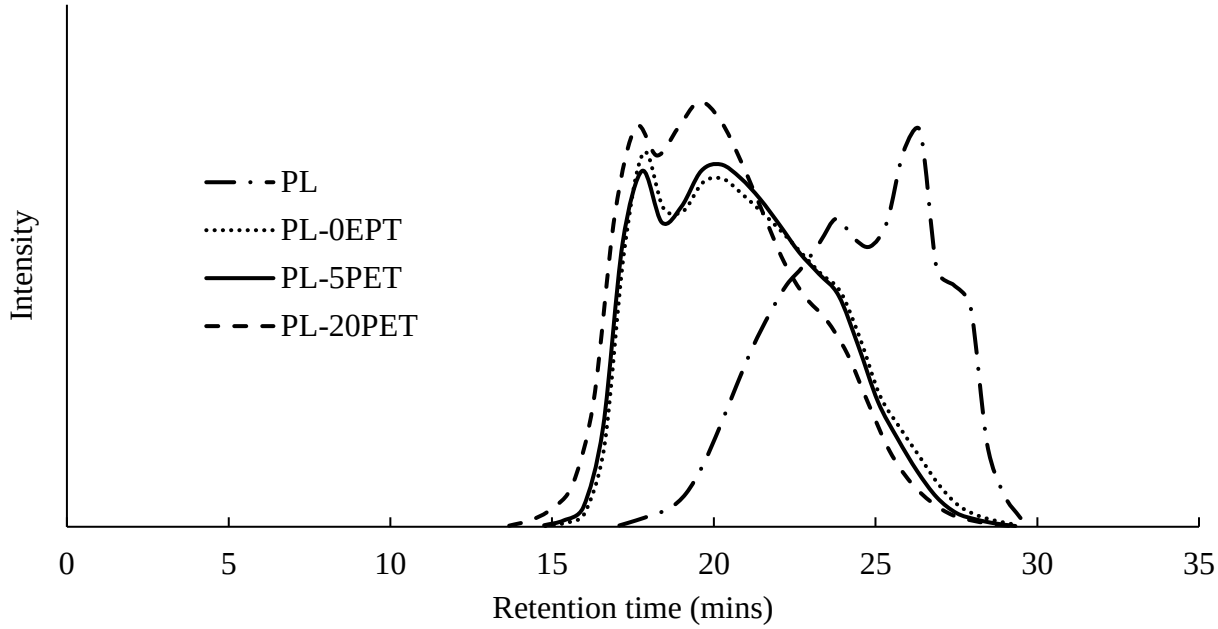

Figure 4.2 GPC curves of THF soluble fractions of different polymers.

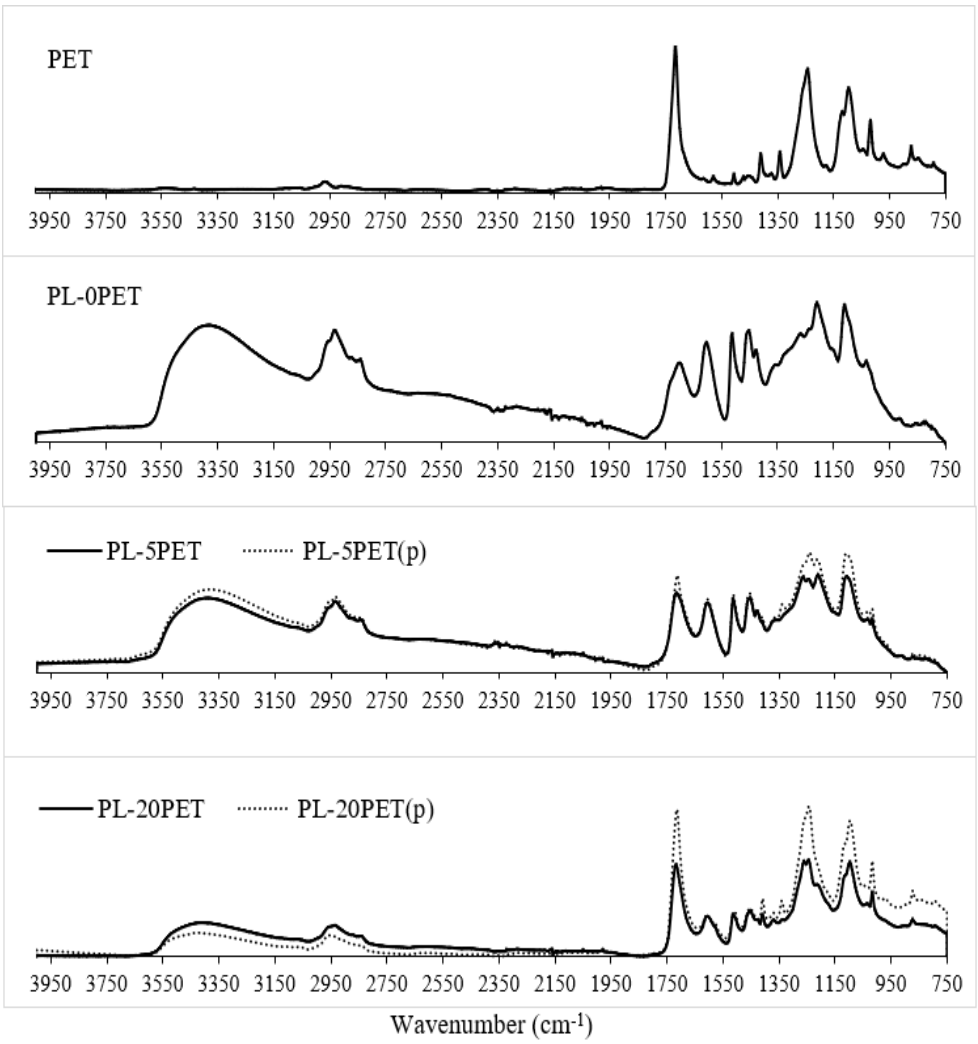

Figure 4.3 FTIR spectra of different polymers.

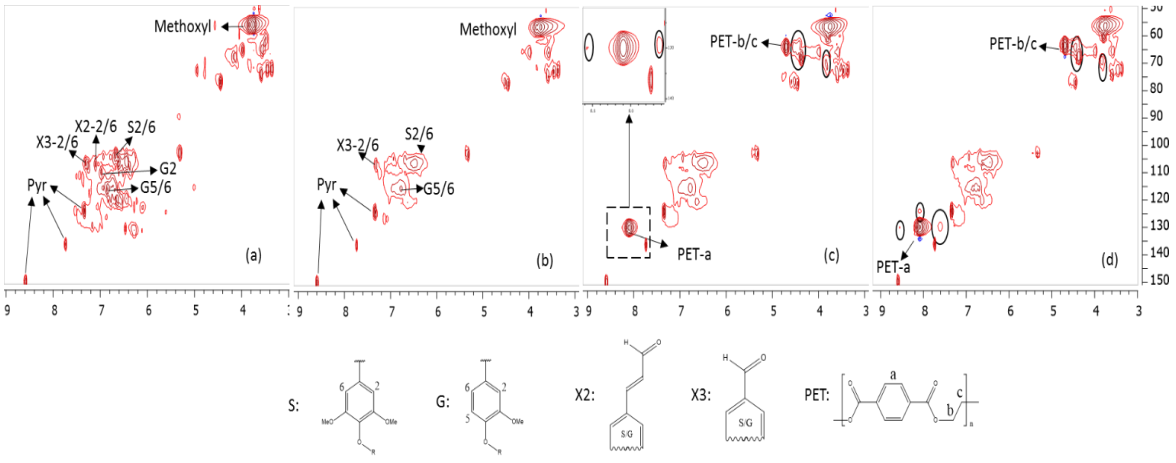

Figure 4.4 HSQC spectrum: (a). PL; (b). PL-0PET; (c). PL-5PET; (d). PL-20PET.

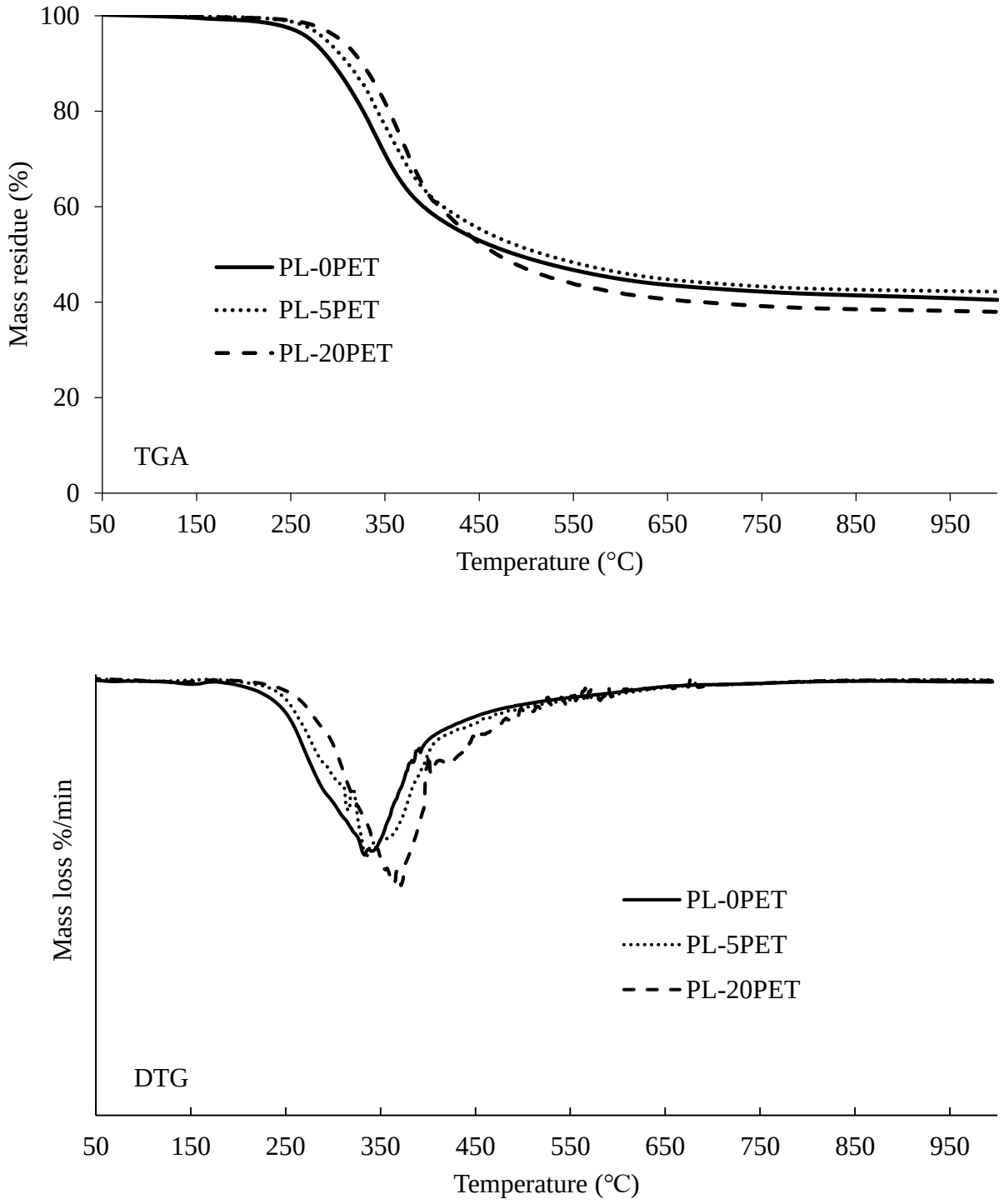

Figure 4.5 TGA and DTG curves of different polymers.

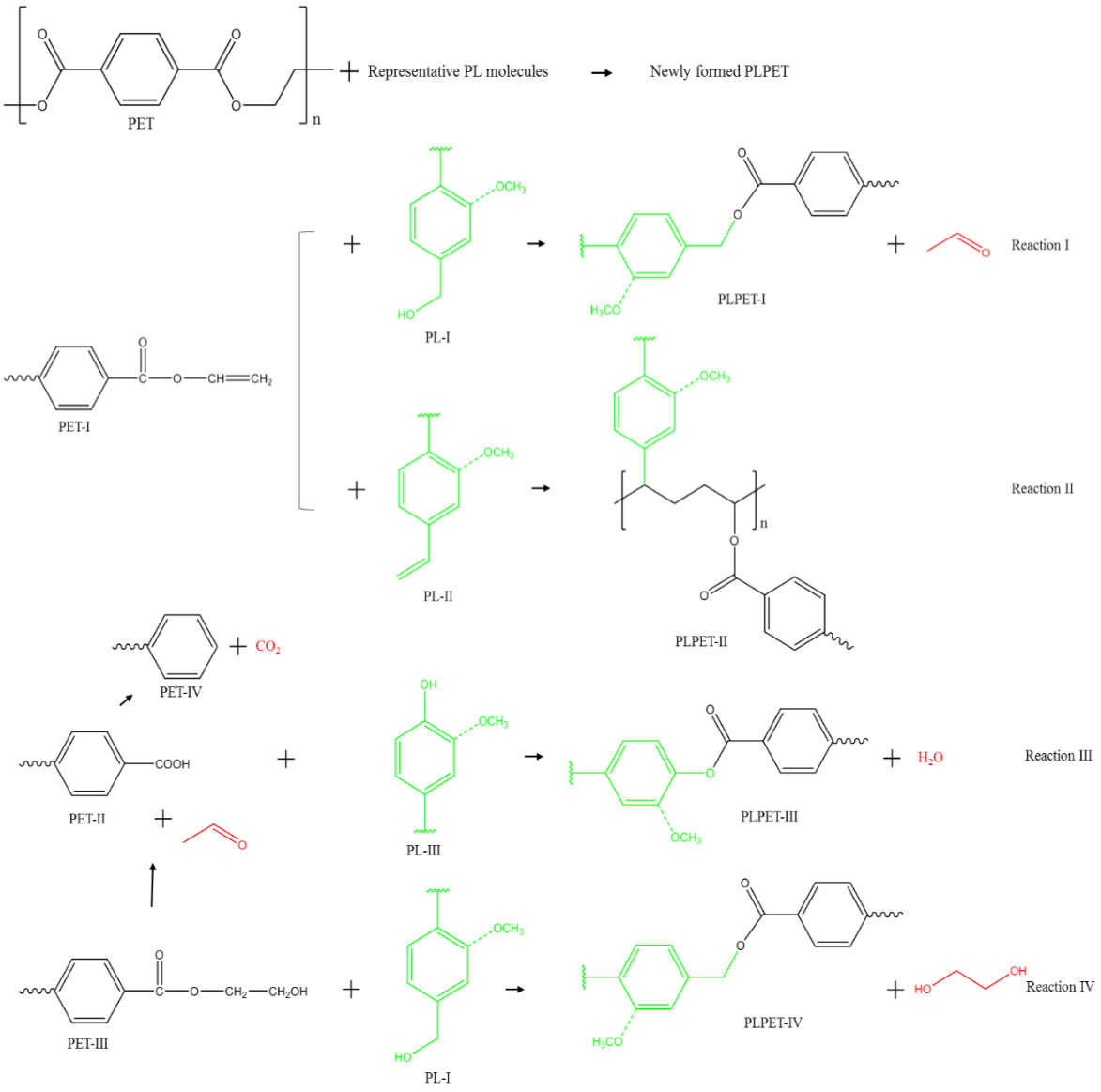

Figure 4.6 Proposed reactions between PL and PET during co-polymerization.

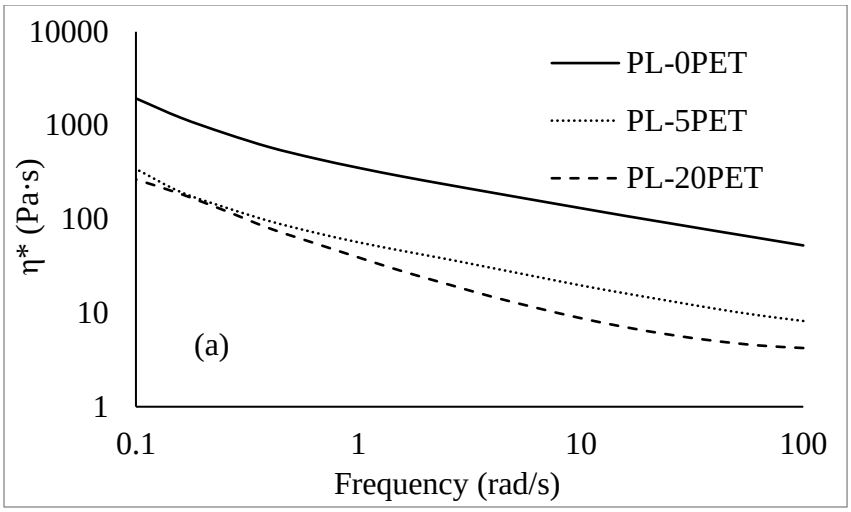

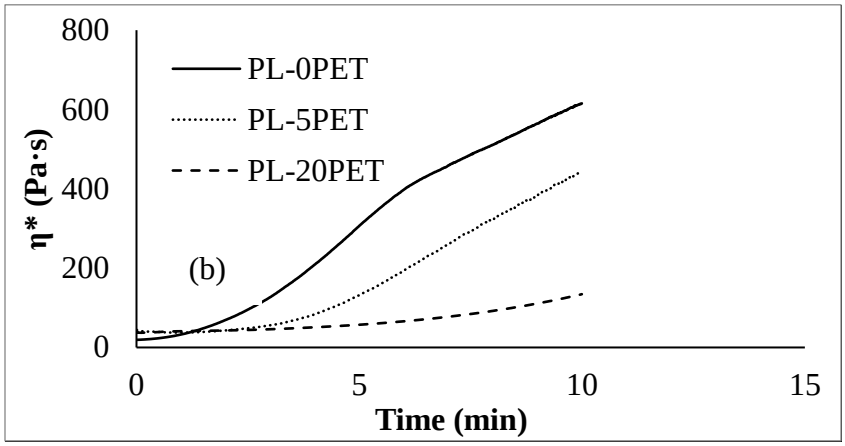

Figure 4.7 Frequency sweep (a) and isothermal sweep (b) of polymers measured at 200 ℃.

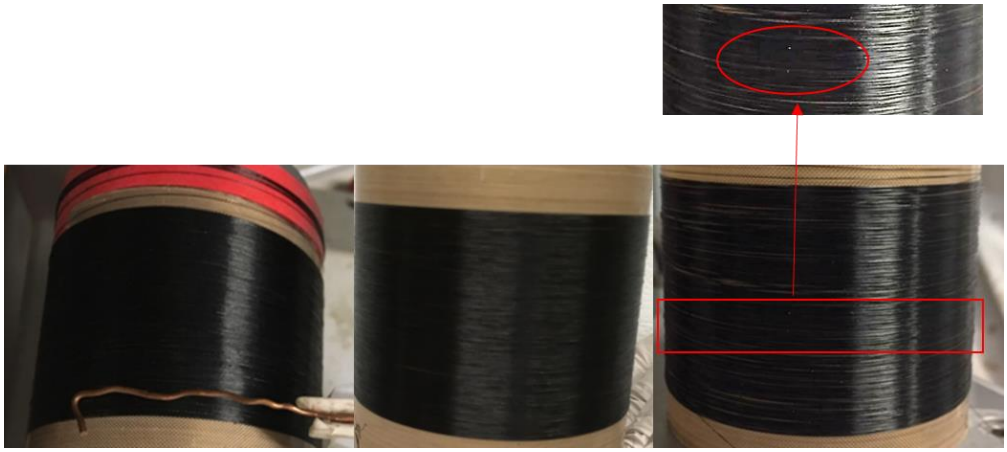

Figure 4.8 As-spun fibers from PL-0PET (left), PL-5PET (middle), and PL-20PET (right).

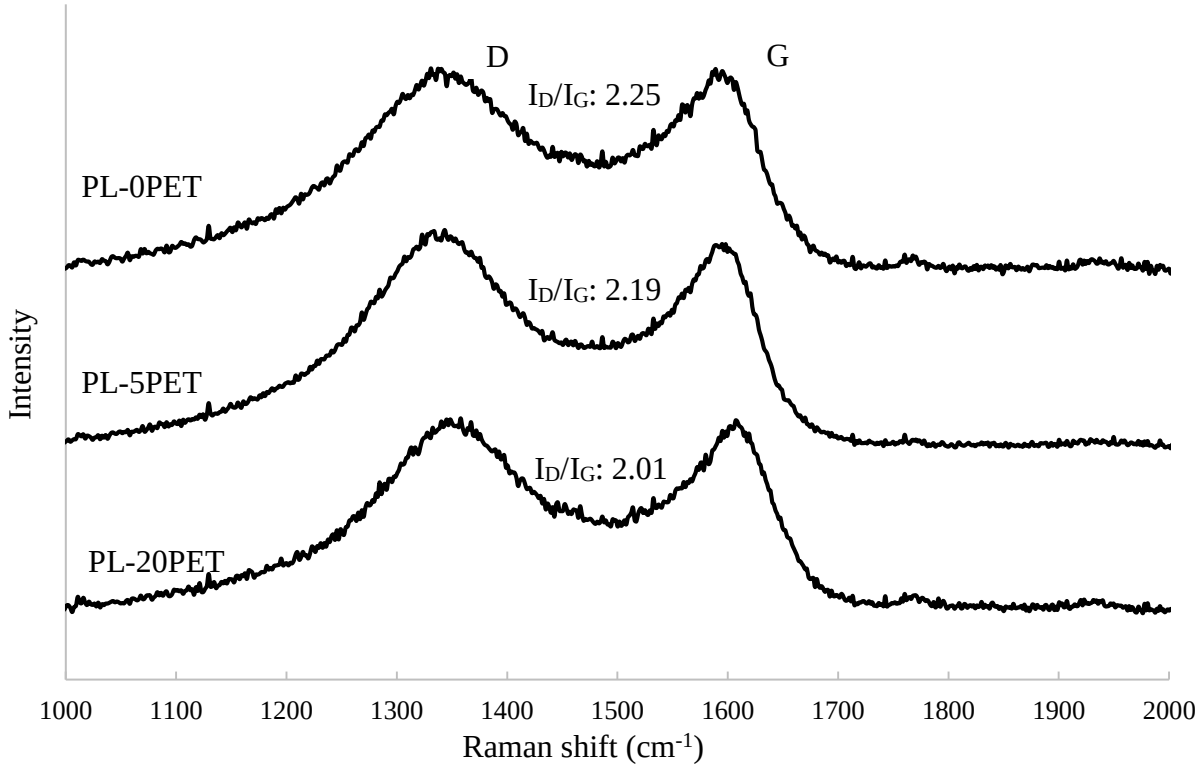

Figure 4.9 Raman spectra of carbon fibers derived from different polymers.

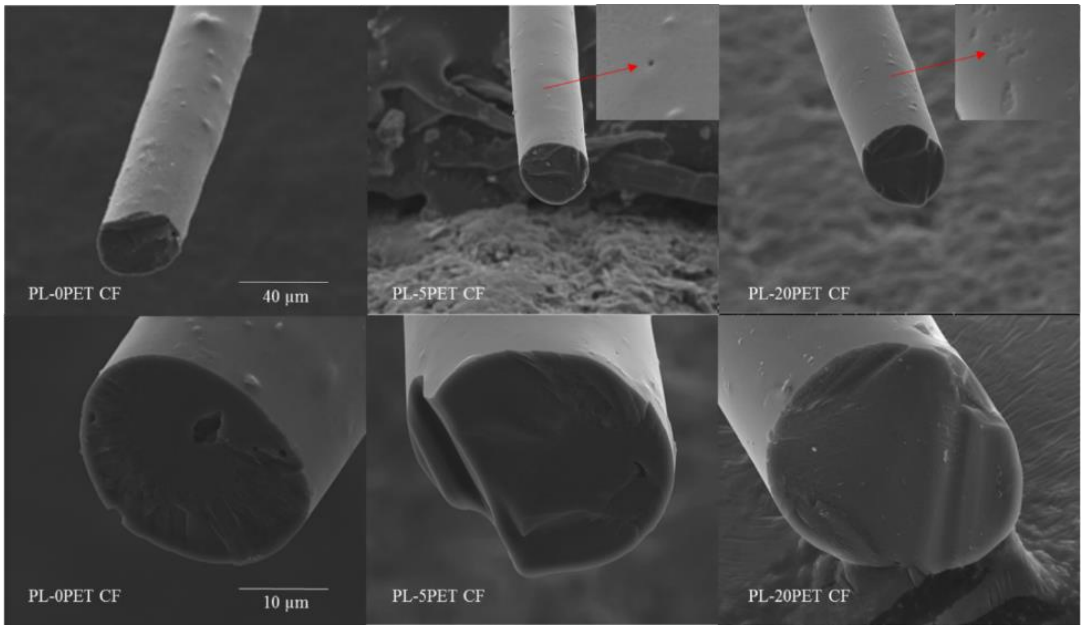

Figure 4.10 SEM images of carbon fibers derived from different polymers.

4.6 References

1. Frank, E., F. Hermanutz, and M.R. Buchmeiser, *Carbon fibers: precursors, manufacturing, and properties.* Macromolecular materials and engineering, 2012. **297**(6): p. 493-501.
2. Liu, Y. and S. Kumar, *Recent progress in fabrication, structure, and properties of carbon fibers.* Polymer Reviews, 2012. **52**(3): p. 234-258.
3. Baker, D.A. and T.G. Rials, *Recent advances in low-cost carbon fiber manufacture from lignin.* Journal of Applied Polymer Science, 2013. **130**(2): p. 713-728.
4. Norgren, M. and H. Edlund, *Lignin: recent advances and emerging applications.* Current Opinion in Colloid & Interface Science, 2014. **19**(5): p. 409-416.
5. Pan, X., et al., *Biorefining of softwoods using ethanol organosolv pulping: Preliminary evaluation of process streams for manufacture of fuel-grade ethanol and co-products.* Biotechnology and bioengineering, 2005. **90**(4): p. 473-481.
6. Kadla, J., et al., *Lignin-based carbon fibers for composite fiber applications.* Carbon, 2002. **40**(15): p. 2913-2920.
7. Saito, T., et al., *Methanol fractionation of softwood kraft lignin: Impact on the lignin properties.* ChemSusChem, 2014. **7**(1): p. 221-228.
8. Li, Q., et al., *Quality carbon fibers from fractionated lignin.* Green Chemistry, 2017. **19**(7): p. 1628-1634.
9. Norberg, I., et al., *A new method for stabilizing softwood kraft lignin fibers for carbon fiber production.* Journal of Applied Polymer Science, 2013. **128**(6): p. 3824-3830.
10. Zhang, M. and A.A. Ogale, *Carbon fibers from dry-spinning of acetylated softwood kraft lignin.* Carbon, 2014. **69**: p. 626-629.
11. Ding, R., et al., *Processing and characterization of low-cost electrospun carbon fibers from organosolv lignin/polyacrylonitrile blends.* Carbon, 2016. **100**: p. 126-136.
12. Kai, D., et al., *Towards lignin-based functional materials in a sustainable world.* Green Chemistry, 2016. **18**(5): p. 1175-1200.
13. Frank, E., et al., *Carbon fibers: precursor systems, processing, structure, and properties.* Angewandte Chemie International Edition, 2014. **53**(21): p. 5262-5298.
14. Zhou, S., et al., *Lignin valorization through thermochemical conversion: comparison of hardwood, softwood and herbaceous lignin.* ACS Sustainable Chemistry & Engineering, 2016. **4**(12): p. 6608-6617.
15. Li, Q., et al., *Quality carbon fibers from fractionated lignin.* Green Chemistry, 2017. **19**(7): p. 1628-1634.
16. Thunga, M., et al., *Bio-renewable precursor fibers from lignin/polylactide blends for conversion to carbon fibers.* Carbon, 2014. **68**: p. 159-166.
17. Kubo, S. and J. Kadla, *Lignin-based carbon fibers: Effect of synthetic polymer blending on fiber properties.* Journal of Polymers and the Environment, 2005. **13**(2): p. 97-105.
18. Dzięcioł, M. and J. Trzeszczyński, *Volatile products of poly (ethylene terephthalate) thermal degradation in nitrogen atmosphere.* Journal of Applied Polymer Science, 2000. **77**(9): p. 1894-1901.
19. Pacheco, J.J., et al., *Route to renewable PET: reaction pathways and energetics of Diels–Alder and dehydrative aromatization reactions between ethylene and biomass-*

derived furans catalyzed by lewis acid molecular sieves. ACS Catalysis, 2015. **5**(10): p. 5904-5913.

20. Wang, Z., et al., *Comparative study on polycyclic aromatic hydrocarbons, light hydrocarbons, carbon monoxide, and particulate emissions from the combustion of polyethylene, polystyrene, and poly (vinyl chloride).* Energy & Fuels, 2003. **17**(4): p. 999-1013.
21. Peterson, J.D., S. Vyazovkin, and C.A. Wight, *Kinetics of the thermal and thermo-oxidative degradation of polystyrene, polyethylene and poly (propylene).* Macromolecular Chemistry and Physics, 2001. **202**(6): p. 775-784.
22. Mohan, D., C.U. Pittman, and P.H. Steele, *Pyrolysis of wood/biomass for bio-oil: a critical review.* Energy & fuels, 2006. **20**(3): p. 848-889.
23. Scholze, B., C. Hanser, and D. Meier, *Characterization of the water-insoluble fraction from fast pyrolysis liquids (pyrolytic lignin): Part II. GPC, carbonyl goups, and 13C-NMR.* Journal of Analytical and Applied Pyrolysis, 2001. **58**: p. 387-400.
24. Kim, K.H., et al., *Quantitative investigation of free radicals in bio-oil and their potential role in condensed-phase polymerization.* ChemSusChem, 2015. **8**(5): p. 894-900.
25. Qin, W. and J. Kadla, *Carbon fibers based on pyrolytic lignin.* Journal of Applied Polymer Science, 2012. **126**(S1).
26. Qu, W., et al., *Repolymerization of pyrolytic lignin for producing carbon fiber with improved properties.* Biomass and Bioenergy, 2016. **95**: p. 19-26.
27. Pollard, A., M. Rover, and R. Brown, *Characterization of bio-oil recovered as stage fractions with unique chemical and physical properties.* Journal of Analytical and Applied Pyrolysis, 2012. **93**: p. 129-138.
28. Hayes, N., et al., *Crystallisation of PET from the amorphous state: observation of different rates for surface and bulk using XPS and FTIR.* Surface and interface analysis, 1996. **24**(10): p. 723-728.
29. Holland, B. and J. Hay, *The thermal degradation of PET and analogous polyesters measured by thermal analysis–Fourier transform infrared spectroscopy.* Polymer, 2002. **43**(6): p. 1835-1847.
30. Guevremont, J., et al., *Orientation and conformation in poly (ethylene terephthalate) with low draw ratios as characterized by specular reflection infra-red spectroscopy.* Polymer, 1995. **36**(17): p. 3385-3392.
31. Vijayakumar, S. and P. Rajakumar, *Infrared spectral analysis of waste pet samples.* International Letters of Chemistry, Physics and Astronomy, 2012. **4**: p. 58-65.
32. Faix, O., *Classification of lignins from different botanical origins by FT-IR spectroscopy.* Holzforschung-International Journal of the Biology, Chemistry, Physics and Technology of Wood, 1991. **45**(s1): p. 21-28.
33. El Mansouri, N.-E. and J. Salvadó, *Structural characterization of technical lignins for the production of adhesives: Application to lignosulfonate, kraft, soda-anthraquinone, organosolv and ethanol process lignins.* Industrial Crops and Products, 2006. **24**(1): p. 8-16.
34. Qu, W., et al., *Potential of producing carbon fiber from biorefinery corn stover lignin with high ash content.* Journal of Applied Polymer Science, 2018. **135**(4).
35. Hiemenz, P.C. and T.P. Lodge, *Polymer chemistry*. 2007: CRC press.

36. Utracki, L.A., *Thermodynamics of Polymer Blends*, in *Polymer Blends Handbook*, L.A. Utracki, Editor. 2003, Springer Netherlands: Dordrecht. p. 123-201.
37. Gewert, B., M.M. Plassmann, and M. MacLeod, *Pathways for degradation of plastic polymers floating in the marine environment.* Environmental Science: Processes & Impacts, 2015. **17**(9): p. 1513-1521.
38. Venkatachalam, S., et al., *Degradation and recyclability of poly (ethylene terephthalate)*, in *Polyester*. 2012, InTech.
39. Baker, D.A., N.C. Gallego, and F.S. Baker, *On the characterization and spinning of an organic-purified lignin toward the manufacture of low-cost carbon fiber.* Journal of Applied Polymer Science, 2012. **124**(1): p. 227-234.
40. Kim, J.W. and J.S. Lee, *Preparation of carbon fibers from linear low density polyethylene.* Carbon, 2015. **94**: p. 524-530.
41. Braun, J., K. Holtman, and J. Kadla, *Lignin-based carbon fibers: Oxidative thermostabilization of kraft lignin.* Carbon, 2005. **43**(2): p. 385-394.
42. Tapia-Picazo, J., et al., *Polyester fiber production using virgin and recycled PET.* Fibers and Polymers, 2014. **15**(3): p. 547-552.
43. Oroumei, A., B. Fox, and M. Naebe, *Thermal and rheological characteristics of biobased carbon fiber precursor derived from low molecular weight organosolv lignin.* ACS Sustainable Chemistry & Engineering, 2015. **3**(4): p. 758-769.
44. Sadezky, A., et al., *Raman microspectroscopy of soot and related carbonaceous materials: spectral analysis and structural information.* Carbon, 2005. **43**(8): p. 1731-1742.

CHAPTER 5. CONTROLLED RADICAL POLYMERIZATION OF CRUDE LIGNIN BIO-OIL FOR BIOBASED POLYMERS AND THE POTENTIAL APPLICATIONS

(A manuscript to be submitted to ACS Sustainable Chemistry & Engineering)

ABSTRACT

In this work, methacrylate polymers with different thermal and viscoelastic properties were synthesized from red oak lignin bio-oil. The bio-oil, also called pyrolytic lignin (PL), consisted of various phenolic monomers and oligomers with average hydroxyl content of 3.04 mol/mol. The PL was first esterified with different amounts of methacryloyl chloride and acetyl chloride to form PL methacrylates and then subjected to controlled radical polymerization. Polymerization of fully methacrylated PL caused gelation to yield a cross-linked polymer. On the other hand, polymerization of partly methacrylated PL was able to suppress crosslinking and gelation to yield a thermoplastic polymer with glass transition temperature (T_g) of 161 ℃ and thermal decomposition temperature (T_d) of 241 ℃. In comparison, the functionalization of PL by partial methacrylation and subsequent acetylation reduced T_g of the resulting polymer to 130 ℃, while increasing T_d to 250 ℃. This latter polymer is melt-spinnable and demonstrated highly attractive properties as ideal carbon fiber precursor. Unlike previously reported phenolic monomer-based methacrylate polymers that cannot withstand high temperature pyrolysis, the polymer produced from this study could be pyrolyzed at 1000 ℃ to carbonize. More importantly, the polymer has a linear molecular orientation that is critical in obtaining high-quality carbon fiber.

Keywords: Lignin, bio-oil, methacrylation, acetylation, polymer, carbon fiber

5.1. Introduction

Lignin is the second most abundant biopolymer next to cellulose [1]. Isolated lignin is abundantly available as byproduct from pulp and paper industry, as well as emerging biorefineries [2]. According to the Department of Energy report, 1.3 billion tons of lignocellulosic biomass is available for biorefinery in the U.S. alone, which could produce more than 225 million tons of lignin [3]. Lignin is currently burned as low-grade boiler fuel for heat with estimated value lower than $50 per ton. Moving forward, value-added products from lignin will play a critical role in sustaining biorefineries. To date, significant research effort has been dedicated to lignin volatilization. In addition to biofuels and chemicals, lignin has also been used to produce green polymers [4], carbon fibers [5] and composites [6, 7]. Although progress has been made, lignin has several drawbacks as a feedstock. Lignin structure and its properties highly depend on lignin extraction methods and biomass species [1]. For instance, glass transition temperature, molecular weight and dispersity vary by lignin type. High dispersity of lignin is due to fragmentation and re-condensation during lignin extraction process [1]. Lignin also has low reactivity, low thermal stability and poor solubility [8, 9]. Moreover, raw lignin is a randomly cross-linked macropolymer lacking in defined molecular orientation unlike cellulose and synthesized polymers.

Alternatively, lignin-derived monomers and/or oligomers could be used as feedstock to take advantages of their higher reactivity and reduced heterogeneity compared to lignin [10-13]. Since they are produced by depolymerizing lignin, the molecular sizes are significantly reduced compared to parent lignin. Also, there are various functional groups in the molecules that could serve as the reactive sites to initiate many interesting reactions. Therefore, there is a possibility to obtain a broad range of lignin-based polymers using the lignin-derived phenolic compounds as building blocks. For example, Mahmood et al. used a solvent-liquefied lignin to synthesize a bio-based polyurethane that has better compression modulus and strengths than sucrose-based

polyurethane [14]. Qu et al. repolymerized lignin-derived bio-oil in the presence of sulfuric acid to produce a melt-spinnable polymer with glass transition temperature (T_g) of 101 ℃ [15]. The resulting polymer was further fabricated to obtain carbon fiber with improved tensile strength and modulus. More often, however, phenolic monomers were used as lignin-derivable model monomers to synthesize bio-based polymers. For example, Mialon et al. produced poly(dihydroferulic acid) from vanillin and reported it's thermal properties to be similar to that of polyethylene terephthalate [13]. In another study, Stanzione et al. polymerized methacrylated phenolic monomers to produce thermoset resin [10]. They further concluded that the phenolic monomers could replace petroleum-based styrene in the synthesis of vinyl ester resin. Holmberg et al. also synthesized thermoplastic polymers from esterified syringol and guaiacol-based monomers through radical polymerization [11, 12].

The phenolic monomer-derived thermoset and thermoplastic synthesized are highly attractive value-added products, as they can serve as alternatives of petroleum-based polymers in many applications. However, obtaining phenolic monomers from lignin at high purity and reasonable cost is often very difficult based on state-of-the art techniques. Due to its amorphous structure, lignin usually depolymerizes to yield crude bio-oil which is a complex mixture containing hundreds of phenolic monomers and oligomers vary in molecular sizes and functional groups [16, 17]. Not only selectively producing a few monomers at high yields is difficult, but also isolating and purifying the monomers from the crude bio-oil are technically and economically challenging. Therefore, a few model monomers were mixed in some of previous studies in order to mimic lignin bio-oil [10, 11]. Unfortunately, such mixtures of three to four pure monomers are too ideal for representing actual bio-oil with far more complex composition. Thus, directly using

crude bio-oil as the feedstock of the synthesis could significantly improve economic feasibility of the biobased polymers.

The focuses of the present study are: 1) to investigate the synthesis of methacrylate polymers using crude lignin bio-oil, and 2) to explore the potential applications of the resulting polymers. While using crude bio-oil instead of pure monomers as the feedstock brings clear economic advantages, this approach may also present new technical challenges. For instance, while Holmberg et al. successfully produced thermoplastic polymers from the monomers containing single esterificable site (i.e., one hydroxyl per molecule, thus a single radically polymerizable site after methacrylation), crude bio-oil is most likely a mixture of monomers and oligomers with multi-esterificable sites. Although methacrylation of all the esterificable sites in the monomers and oligomers will ensure the bio-oil is radically polymerizable, having too many polymerizable sites on per molecule may promote crosslinking and could result in gelation. This problem may be avoidable by controlling the extent of methacrylation to limit the crosslinking and branching. Previously, Cochran successfully synthesized thermoplastics from multi-functional soybean oil monomers by limiting polymerizable sites on the molecules [18].

In the present study, lignin bio-oil obtained from pyrolysis of red oak was converted to biobased methacrylate polymers by employing controlled polymerization technique. To better explore the use of crude bio-oil as a feedstock, the bio-oil was first functionalized with three different methods, which are full methacrylation, partial methycryaltion, and the combination of partial methacrylation and acetylation. The functionalized bio-oils were further subjected to reversible addition-fragmentation chain transfer (RAFT) polymerization. The produced polymers were characterized, and their potential applications, mainly as carbon fiber precursor, were discussed.

5.2. Experimental Section

5.2.1 Materials

Lignin bio-oil used in this study was provided by BioCentury Research Farm of Iowa State University. The process for producing the bio-oil is described elsewhere [19]. Briefly, red oak (Quercus rubra) was fast pyrolyzed at 500 ℃ in a fluidized reactor equipped with a condenser train. The recovered bio-oil was washed with cold water to isolate lignin bio-oil, also called pyrolytic lignin (PL). Methylene chloride (DCM), triethylamine (TEA), methacryloyl chloride (MC), acetyl chloride (AC), sodium bicarbonate, 1, 4-dioxane and 2, 2-azobisisobutyronitrile (AIBN) were purchased from Sigma Aldrich. The as-received AIBN was purified and recrystallized in methanol and stored at -20 ℃ prior to use. Chain transfer agent was synthesized in the lab (CYCART) and also stored at -20 ℃.

5.2.2 PL Functionalization

The polymer synthesis included two steps: esterification of PL followed by RAFT polymerization of the esterified PL. In this study, the PL esterification was carried out using three different methods. In the first method, hydroxyl groups in PL were fully methacrylated; in the second method, hydroxyl groups were partially methacrylated; in the third method, hydroxyl groups were also partially methacrylated but the residue hydroxyl groups were subsequently acetylated. Typical functionalization process of PL is described as below: 15g of PL was dissolved in 300 mL DCM and then stirred vigorously for 30 mins. Next, TEA was added in the solvent followed by adding an equal amount mole of MC drop wisely. The sample was left inside a fume hood at room temperature for overnight reaction. Next, 200 mL of deionized (DI) water was added into the solution and stirred for 30 mins. Afterwards, the functionalized PL (PL methacrylate, PLMA) in DCM was collected using a separating funnel. In the case of acetylation, the

methacrylated PL was further acetylated with an excess amount of AC and equal mole of TEA to eliminate residual hydroxyls. Finally, the PLMA was washed with DI water again, followed by washing with sodium bicarbonate solution (8g/100mL) twice to remove remaining acid. The PLMA in DCM was first rotary evaporated and further dried in a vacuum oven overnight to eliminate DCM. Based on the amount of MC and AC added, three PLMAs, denoted as PLMA1, PLMA2, and PLMA3 were obtained. The amounts of MC and AC used for each case are summarized in Table 5.1.

5.2.3 Polymer Synthesis

Five grams of PLMAs produced from the above processes were dissolved in 15 mL of 1, 4-dioxane in a flask. AIBN (~ 1wt %) and CTA with targeted molecular weight of 20,000 g/mol were added to the solution. The flask was then sealed and purged with argon for 30 mins. After purging, the flask was transferred to an oil bath at 90 ℃ for polymerization. The reaction was conducted for 4 hrs. After reaction, the solutions were cooled to room temperature and then vacuum dried at room temperature overnight to eliminate 1,4-dioxane. The PL methacrylate polymers (PLMAP1, PLMAP2, and PLMAP3) were then precipitated in methanol twice and further dried in the vacuum oven. The yield of the polymer was calculated by dividing the mass of the final PLMAPs over the initial mass of PLMAs.

5.2.4 Characterizations

Fourier Transform Infrared (FTIR) analysis was conducted using a Thermo Scientific Nicolet iS10 (Thermo Fisher Scientific Inc., Waltham, MA) equipped with a Smart iTR accessory. The wave numbers of the FTIR analysis ranged from 750 cm^{-1} to 4000 cm^{-1}. Each sample was scanned 32 times at a resolution of 4 cm^{-1} and interval of 1 cm^{-1}.

An Agilent 7890B gas chromatography (GC) with Agilent 5977A mass-selective-detector (MSD) and flame ionization detector (FID) system was used to identify the monomer composition in PL. The capillary column used in the GC was a ZB-1701 (60 m × 250 mm × 0.25 mm). The injection temperature at the GC was 250 ℃. The oven temperature was kept at 40 ℃ for 3 mins and then ramped to 280 ℃ at 3 ℃/min.

Gel permeation chromatography (GPC) analysis was conducted using Dionex Ultimate 3000 series high performance liquid chromatography (HPLC) equipped with a Shodex Refractive Index (RI) and Diode Array Detectors (DAD). A UV detector (254 nm) was used to detect the peaks. GPC column was calibrated with six monodispersed polystyrene standards ranging from 162 g/mol to 45120 g/mol. Tetrahydrofuran (THF) was used as both the solvent and eluent in the column. The viscosity measurement was conducted using a Malvern 270 Dual detector.

Glass transition temperature, T_g, was determined using a differential scanning calorimeter (DSC, Q2000, TA instruments). First, about 5 mg of sample was rapidly heated to 200 ℃ and then cooled to 0 ℃ to eliminate thermal history. Subsequently, the sample was reheated to 200 ℃ at a heating rate of 10 ℃/min to determine T_g. Nitrogen with a flow rate of 50 mL/min was used as the purge gas. The midpoint T_g of the polymer was determined using the TA software.

Thermal stability of PLMAPs was determined using a thermal gravimetric analyzer (TGA/DSC 1 STARe system, Mettler Toledo). About 10 mg samples were first dried in the vacuum oven at 40 ℃ overnight and then pyrolyzed by the TGA at 10 ℃/min using nitrogen gas with a flow rate of 100 mL/min until the temperature reached 1000 ℃. The thermal decomposition temperature (T_d) was defined as the temperature corresponding to a 5% of mass loss.

^{1}H NMR spectroscopy of PL and PLMAs was conducted using Bruker Biospin Advance 600 MHz, and $CDCl_3$ as solvent with 4-nitrobenzaldehyde as internal standard (IS). PL was acetylated with acetyl chloride prior to the analysis. For quantification of C=C, the peak difference between 6-7 ppm for acetylated PL and PLMAs were used. The integration of peaks, masses of PLMAs and IS, were provided in Fig. S5.2 and Table S5.1. ^{1}H-^{13}C correlation NMR (2D NMR) spectroscopy (Bruker Biospin Advance 600 MHz, DMSO) of the acetylated PL was also conducted and analyzed according to reference [20].

Rheology analysis of the PLMAPs was performed using a Discovery hybrid rheometer (DHR-2, TA Instruments) with 25 mm parallel-plate geometry. Temperature ramp was conducted with a maximum temperature of 250 ℃ with fixed angular frequency of 10 rad/s and strain of 1.25%. Frequency sweep at 210 ℃ was also conducted for the angular frequency between 0.1 to 100 rad/s at fixed strain of 1.25%. Isothermal time sweep was also conducted at 210 ℃.

5.3. Results and Discussion

5.3.1 Characterizations of PL

The PL was a highly viscous liquid at room temperature with a good solubility in many polar solvents such as THF, acetone, and methanol. This differentiates PL from lignin as usually lignin has to be esterified to enhance its solvent solubility [21]. The weight average molecular weight (M_w) of PL was 566 g/mol and its dispersity was 2.44. In comparison, the M_ws of red oak lignin were 1769~5364 g/mol in previous study depending on lignin isolation method [22]. Since lignin is made of three monolignols (i.e., P-coumaryl alcohol, coniferyl alcohol and sinapyl alcohol) with their respective molecular weights of 150, 180 and 210 g/mol [23], the average degree of polymerization of the PL is about 3. The GC/MS chromatogram of PL is given in Fig. 5.1. A number of peaks appeared in the chromatogram, implying the complex composition of the PL.

Among the peaks, 14 major peaks identified were various phenolic monomers containing hydroxyl, methoxyl, methyl, propanol, vinyl and/or aldehyde groups on side chain. Although not quantified in this study, the concentration of each phenolic monomer is usually low, mostly below 1% [22]. It should be noted that only the compounds with low molecular weights (<200-220 g/mol) and with sufficient volatility can be detected by GC/MS. Thus, the phenolic oligomers are not detected by GC/MS due to their larger molecular weights although they are also abundantly present in PL. The plausible structures of the oligomers are previously suggested and given in literature [16].

The complexity of its composition is further evident from the FTIR and NMR results of PL. In the FTIR spectrum of PL given in Fig. 5.2, the large peak appears at 3400 cm^{-1} corresponds to hydroxyls. Peaks representing methyl/methylene (2842-3000 cm^{-1}), carbonyls (1738 cm^{-1}), esters (1221 cm^{-1}), and ether bonds (1080 cm^{-1}) were also observed. The 2D-NMR spectrum of PL is given in Fig. S5.1. From the spectrum, aromatic (δ_C-δ_H 100-150/6-7.5 ppm), syringyls 2/6 (S and S'), guaiacyls 2/5/6 (G) derived units, benzaldehydes (X3) and cinnamaldehyde (X2) units were identified. In addition, oxygenated aliphatic groups (δC-δH 50-100/3-4 ppm) attached to aromatic rings were also identified [20, 24]. The ^{1}H-NMR spectra shown in Fig. S5.2 (a) was used to quantify the contents of phenolic hydroxyls (δ 2.20-2.35 ppm), aliphatic hydroxyls (δ 2.00-2.10 ppm) and methoxyls (δ 3.75-4.00 ppm). Based on the results, the content of phenolic hydroxyls and aliphatic hydroxyls were 2.58 mol/mol and 0.46 mol/mol, giving the total amount of hydroxyls in average PL molecules to be 3.04 mol/mol. For the PL compounds, aromatic hydroxyls could include phenolic and catechol hydroxyls, and aliphatic hydroxyls include hydroxyls on both primary alcohols and secondary alcohols. The NMR result also showed that the amount of methoxyl group in PL to be 1.59 mol/mol. The amount of methoxyls was low in PL due to

demethoxylation during lignin pyrolysis [22]. The properties of PL based on GPC and 1H-NMR analyses are also summarized in Table 5.2.

5.3.2 Functionalization of PL to PLMAs

The abundant hydroxyl groups in PL could serve as the most sensible site for esterification. The reaction schemes of typical monomers and oligomers in PL based on the three proposed functionalization methods are illustrated in Fig. 5.3. All resulting PLMAs were flowable at room temperature but their viscosity increased compared to PL. Their molecular weights are given in Table 5.3. The M_w of PLMA1, for the case hydroxyl group in PL was fully methacrylated, increased to over 1000 Da due to the substitution of hydroxyls with methacrylic groups. PLMA2, for the case PL was partly methacrylated, had similar M_w as that of PL but a decreased dispersity. Since hydroxyls of PL were partly esterified, it is possible that some hydroxyl containing molecules with stronger polarity remained as DCM insoluble. Only less polar molecules were dissolved and recovered as PLMA2, thus reporting the reduced M_w and dispersity. The M_w of PLMA3, for the case hydroxyl group in PL was partly methacrylated and remaining hydroxyls were captured by acetyl groups, increased to over 800 Da due to the introduction of both methacryloyl group and acetyl group. Since hydroxyls were fully esterified, the polarities were reduced and all the molecules after esterification were able to be dissolved in DCM and recovered as PLMA3.

FTIR spectra of PLMAs are also shown in Fig. 5.2 to compare with the spectra of PL. The peaks at 3400 cm^{-1} stands for hydroxyls dramatically decreased at both PLMA1 and PLMA3, which imply a thorough functionalization of hydroxyls. In comparison, this peak was much more pronounced in PLMA2 since some of hydroxyl groups were left unesterified. In the spectra, the appearance of peaks at 1750 cm^{-1} (C=O), 1240 cm^{-1} (acetyl-O-aromatics), and 1080 cm^{-1} (C-O) are

indicative of successful introduction of methacrylates (and acetyls in PLMA3). The peak appears at 1640 cm^{-1} is a good indicator of C=C bonds [10]. This peak was not identifiable in PL probably because of its low abundancy, but it became noticeable in all the PLMAs. The C=C peak was sharper and most intense at PLMA1, indicating PLMA1 contains more C=C due to a higher extent of hydroxyl substitution by methacrylate. PLMA2 and PLMA3 showed smaller C=C peaks since they were both partially methacrylated.

The amount of added C=C bonds for PLMAs were also quantified based on their ^{1}H NMR spectra (Fig. S5.2(b)-(d)). As shown in Table 5.3, the C=C concentration was 3.58 mol/mol for PLMA1. Considering OH concentration in PL was 3.04 mol/mol, this result implies that hydroxyls were fully methacrylated in PLMA1. Since methacrylation of each mole of OH should result in an equal mole of C=C, the higher C=C concentration than 3.04 mol/mol may be due to original C=C concentration in PL side chains (although it was not obvious with the FTIR spectrum of PL). For instant, C=C is found in phenolic vinyl and propanol identified in the GC/MS analysis of PL, as previously shown in Fig. 5.1. For PLMA2, the C=C concentration was 0.78 mole/mole, despite methacrylating 1 mol/mol of OH is supposed to create the same mole of new C=C in PLMA2. The lower than expected C=C concentration suggests that some molecules were also methacrylated, but they stayed as DCM insoluble due to the high polarity caused by other unesterified hydroxyls in the same molecules. It should be noted that hydroxyl groups are not eventually distributed among individual the phenolic monomers and oligomers in PL. Some could contain more than three hydroxyls per molecule, while others could contain much fewer hydroxyls per molecule. For PLMA3, the C=C concentration was 1.26 mol/mol. PLMA3 could be fully recovered in DCM since its residual hydroxyls were captured with less polar acetyls.

5.3.3 RAFT Polymerization to PLMAs

The polymer yields, Mws and dispersity of PLMAPs after 4 hrs of reactions are given in Table 5.4. During the reaction, PLMAP1 started to gel only after 30 minutes and its yield reached 89% after 4hrs. Gelation is a result of extensive intermolecular crosslinking. During the polymerization, the chain propagation and branching occur simultaneously [25]. Since excess functionalization led to the formation of multiple radically polymerizable C=C sites on the molecules of PLMA1, the rapid branching could surpass chain propagation and eventually form extensively crosslinked polymer that is insoluble.

Gelation was not observed in either PLMAP2 or PLMAP3 during their respective synthesis processes, contributed to the reduced C=C sites in PLMA2 or PLMA3 that reduces the possibility for developing crosslinking. After 4 hrs, the M_w of PLMA2 reached 11282 g/mol and its dispersity was remained low at 1.55. The polymer yield of PLMA2 was only 18.51%. Since hydroxyl groups were not fully functionalized, the residue hydroxyl groups could act as radical inhibitors to hinder the polymerization initiation and effective chain propagation. Also, recall that the concentration of C=C was only 0.78 mol/mol in PLMA2 (the DCM soluble fraction). Since there was average less than one radically polymerizable site on each molecule, some individual molecules with no C=C could not participate in the radical polymerization process. The M_w of PLMAP3 was 15984 g/mol, closer to the target M_w. The corresponding dispersity was 1.53 and the yield was 42.5%. Since hydroxyl groups were either methacrylated or acetylated, their radical inhibitor effect was reduced in PLMA3. The C=C content in PLMA3 was also higher, and thus better chain initiation and propagation. Both PLMAP2 and PLMAP3 had dispersity well below 2, which is contributed by RAFT technique applied in this study. As shown in Fig. S5.3, PLMAP1 appeared to be a dark brown material, the similar color as the original PL. In comparison, the dark color of original PL

was significantly removed and both PLMAP2 and PLMAP3 appeared to light brownish materials. Owing to PL's complex compositions, PLMAP2 and PLMAP3 are likely the polymers with linear methacrylate backbones and various pendant aromatic structures. The viscometry and GPC data of PLMAP2 and PLMAP3 were combined to form the Mark-Houwink plot and shown in Fig. S5.4. The Mark-Houwink equation, $[\eta] = KM^{\alpha}$, is a classical result of polymer physics that relates the intrinsic viscosity of a polymer solution to its molecular weight through the hydrodynamic volume. The determination of α value is capable of understanding the molecular confirmation of polymers. For most of the technical lignins, α is low at 0.14-0.25 pointing toward their spherical structures [26]. In this study, α is 1.16 for PLMAP2, and 0.86 for PLMAP3, indicating both polymers have developed relatively linear and stretched structures as proposed. PLMAP2 is a more rigid polymer than PLMAP3, possibly because residue hydroxyls on pendants increase inter- or intra- molecular interactions through hydrogen bonding.

5.3.4 Thermal Properties of PLMAPs

The DSC curves of PLMAPs are given in Fig. S5.5. No fluctuation was observed in the curve of PLMAP1, indicating the absence of glass transition temperature below 200 ℃. Since PLMAP1 is highly crosslinked, the movement of molecular chains was severely restricted. The DSC curves of both PLMAP2 and PLMAP3 were similar to those observed with lignin or other lignin-based materials [27, 28]. Instead of sharp peaks commonly observed with well-defined polymer materials, only small dips representing transition from glassy state to rubbery state were observed. While PLMAP2 and PLMAP3 have linear orientation, their pendant structures are not uniform. . The T_g of PLMAL2 was 161 ℃, higher than that of many biobased polymers [12]. The formation of hydrogen bonding among the chains associated with the presence of residue hydroxyls could be one of the reasons for the high T_g of the polymer. The T_g of PMAPL3 was 130

℃ . The substitution of residue hydroxyls by acetyls lowered the molecular interactions, and thus lowered the T_g [29]. The T_gs of the methacrylate polymers can also be affected by the pendant structures. Previously, Holmberg et al. showed that the T_gs of the methacrylate polymers depended on side chain functional groups on the feedstock monomers, increasing in the order of ethyl guaiacol<guaiacol<cresol<vanillin<syringol [11, 12]. Overall, the alkyl group lowers T_g whereas aldehyde group increases T_g. Syringol-based polymer had the highest T_g possibly because symmetric methoxyl groups could restrict molecular rotation. As previously described, PL consists of many phenolic molecules vary in molecular sizes and functionalities. Therefore, the T_g of the methacrylate polymer is likely to strongly depend on the composition of PL. In addition to PL composition, polymer synthesis conditions (temperature, initiator ratio, reaction time, etc.) and molecular weights of the polymer could also influence T_g of the resulting polymer.

The results from thermogravimetric analysis (TGA) are plotted in Fig. 5.4. PLMAP3 showed best thermal stability among the three polymers. Its T_d was 250 ℃, much higher than its T_g. This result suggests that there is a sufficiently wide temperature range at where the polymer can be melt-processed without causing polymer degradation. The T_d of PLMAP2 was slightly lower at 241 ℃ because of the absence of thermally stable acetyl groups. The T_g of PLMAP1 was 203 ℃, which was lowest. Probably, the methyl groups in PLMAP1 could be easily cleaved at low temperatures during pyrolysis. PLMAP1 is expected to contain more methyl groups than PLMAP2 or PLMAP3 because the extent of methyacrylation was highest with PLMA1.

It was also found that PLMAPs could be pyrolyzed at 1000 ℃, leaving solid residues. For all the polymers, the mass losses mostly occurred between their respective T_ds and the temperatures up to about 450 ℃. The mass losses at above 450 ℃ were insignificant at all the polymers, suggesting more aromatized and thermally stable structures were formed among the

solid residues. The yields of solid residues at 1000 ℃ were between 24~28% for the three polymers with the highest yield achieved with PLMAP3. In previous studies, the phenolic monomer-derived methacrylate polymers were completely or nearly completely volatilized at temperature around 500 ℃ [11]. Compared to the monomer-based polymers, the PLMAPs have bulkier pendants attached to the methacrylate backbones. When the PLMAPs degrade at elevated temperatures, the bulkier pendants are less likely to volatilize than smaller pendants made of simple monomers. Moreover, the bulky pendants with various functional groups could also react with nearby pendants under elevated temperatures to form polyaromatic structures through thermally induced condensation reactions. As a result, heat tolerance of PLMAPs at high temperatures was significantly better than the monomer-based polymers.

5.3.5 Melt Rheology of PLMAPs

Temperature sweep of PLMAPs was conducted and the results are shown in Fig. 5.5. Storage modulus (G') measures the material's ability to store energy and represents elastic property of a material. Loss modulus (G") measures energy dispersed as heat and it represents viscous property of a material. The G' of PLMAP1 was constantly higher than G'', indicating this polymer is cross-linked and behaves as an elastic solid. It can be found that there is not a significant decrease in the G' value along with increasing temperature even after the polymer started to degrade. On the other hand, the G" of PLMAP2 was higher than its G' at temperature below 228 ℃, indicating its viscous behavior at the given temperature range. The G' and G'' crossed at higher temperatures where the polymer turned into an elastic material. As previously shown in the TGA results (Fig. 5.4), the polymer degradation occurred at similar temperature range where the G' and G'' crossed. Thus, this transition of viscous material to elastic material is likely related to the polymer degradation as a result of cross-linking and cracking. For PLMAP3, G' was also lower

than G'' before they crossed at 230 ℃, demonstrating its viscous behavior at the corresponding temperature region. For all the polymers, the complex viscosity (η^*) decreased with increasing temperature before it reversed the trend to increase at higher temperatures. The η^* was lowest with PLMAP3, since incorporating inert acetyls in PLMA3 reduced molecular interactions and improved their chain mobility. The η^* increase at higher temperatures is an indicative of the development of crosslinking within the polymers. The crosslinking temperatures T_cs, at where η^* reverses its trend, were 230 ℃, 205 ℃ and 227 ℃ for PLMAP1, PLMAP2 and PLMAP3, respectively. The T_c was lowest with PLMAP2 among the three polymers. Considering phenolic hydroxyls are highly reactive toward polycondensation reactions [29], the residue hydroxyls present in PLMAP2 could serve as the active sites to promote the crosslinking. Nevertheless, T_cs of PLMAP2 and PLMAP3 were both sufficiently higher than their respective T_gs. Thus, both PLMAP2 and PLMAP3 are thermoplastics at temperatures below their corresponding T_cs.

The rheology tests indicate PLMAP2 and PLMAP3 are both melt-processable. In comparison to PLMAP2, PLMAP3 exhibited much lower viscosity. At temperature range of 200~232 ℃, η^* of PLMAP3 was between 100 and 1000 Pa·s. It was suggested that a polymer within this viscosity range is suitable for spinning continuous filament [30]. In the present study, melt-rheology of PLMAP3 was further investigated at 210 ℃. According to the results of TGA and rheological analyses, neither the crosslinking reactions nor polymer degradation occur at this temperature. The result of frequency sweep is given in Fig. 5.6 (a). The G'' was constantly higher than G', showing the polymer remains as a viscous material at the entire frequency range. PLMAP3 also showed typical shear-thinning behavior of a lignin-based polymer [26]. Its near zero shear η^* was 3911 Pa·s and decreased at higher frequencies since the interaction between molecules due to chain entanglement was reduced as the frequency increases [31]. The isothermal

rheology of PLMAP3 is shown in Fig. 5.6 (b). The η^* increase as increasing retention time was not significant, as it changed from initial 376 Pa·s to 878 Pa·s after 10 mins. On the other hand, the slight increase in viscosity could be related to the reactivity of the pendant structures for thermally induced polycondensation. As described above, there present various functional groups other than hydroxyl on the phenolic monomers and oligomers that later become the source of the pendants in the PLMAPs. The polycondensation of PL molecules (also called bio-oil aging) can be accelerated at elevated temperatures [32].

5.3.6 Potential Application of PLMAP3 as Precursor of Carbon Fiber

As demonstrated above, methacrylate polymers could be synthesized directly from crude lignin bio-oil by skipping costly extraction and purification for monomers. The derived polymers could join other biobased polymers in various applications. The polymers produced in this study have relatively good thermal stability and high T_gs, thus could potentially be used in high temperature applications, such as machine parts, asphalt components, composites, and insulators [33]. Furthermore, PLMAP3 produced in this study demonstrated several attractive properties that are highly desirable toward carbon fiber production. Therefore, the applicability of PLMAP3 as a precursor of lignin-based carbon fiber is exclusively discussed in below section.

Carbon fiber is a light-weight material with high tensile strength. Two basic requirements of a carbon fiber precursor are its spinnability and the ability to carbonize. Lignin-based carbon fiber is usually fabricated using three steps: first the precursor is spun into fiber, followed by oxidative stabilization to increase fiber rigidity, and then finally carbonized at high temperatures (1000 ℃ or above) to remove non-carbon atoms. Melt spinning is preferred over wet-spinning or electrospinning due to its low cost. In most of previous studies, lignin was either directly melt processed or co-extruded with other polymers [5]. The limitation of the state-of-the art lignin-based carbon fibers compared to polyacrylonitrile based carbon fiber is its poor mechanical

properties. The requirements of ideal precursor for producing high-quality carbon fiber, as well as the limitations of lignin as the precursor material have been discussed in several articles [5, 8]. Baker et al. indicated that the lignin-based precursor should have narrower molecular distribution and low impurities. They also suggested that T_g of the precursor should be low enough so that the precursor can be melt-spun, yet it has to be high enough in order for the precursor fiber to be oxidatively stabilized with reasonable heating rates. The viscosity of the precursor needs to be within acceptable range. A lignin precursor with too low viscosity is difficult to form fiber, whereas the precursor with high viscosity cannot be drawn into continuous and uniform filament. Nevertheless, the lignin precursors that could meet these requirements still not able to deliver carbon fiber with satisfactory quality [9]. More recently, Frank et al. compared carbon fibers derived from different precursor materials and concluded that it is critical for the precursor to have molecular orientation in order to produce high-quality carbon fiber. The authors further pointed out that the molecular orientation of the precursor must be achieved before the fiber is stabilized or carbonized because high temperature processing cannot improve the molecular orientation. However, this critical requirement was impossible to meet with raw lignin, as lignin is intrinsically lack of molecular orientation due to its three-dimensional, amorphous, and randomly cross-linked structure.

Our present study showed that PLMAP3, the PL-based methacrylate polymer, could meet the abovementioned requirements and thus potentially be an ideal precursor of carbon fiber. The molecular weight of PLMAP3 is much higher than technical lignin [34], whereas the dispersity is much lower (<2). The T_g of PLMAP3 also lies in a suitable range for melt-spinning [30]. There is a temperature range at where the polymer can be drawn into fibers continuously without being affected by significant crosslinking or degradation. It is known that the precursor degradation

during the melt-spinning could result in carbon fibers with pores, therefore greatly weakening its mechanical strengths. Also, crosslinking during fiber spinning would increase the precursor viscosity and cause uneven fibers. On the other hand, crosslinking is desired at subsequent stabilization process of fibers since the precursor that does not crosslink is difficult to be stabilized. As previously shown in Fig. 5.5, the viscosity increase of PLMAP3 was observed at temperatures above T_c, indicating certain functionalities in the polymer (mostly on the pendant structures) could become reactive at elevated temperatures to develop crosslinking. Therefore, the precursor fiber should be able to be stabilized and turn into rigid solid by oxidation. Moreover, PLMAP3 can be carbonized at 1000 ℃, thus further satisfying the requirement as a carbon fiber precursor. Most importantly, PLMAP3 is a linear polymer with the methacrylate backbone as illustrated in Fig. 5.7. Such superior molecular orientation has not been found in any other lignin-based precursors to date. As described previously, establishing molecular orientation in a precursor is critical in order to produce high-quality carbon fiber. In the present study, PLMAP2 was also a linear thermoplastic polymer with melt-processability. Moreover, it could more easily be stabilized since residual hydroxyl groups intentionally left in the polymer promote crosslinking. However, the present of hydrogen bonding between hydroxyls also increased both T_g and viscosity of PLMAP2, making it a less desirable for melt-spinning. Further process is being developed to convert the as-spun PLMAP3 to high quality carbon fiber.

5.4. Conclusions

In this study, crude lignin bio-oil (PL) obtained from pyrolysis of red oak was synthesized to methacrylate polymers by employing RAFT polymerization technique. Polymerization of fully methacrylated PL resulted in gelation due to the extensive crosslinking to form a polymer with no detectable T_g. On the other hand, polymerization of partly methacrylated PL inhibited gelation to

yield a linear thermoplastic polymer with dispersity of 1.55, T_g of 161 ℃ and T_d of 241 ℃. However, the radical inhibitory effect of the residual hydroxyls was found to lower the M_w and polymer yield. In comparison, partial methacryation of PL followed by acetylation eliminated inhibitory effect of hydroxyl to enhance the polymerization. It was found that PLMAP3 demonstrates several attractive characteristics that are highly desirable toward carbon fiber production. Its M_w was around 16k g/mol while dispersity was as low as 1.53. The T_d of PLMAP3 was 250 ℃, much higher than its T_g of 130 ℃. Rheological results showed that the viscosity of PLMAP3 at temperature range of 190 to 230 ℃ was between 100~1000 Pa·s, suggesting the polymer could be continuously spun into filament without causing polymer degradation. PLMAP3 could also be pyrolyzed, leaving 28% of solid residue at 1000 ℃. Most importantly, PLMAP3 was a linear polymer, thus providing superior molecular orientation that is critical in order to produce high-quality carbon fiber. In summary, such a polymer with these ideal properties for carbon fiber precursor was for the first time produced from lignin. In future studies, the properties of the precursor polymer will be tuned, by such as changing target molecular weight or adjusting the reaction conditions. The relationship between the precursor polymer's properties and carbon fiber processing will also be investigated.

5.5 Tables and Figures

Table 5.1 Functionalization of PLMAs

		PLMA1	PLMA2	PLMA3
		(mol/mol PL)		
Step 1	MC	3	1	1
	TEA	3	1	1
Step 2	AC	2	0	4
	TEA	2	0	4

Table 5.2 Properties of PL based on GPA and ^{1}H NMR analyses

GPC		^{1}H NMR (mol/mol PL)		
M_w (Da)	Dispersity	Phenolic OH	Aliphatic OH	Methoxyl
566	2.44	2.58	0.46	1.59

Table 5.3 Properties of PLMAs based on GPC and ^{1}H NMR analyses

	PLMA1	PLMA2	PLMA3
		GPC	
M_w (Da)	1046	561*	803
Dispersity	2.62	1.58*	2.22
		^{1}H NMR	
Calculated C=C (mol/mol)	3.58	0.78	1.26

* Only DCM soluble fraction

Table 5.4 Yields of PLMAPs after 4hrs reaction and their molecular properties

	PLMAP1	PLMAP2	PLMAP3
Yield (%)	89.3	18.5	42.5
M_w	∞	11282	15984
M_n	∞	7276	10420
Dispersity	-	1.55	1.53

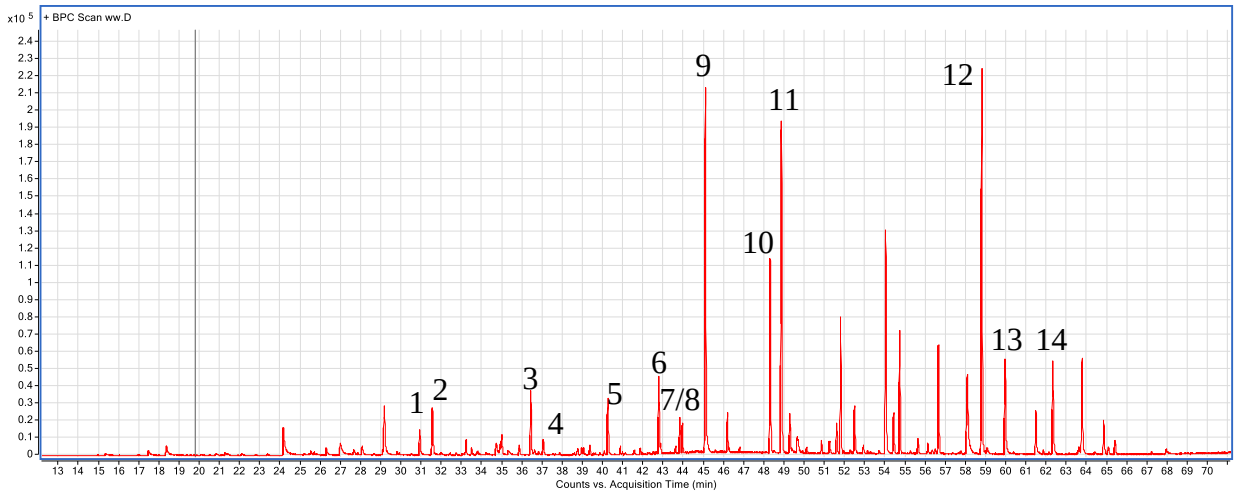

Figure 5.1 GC/MS detectable phenolic monomers in PL: 1. Phenol; 2. Phenol, 2-methoxy-; 3. 2-Methoxy-5-methylphenol; 4. Phenol, 3,5-dimethyl-; 5. Phenol, 3,4-dimethyl-; 6. 2-Methoxy-4-vinylphenol; 7. 3-Allyl-6-methoxyphenol; 8. Phenol, 2-methoxy-4-propyl-; 9. Phenol, 2,6-dimethoxy-; 10. trans-Isoeugenol; 11. 1,2,4-Trimethoxybenzene; 12. Phenol, 2,6-dimethoxy-4-(2-propenyl)-; 13. Benzaldehyde, 4-hydroxy-3,5-dimethoxy-; 14. Ethanone, 1-(4-hydroxy-3,5-dimethoxyphenyl)-.

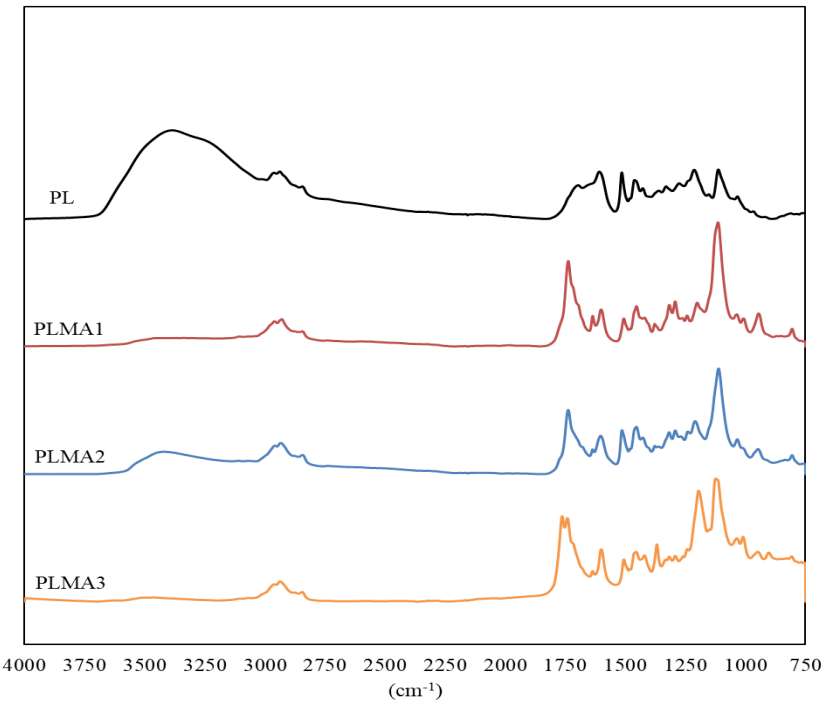

Figure 5.2 FTIR spectra of PLMAs.

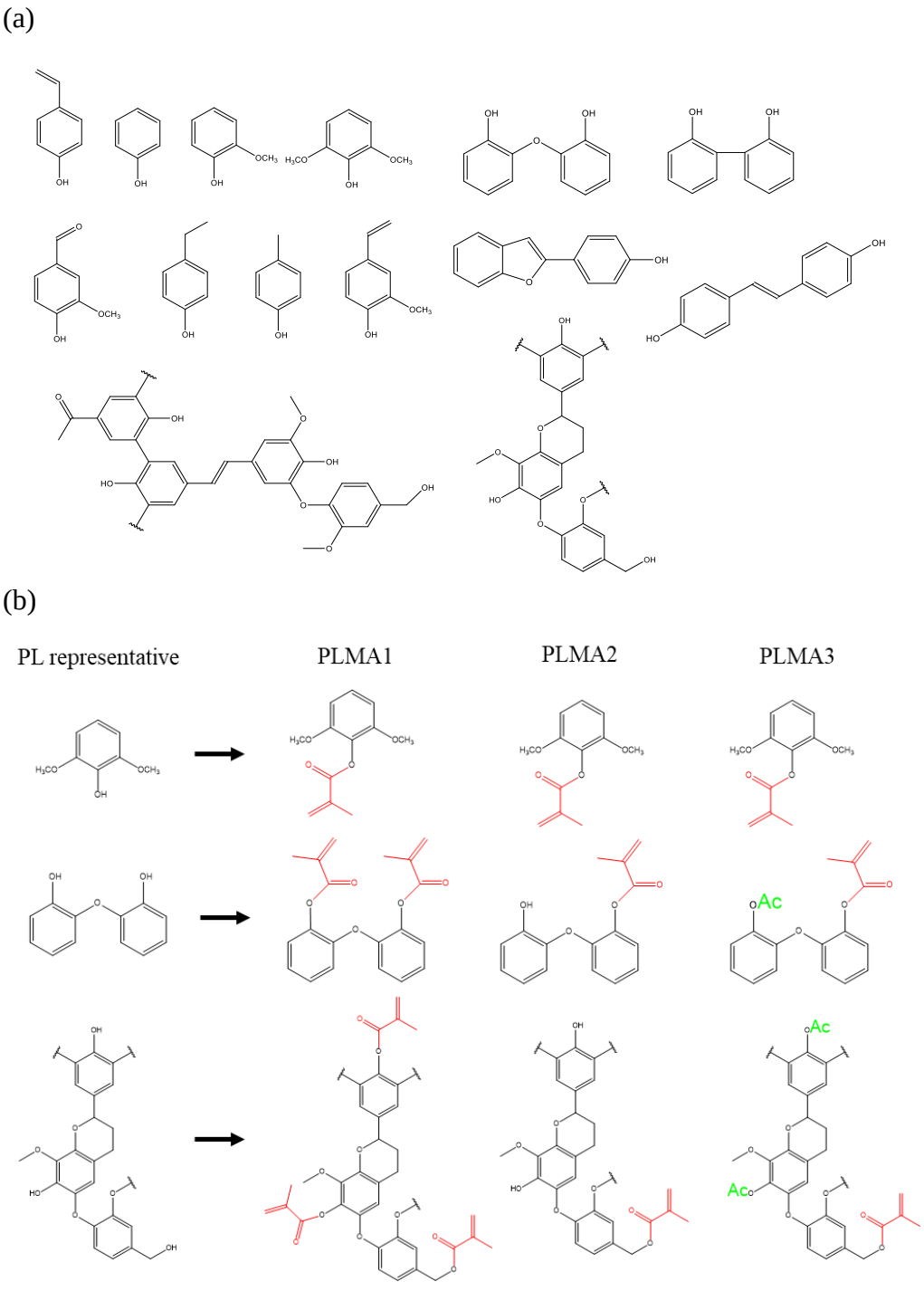

Figure 5.3 a) Examples of phenolic compounds found in PL. The plausible structure of dimers and trimers are based on reference [16]; b) Functionalization of representative phenolic monomer and oligomers based on three different methods.

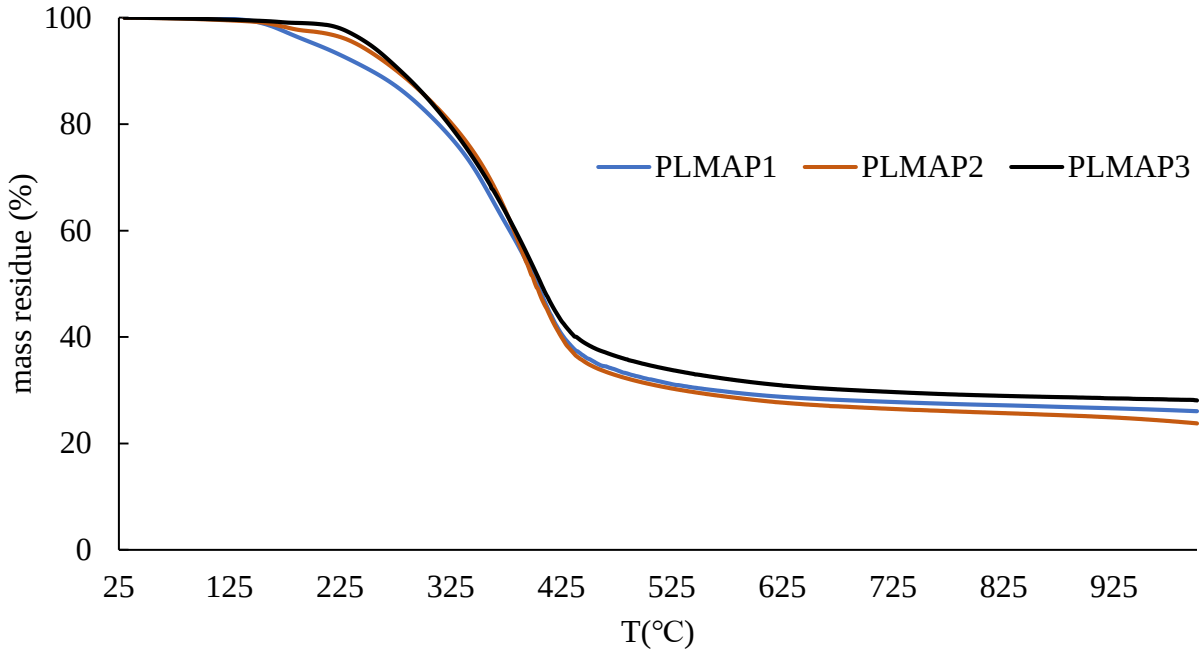

Figure 5.4 TGA curves of PLMAPs.

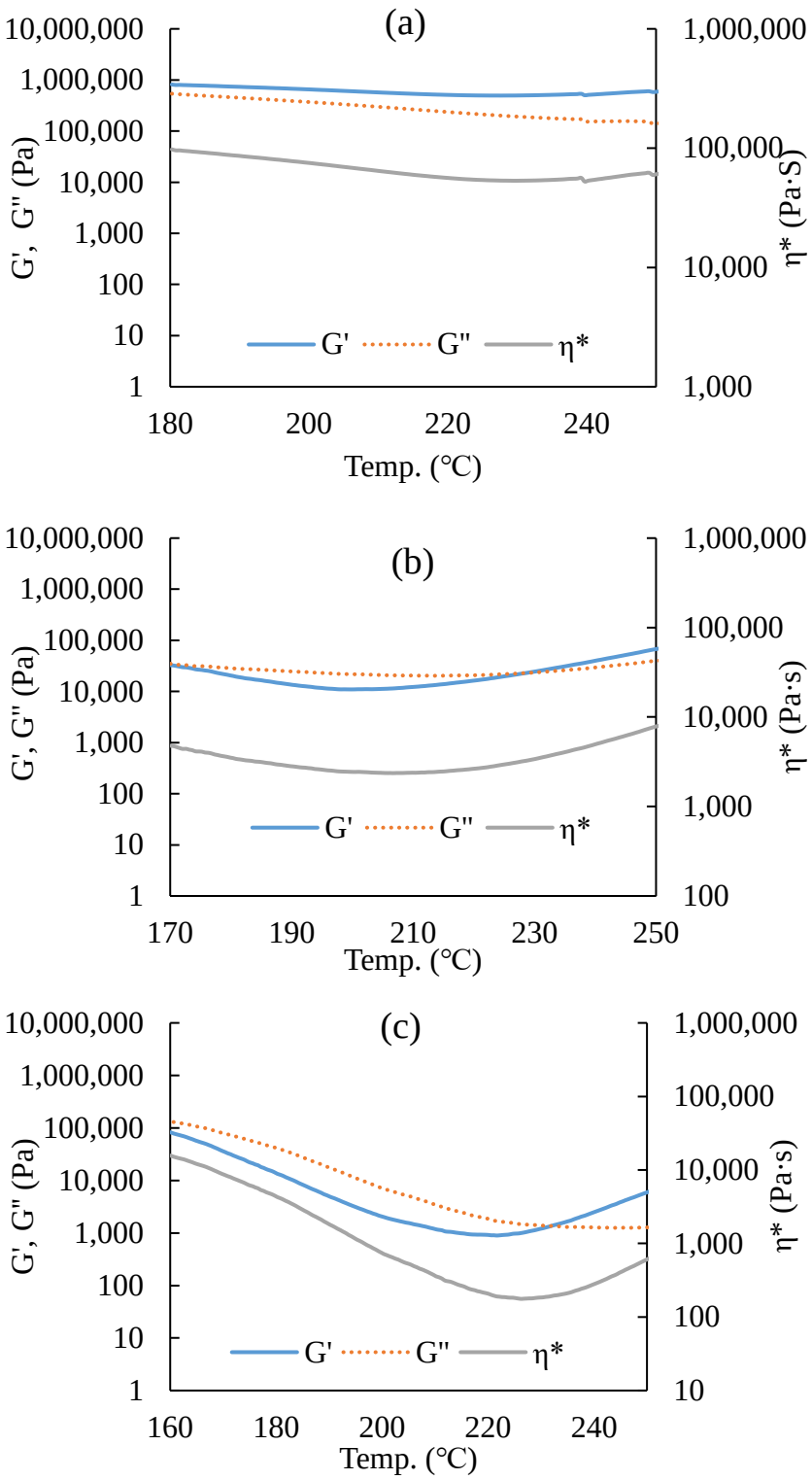

Figure 5.5 Temperature sweep of PLMAPs; (a). PLMAP1; (b). PLMAP2; (c). PLMAP3. G'-storage modulus; G"-loss modulus; η*- complex viscosity.

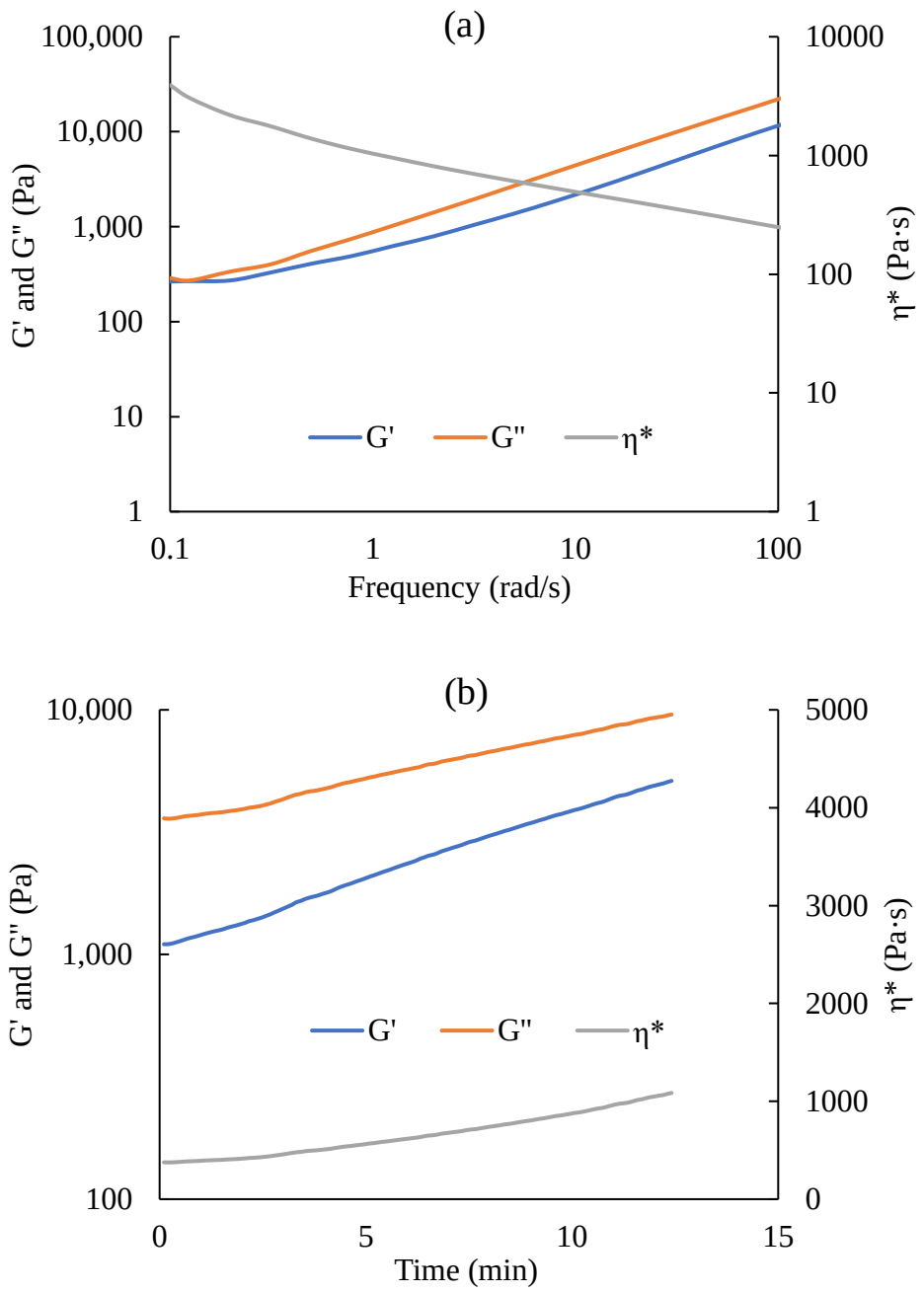

Figure 5.6 (a) Frequency sweep and (b) isothermal sweep of PLMAP3 at 210 ℃

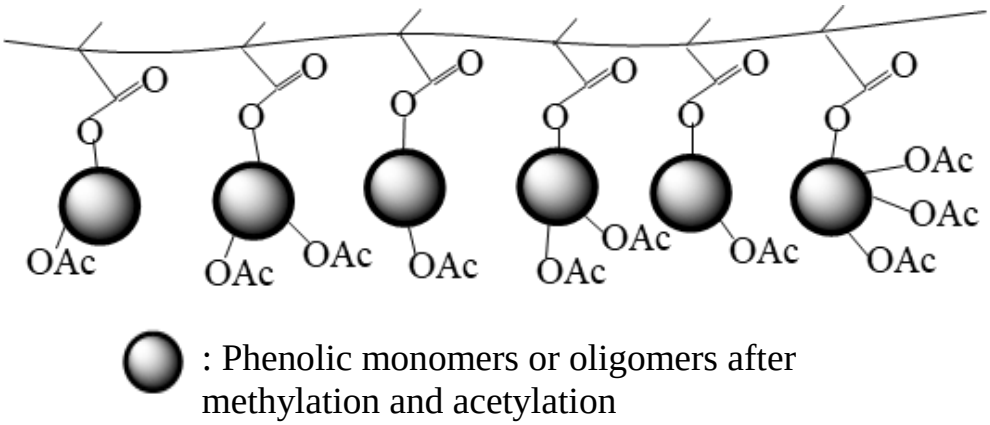

Figure 5.7 Representative structure of PLMAP3.

5.6 Supplemental Tables and Figures

Table S5.1 Datasheet used for quantification of added C=C for PLMAs.

	Mw (Da)	Mass (mg)	Internal standard (mg)	Peak area (6-7 ppm)	C=C/PLMA (mol/mol)
Original PL	600*	24.75	4.02	5.07	NA
PLMA1	1046	23.5	3.99	8.88	3.58
PLMA2	561	23.97	2.83	11.06	0.78
PLMA3	803	24.12	4.05	6.51	1.26

* Slightly increase due to acetylation

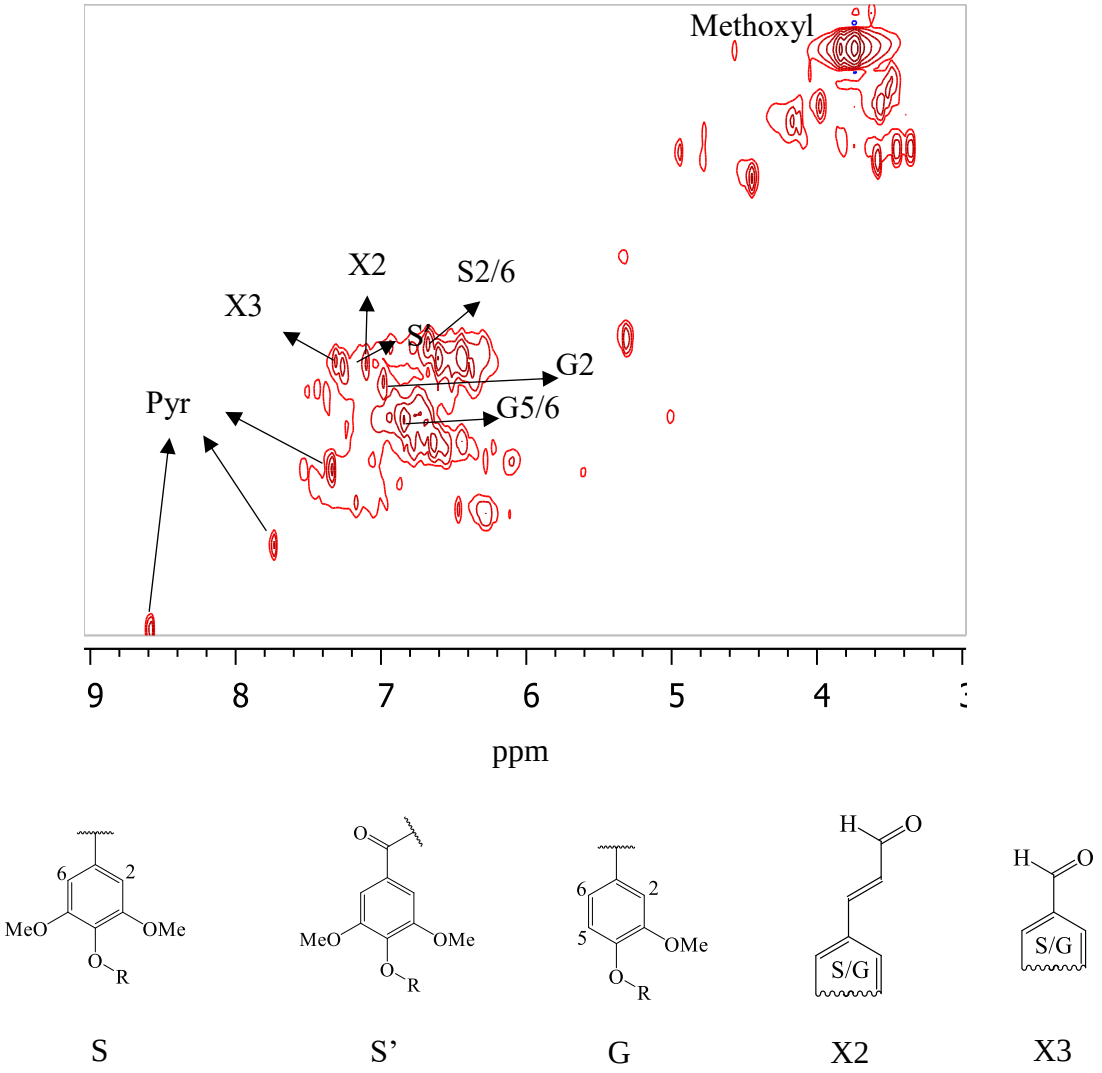

Figure S5.1 2D NMR spectrum of PL.

(a)

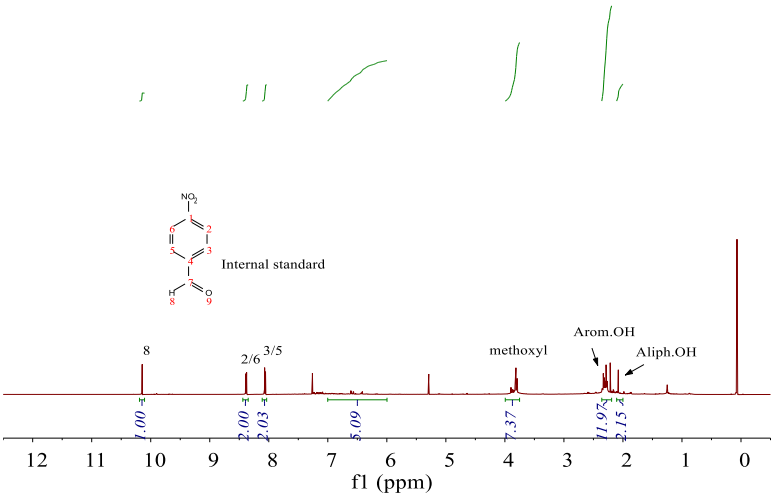
Internal standard
8
2/6
3/5
methoxyl
Arom.OH
Aliph.OH
1.00
2.00
2.03
5.09
7.37
11.97
2.15
12 11 10 9 8 7 6 5 4 3 2 1 0
f1 (ppm)

(b)

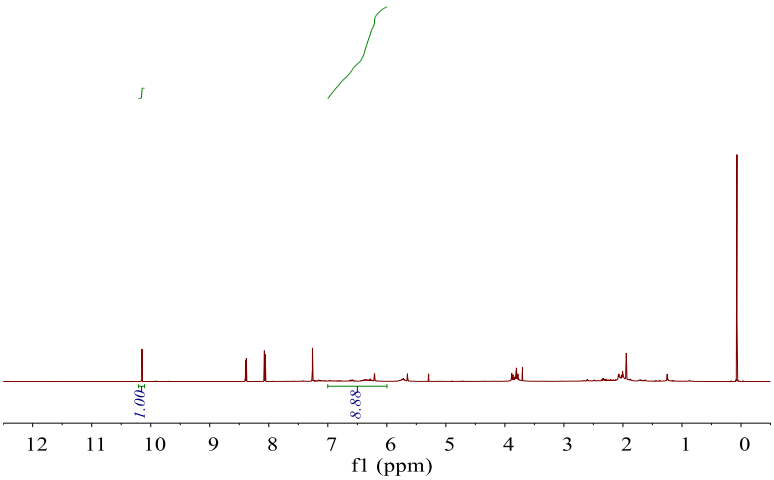
1.00
8.88
12 11 10 9 8 7 6 5 4 3 2 1 0
f1 (ppm)

(c)

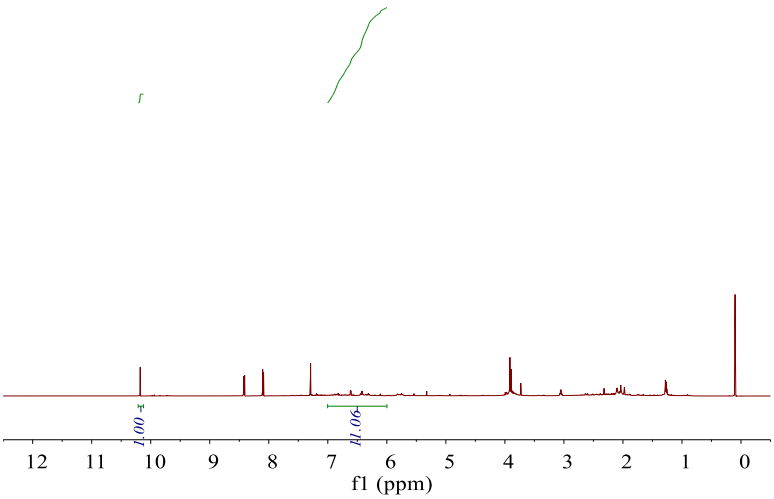
1.00
11.06
12 11 10 9 8 7 6 5 4 3 2 1 0
f1 (ppm)

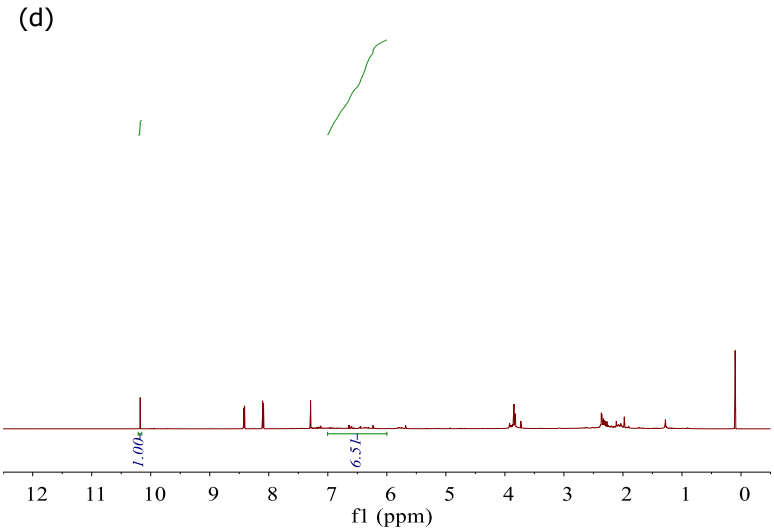

Figure S5.2 ^{1}H NMR spectra of (a) acetylated PL (b) PLMA1 (c) PLMA2 (d) PLMA3.

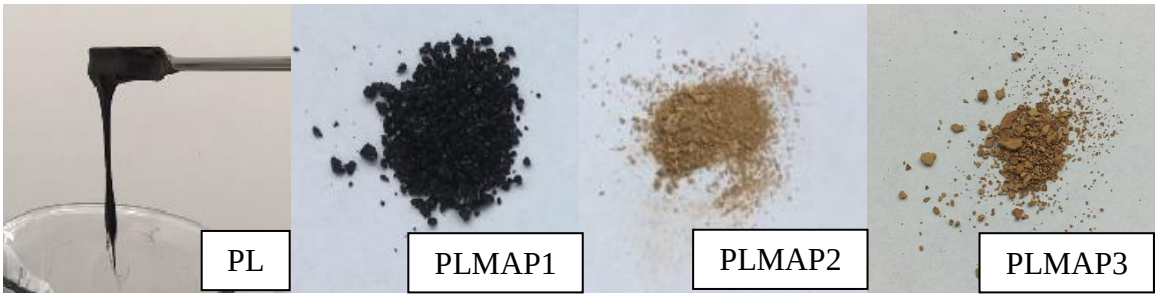

Figure S5.3 Appearances of PL and PLMAPs.

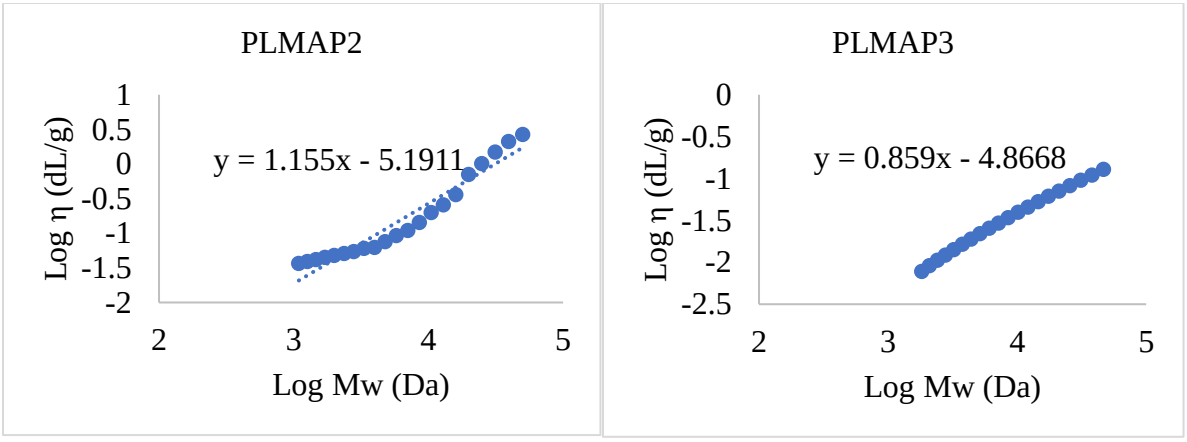

Figure S5.4 Mark-Houwink plot for PLMAP2 and PLMAP3.

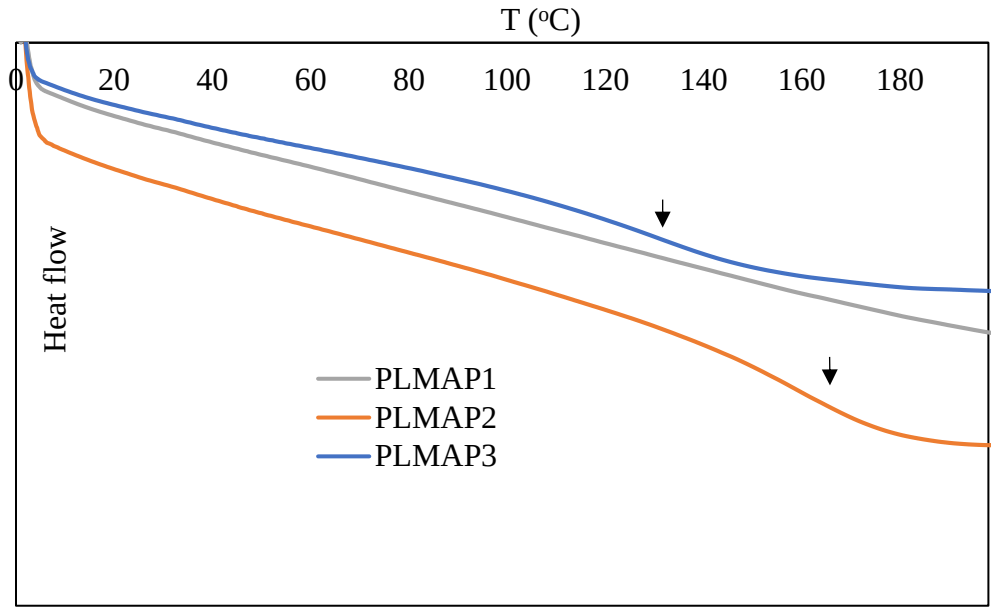

Figure S5.5 DSC curves of PLMAPs.

5.7 References

1. Kai, D., et al., *Towards lignin-based functional materials in a sustainable world.* Green Chemistry, 2016. **18**(5): p. 1175-1200.
2. Ragauskas, A.J., et al., *Lignin valorization: improving lignin processing in the biorefinery.* Science, 2014. **344**(6185): p. 1246843.
3. Liu, H.C., et al., *Processing, structure, and properties of lignin-and CNT-incorporated polyacrylonitrile-based carbon fibers.* ACS Sustainable Chemistry & Engineering, 2015. **3**(9): p. 1943-1954.
4. Thakur, V.K., et al., *Progress in green polymer composites from lignin for multifunctional applications: a review.* ACS Sustainable Chemistry & Engineering, 2014. **2**(5): p. 1072-1092.
5. Baker, D.A. and T.G. Rials, *Recent advances in low-cost carbon fiber manufacture from lignin.* Journal of Applied Polymer Science, 2013. **130**(2): p. 713-728.
6. Gordobil, O., et al., *Kraft lignin as filler in PLA to improve ductility and thermal properties.* Industrial Crops and Products, 2015. **72**: p. 46-53.
7. Gordobil, O., et al., *Physicochemical properties of PLA lignin blends.* Polymer Degradation and Stability, 2014. **108**: p. 330-338.
8. Frank, E., et al., *Carbon fibers: precursor systems, processing, structure, and properties.* Angewandte Chemie International Edition, 2014. **53**(21): p. 5262-5298.
9. Qu, W., et al., *Potential of producing carbon fiber from biorefinery corn stover lignin with high ash content.* Journal of Applied Polymer Science, 2018.
10. Stanzione III, J.F., et al., *Lignin-based bio-oil mimic as biobased resin for composite applications.* ACS Sustainable Chemistry & Engineering, 2013. **1**(4): p. 419-426.

11. Holmberg, A.L., et al., *Softwood lignin-based methacrylate polymers with tunable thermal and viscoelastic properties.* Macromolecules, 2016. **49**(4): p. 1286-1295.
12. Holmberg, A.L., et al., *Syringyl methacrylate, a hardwood lignin-based monomer for high-T g polymeric materials.* ACS macro letters, 2016. **5**(5): p. 574-578.
13. Mialon, L., A.G. Pemba, and S.A. Miller, *Biorenewable polyethylene terephthalate mimics derived from lignin and acetic acid.* Green Chemistry, 2010. **12**(10): p. 1704-1706.
14. Mahmood, N., et al., *Hydrolytic liquefaction of hydrolysis lignin for the preparation of bio-based rigid polyurethane foam.* Green Chemistry, 2016. **18**(8): p. 2385-2398.
15. Qu, W., et al., *Repolymerization of pyrolytic lignin for producing carbon fiber with improved properties.* Biomass and Bioenergy, 2016. **95**: p. 19-26.
16. Bayerbach, R. and D. Meier, *Characterization of the water-insoluble fraction from fast pyrolysis liquids (pyrolytic lignin). Part IV: Structure elucidation of oligomeric molecules.* Journal of Analytical and Applied Pyrolysis, 2009. **85**(1-2): p. 98-107.
17. Bai, X., et al., *Formation of phenolic oligomers during fast pyrolysis of lignin.* Fuel, 2014. **128**: p. 170-179.
18. Yan, M., et al., *Gel point suppression in RAFT polymerization of pure acrylic cross-linker derived from soybean oil.* Biomacromolecules, 2016. **17**(8): p. 2701-2709.
19. Rover, M.R., et al., *Stabilization of bio-oils using low temperature, low pressure hydrogenation.* Fuel, 2015. **153**: p. 224-230.
20. McClelland, D.J., et al., *Functionality and molecular weight distribution of red oak lignin before and after pyrolysis and hydrogenation.* Green Chemistry, 2017. **19**(5): p. 1378-1389.
21. Dodd, A.P., J.F. Kadla, and S.K. Straus, *Characterization of fractions obtained from two industrial softwood kraft lignins.* ACS Sustainable Chemistry & Engineering, 2014. **3**(1): p. 103-110.
22. Zhou, S., et al., *Lignin valorization through thermochemical conversion: comparison of hardwood, softwood and herbaceous lignin.* ACS Sustainable Chemistry & Engineering, 2016. **4**(12): p. 6608-6617.
23. Bayerbach, R., et al., *Characterization of the water-insoluble fraction from fast pyrolysis liquids (pyrolytic lignin): Part III. Molar mass characteristics by SEC, MALDI-TOF-MS, LDI-TOF-MS, and Py-FIMS.* Journal of analytical and applied pyrolysis, 2006. **77**(2): p. 95-101.
24. Fernández-Costas, C., et al., *Structural characterization of Kraft lignins from different spent cooking liquors by 1D and 2D Nuclear Magnetic Resonance spectroscopy.* Biomass and Bioenergy, 2014. **63**: p. 156-166.
25. Gao, H., K. Min, and K. Matyjaszewski, *Determination of gel point during atom transfer radical copolymerization with cross-linker.* Macromolecules, 2007. **40**(22): p. 7763-7770.
26. Steudle, L.M., et al., *Carbon fibers prepared from melt spun peracylated softwood lignin: an integrated approach.* Macromolecular Materials and Engineering, 2017. **302**(4).
27. Passoni, V., et al., *Fractionation of industrial softwood Kraft lignin: solvent selection as a tool for tailored material properties.* ACS Sustainable Chemistry & Engineering, 2016. **4**(4): p. 2232-2242.
28. Sun, Q., et al., *A study of poplar organosolv lignin after melt rheology treatment as carbon fiber precursors.* Green Chemistry, 2016. **18**(18): p. 5015-5024.

29. Zhang, M., *Carbon fibers derived from dry-spinning of modified lignin precursors.* 2016.
30. Baker, D.A., N.C. Gallego, and F.S. Baker, *On the characterization and spinning of an organic-purified lignin toward the manufacture of low-cost carbon fiber.* Journal of Applied Polymer Science, 2012. **124**(1): p. 227-234.
31. Ouyang, Q., et al., *Fabrication of partially biobased carbon fibers from novel lignosulfonate–acrylonitrile copolymers.* Journal of Materials Science, 2017. **52**(12): p. 7439-7451.
32. Kim, K.H., et al., *Quantitative investigation of free radicals in bio-oil and their potential role in condensed-phase polymerization.* ChemSusChem, 2015. **8**(5): p. 894-900.
33. Chen, X., et al., *A thermally re-mendable cross-linked polymeric material.* Science, 2002. **295**(5560): p. 1698-1702.
34. Gordobil, O., et al., *Assesment of technical lignins for uses in biofuels and biomaterials: Structure-related properties, proximate analysis and chemical modification.* Industrial crops and products, 2016. **83**: p. 155-165.

CHAPTER 6. SUMMARY AND FUTURE PERSPECTIVE

In Chapter 2, a biorefinery corn stover lignin with high ash content was successfully converted into carbon fiber. Methanol fractionation was used to purify raw lignin and selectively remove the lignin with high Mw. However, neither ML nor thermally pretreated ML (0AT-ML) was spinnable, due to the coupled effect of high viscosity of the precursors upon melting and precursor devolatilizations at low temperatures. A two-step acetylation of ML rendered thermally stable and spinnable precursors. Among precursors with different acetylation degree, the optimum precursor had an acetylation degree of 0.59, T_g of 85 °C, and Mw of 3594 Da. The average tensile strength and modulus of the carbon fiber produced upon oxidative stabilization of the 0.75AT-ML as-spun fiber followed by carbonization at 1000 °C were 0.454 GPa and 62 GPa. The I_D/I_G ratio of the carbon fiber was 2.53 based on Raman spectroscopy.

In Chapter 3 to 5, depolymerized lignin (PL) with much smaller molecule size was obtained by pyrolyzing biomass/lignin. PL was repolymerized via different routes to produce lignin precursor with modified structure. In Chapter 3, PL was first washed with toluene to remove low-Mw compounds and to narrow the Mw distribution. PL was then repolymerized in present of acid catalyst to increase both thermal stability and T_g of the precursor. After melt-spinning, oxidative stabilization and carbonization, the produced carbon fiber had attractive tensile strength of 0.855 GPa with single filament reach to 1.01 GPa. The work encourages the use of PL (i.e. decomposed lignin) as carbon fiber precursor. In Chapter 4, PL was co-treated with PET to produce a lignin-based melt-spinnable polymer with improved molecular orientation. The highly reactive PL was able to initiate chain scission and fragmentation of PET at a temperature significantly lower than standard degradation temperature of PET. The resulting PET fragments containing carboxylic, vinyl, and hydroxyl groups further reacted with the PL

molecules to form the PL-PET polymers, which have linear backbone of PET. The co-polymerization was found to lower T_gs and improve thermal stability of the PL-PET polymers despite of their increased Mws. During melt rheology testing, complex viscosity decreased with the PL-PET polymers because of reduced crosslinking and improved flow orientability in the polymer chains. The melt spinning temperature was lowest with PL-20PET due to the higher content of linear backbones and better molecular orientation. The improved molecular orientation in the PL-PET polymers also resulted in the stabilized fibers with higher strains and carbonized fibers with lower I_D/I_G ratios and higher tensile strengths. This preliminary study demonstrated an approach to improve molecular and flow orientability of lignin-based polymer. In Chapter 5, PL was used as the monomers/oligomers for polymerization reaction. The large presence of hydroxyls on PL render it a reactive medium for functionalization. Hydroxyls on PL was successfully captured with methacryloyls, making them polymerizable with presence of carbon-carbon double bonds. Different functionalized PL was prepared, and three polymers were synthesized and compared. It was found the synthesized PLMAP3 had Mw of 16K Da with PDI of 1.53. The T_g and T_d of PLMAP3 were 130 ℃ and 250 ℃, respectively. Moreover, PLMAP3 also had a linear structure implying by Mark Houwink plot. Rheological results showed that the viscosity of PLMAP3 at temperature range of 190 to 230 ℃ was between 100~1000 Pa·s, suggesting the polymer could be continuously melt-spun into fiber filament without causing polymer degradation. PLMAP3 could also be pyrolyzed, leaving 28% of solid residue at 1000 ℃. These characteristics suggested PLMAP3 could be potentially used as precursor for high-quality carbon fiber production.

Producing carbon fiber from the renewable and low-cost lignin has been received great interest for decades. Unlike PAN, lignin is complexed and cross-linked with seldom consistency

could follow. This is the main obstacles that prevent lignin from converting into orientated and high-quality carbon fiber. Therefore, one of the main tasks in future should be addressed the amorphous structure of lignin. As it was shown in Chapter 5, re-construction of decomposed lignin molecules into lignin-based macromolecules could be an approach to alter the molecular orientation of lignin. The better-orientated lignin is much closer to industrially available linear polymers in properties, and could be treated as the polymer for further processing. Moreover, due to the inherent characteristics of lignin molecules, lignin-based materials always preserve certain amount of fixed carbon upon carbonization, making the PL-based polymer be able to convert to carbon fiber.

Future work of emphasis could be focused on fractionation of PL molecules into different categories with different molecular sizes. This will facilitate the formation of crystallinity in produced polymers. The investigation of relationship between functional groups on PL and kinetics of polymerization will be also of great interest. PL is crude lignin-derived monomers/oligomers with hundreds of compounds, it may perform differently in polymerization compared with model monomers. Understanding the key factors of the polymerization of PL monomers can provide a method to control the properties of the synthesized polymer, thus target a polymer that is most beneficial to produce high quality PL-polymer based carbon fiber.